

Copy No.

122

RM No. L7F13

CONFIDENTIAL

TECH LIBRARY KAFB, NM
REF ID: D3947



RESEARCH MEMORANDUM

001L

RM L7F13

MEASUREMENTS OF AERODYNAMIC CHARACTERISTICS
OF A 35° SWEPTBACK NACA 65-009 AIRFOIL MODEL WITH $\frac{1}{4}$ -CHORD
PLAIN FLAP BY THE NACA WING-FLOW METHOD

By

Harold I. Johnson

Langley Memorial Aeronautical Laboratory
Langley Field, Va.

CLASSIFIED DOCUMENT

This document contains classified information pursuant to the National Defense of the United States. It is illegal to transmit or the revelation of its contents in any manner to an unauthorized person prohibited by law. Information so contained may be imparted only to persons in the military and naval services of the United States, appropriate civilian officers and employees of the Government who have a legitimate need therefor, and to United States citizens of loyalty and discretion who of necessity must be informed thereof.

NATIONAL ADVISORY COMMITTEE
FOR AERONAUTICS

WASHINGTON

August 5, 1947

319.98/c3

Classification canceled (or changed to Unclassified.....)
By Authorizer NASA Tech PubA
(OFFICER AUTHORIZED BY 57 by Jane)

By

Date

GRADE OF OFFICER MAKING CHANGE) NK

DATE 12 Dec 61



0143947

NACA RM No. L7F13

NATIONAL ADVISORY COMMITTEE FOR AERONAUTICS

RESEARCH MEMORANDUM

MEASUREMENTS OF AERODYNAMIC CHARACTERISTICS

OF A 35° SWEPTBACK NACA 65-009 AIRFOIL MODEL WITH $\frac{1}{4}$ -CHORD

PLAIN FLAP BY THE NACA WING-FLOW METHOD

By Harold I. Johnson

SUMMARY

As part of a general investigation of the stability and control characteristics of various airfoil-flap combinations in the transonic speed range, measurements were made by the NACA wing-flow method of the lift, pitching-moment, and hinge-moment characteristics of a 35° sweptback NACA 65-009 airfoil of aspect ratio 3.04, with a full-span $\frac{1}{4}$ -chord unsealed plain flap. The tests covered Mach numbers from 0.55 to 1.10, Reynolds numbers from about 500,000 to 1,300,000, angles of attack from -2° to 15°, and flap deflections from about -20° to 20°. Some of the important results are given below.

The variations of lift and pitching moment with either angle of attack or flap deflection were nearly rectilinear at all Mach numbers tested for moderate angles of attack and flap deflections; similarly, flap hinge moment increased almost rectilinearly with flap deflection. The lift curve slope increased slightly as the Mach number was increased to 0.80 but remained practically unchanged as the Mach number was increased from 0.80 to 1.10. The aerodynamic center shifted rearward steadily from 17 percent of the mean aerodynamic chord below a Mach number of 0.90 to 33 percent of the mean aerodynamic chord at a Mach number of 1.10. Flap effectiveness decreased 40 percent as the Mach number increased from 0.55 to 1.00. The flap effectiveness then remained constant to a Mach number of 1.10. The center of pressure due to flap deflection moved rearward with increasing Mach number from about 65 to 85 percent of the mean aerodynamic chord over the test Mach number range. At small to moderate angles of attack the flap-floating tendency $dC_H/d\alpha$ was zero at all Mach numbers; at large angles of attack the flap had a strong negative floating tendency that was magnified by increasing Mach number. The flap-restoring tendency $dC_H/d\delta$ approximately doubled in going from a Mach number of 0.55 to a Mach number of 1.05.

It was found that in the Mach number range from 0.65 to 0.90 wherein comparable data were obtained increasing the Reynolds number from roughly 600,000 to 1,200,000 caused small changes in the lift-curve slope and position of the aerodynamic center but no changes in the flap lift, pitching-moment, or hinge-moment characteristics.

INTRODUCTION

The NACA is conducting a number of investigations of the aerodynamic characteristics of small models in the transonic speed range by the wing-flow method. One of these investigations is concerned with the measurement of the stability and control characteristics of various general research airfoil-flap combinations. Brief measurements of this type on an unswept model having the geometric characteristics of the horizontal tail of a P-51D airplane have been reported in reference 1. The present report covers more complete measurements of the characteristics of a sweptback research model. These tests represent the first of a series of measurements being made with general research models to investigate flap effectiveness and methods of balancing control surfaces at transonic speeds.

The tests consisted of measurements of the lift, pitching moment, and hinge moment on a model of a 35° sweptback, aspect ratio = 3.04, untapered NACA 65-009 airfoil with a full-span $\frac{1}{4}$ -chord unsealed plain flap. The tests were run for angles of attack from -2° to 15° and for flap angles from about -20° to 20° through a Mach number range from 0.55 to 1.10. The Reynolds numbers varied from about 500,000 to 1,300,000. In the Mach number range from 0.65 to 0.90, comparable data were obtained for Reynolds numbers of approximately 600,000 and 1,200,000 so that the effect of Reynolds number could be determined over this range.

SYMBOLS

The symbols defined in the following list are used in this report.

- | | |
|-------|---------------------------------------|
| M | average Mach number over the model |
| M_A | airplane free-stream Mach number |
| R | Reynolds number |
| q_A | airplane free-stream dynamic pressure |

q	average dynamic pressure over model
C_{LA}	airplane lift coefficient $\left(\frac{\text{Airplane lift}}{q_A S_A} \right)$
C_L	model lift coefficient $\left(\frac{\text{Model lift}}{qS} \right)$
C_M	model pitching-moment coefficient $\left(\frac{\text{Model pitching moment}}{qb_f c^2} \right)$ (measured about axis 16-percent M.A.C. ahead of leading edge of M.A.C.)
C_H	model hinge-moment coefficient $\left(\frac{\text{Model hinge moment}}{qb_f \bar{c}_f^2} \right)$
$\frac{dC_L}{d\alpha}$	variation of model lift coefficient with angle of attack, per degree
$\frac{dC_L}{d\delta}$	variation of model lift coefficient with flap deflection, per degree
$\frac{dC_M}{d\alpha}$	variation of model pitching-moment coefficient with angle of attack, per degree
$\frac{dC_M}{d\delta}$	variation of model pitching-moment coefficient with flap deflection, per degree
$\frac{dC_H}{d\alpha}$	variation of flap hinge-moment coefficient with model angle of attack, per degree
$\frac{dC_H}{d\delta}$	variation of flap hinge-moment coefficient with flap deflection, per degree
$\frac{d\alpha}{d\delta}$	flap relative effectiveness $\left(\frac{dC_L/d\delta}{dC_L/d\alpha} \right)$
α	angle of attack; angle between model chord plane and direction of relative wind
δ	flap deflection; angle between flap chord line and airfoil chord line measured in plane perpendicular to hinge line
Λ	sweepback angle
λ	taper ratio
A	aspect ratio
$b/2$	model span normal to wind direction

- c model chord parallel to wind direction
- c model mean aerodynamic chord
- S total area of model (corresponds to 1/2 the area of a complete wing)
- b_f/2 flap span along hinge line
- c_r flap root-mean-square chord perpendicular to hinge line
- c_f flap chord parallel to wind direction
- S_A airplane wing area

APPARATUS

The airfoil model was mounted on the door of the ammunition compartment on the upper surface of the right wing of a P-51D airplane (fig. 1). The contour of the door had been modified to provide smaller velocity gradients over the model and to place the compression shock on the airplane wing at a position behind the model. Typical chordwise variations of local velocity in the region of the model, as determined from static-pressure measurements on the surface of the door with model removed, are shown in figure 2. Some typical spanwise variations of local velocity over the model, as determined from static-pressure measurements made with the rake shown in figure 3, are given in figure 4. For purposes of converting measured forces and moments on the model into nondimensional coefficients, the local dynamic pressures corresponding to the local Mach numbers were averaged in both a chordwise and a spanwise direction over the model area. In addition to the foregoing, some measurements were made of surface pressures along the span of the airplane wing at the model station. As might be expected, these measurements showed a negligible variation in velocity near the wing surface with spanwise distance along the airplane wing within the accuracy of the measurements.

The airfoil model was machined from solid dural to the dimensions shown in figure 5. A thin circular end plate having a diameter equal to the model chord was fastened to the root of the model in order to simulate half-span test conditions. The end plate was solid except for a $\frac{1}{2}$ -inch-diameter hole through which the flap tang passed.

Also, there were two small openings in the wing surface underneath

the end plate through which the model tang and flap tang passed. These openings undoubtedly allowed some leakage of flow around the root of the model but the effects of this leakage are believed to be very small. The flap gap of approximately 0.02 inch was left unsealed.

The lift, pitching moment, and hinge moment were measured by a strain-gage balance and the flap deflection was measured by a slide-wire potentiometer. These quantities were recorded continuously by a recording galvanometer. The strain-gage balance was equipped with an air-driven motor that oscillated the flap continuously through a deflection range of approximately $\pm 20^\circ$ at a nearly uniform rate of $1\frac{1}{2}$ oscillations per second. In terms of relative flight

speed these figures mean that the flap was deflected 1° while the model travelled 18 chord lengths for the lowest flight speed tested. From this standpoint it appears the effect of aerodynamic lag on the measurements should be negligible.

The airfoil angle of attack was measured with respect to the angle of a freely floating rectangular vane with a wedge-shape cross section that was located $22\frac{1}{2}$ inches outboard of the model station.

(Refer to fig. 1.) In a flight made before the sweptback model was installed, an identical floating vane was installed at the model station so that the direction of air flow at the model location was calibrated as a function of the position of the outboard vane.

In addition to the foregoing instrumentation, standard NACA recording instruments were used to determine the airspeed, altitude, normal and lateral acceleration of the airplane, and the free-air temperature.

TESTS

Flights were made with the model set at angles of -2° , 0° , 2° , 5° , 8° , and 15° relative to the longitudinal axis of the airplane. In addition, a flight was made to determine only the lift of the model when set at 22° from the longitudinal axis of the airplane. Each flight consisted of two runs at different altitudes so that a large Mach number range could be covered for different Reynolds number ranges. In the "high-dive" run the airplane was dived from an altitude of 28,000 feet at an indicated airspeed of 220 miles per hour to an airplane Mach number of 0.73 at an altitude of 18,000 feet whereupon a 4g pull-out was made. During this dive useable data were obtained for Mach numbers over the model ranging from 0.65 to 1.10.

In the "level-flight" run the airplane was slowed down gradually from 450 miles per hour to 300 miles per hour at 5,000 feet altitude following a dive and pull-out from about 12,000 feet altitude. From this run data were obtained for model Mach numbers varying from 0.90 to 0.55. The variation of Reynolds number with Mach number for the high-dive and level-flight runs is shown in figure 6.

ACCURACY

The major variables presented herein are believed to be accurate within the following absolute limits:

Mach number	±0.01
Angle of attack, degrees	±0.2
Flap angle, degrees	±0.3
Lift coefficient	±0.03
Pitching-moment coefficient	±0.015
Hinge-moment coefficient	±0.015

The accuracy of the last three of the foregoing variables is a function of the magnitude of the forces and moments which in turn are a function of the dynamic pressure; the figures given above are for the lowest dynamic pressure used in the tests. At the highest dynamic pressure tested, the accuracies should be four times better than those listed. About half of the loss in accuracy was caused by gradual small shifts in instrument zeros during a run. The other half was caused by inability of the recording galvanometer to produce a unique deflection from a given signal and by small reading errors incurred during the evaluation of the data. In the case of measuring slopes for data plotted against flap deflection, the accuracy should be better than that corresponding to the foregoing because the instrument zeros remained essentially constant during any single flap oscillation.

PRESENTATION OF RESULTS

Standard NACA conventions were used for the signs and coefficients used in presenting the data. The pitching moments were measured about an axis located 16 percent of the chord ahead of the leading edge of the mean aerodynamic chord.

An example of a plot of typical original data obtained from the balance is shown in figure 7. It will be noted that the measurement of lift and pitching moment involved some hysteresis. This time lag

in recording the lift and pitching moment actually amounted to about 0.010 and 0.014 second, respectively; the phenomenon was probably associated with the capabilities of the balance or the recording galvanometer to respond quickly to an impressed force or moment. In this connection, the balance was designed to have a maximum natural oscillation period under 0.020 second. As indicated by figure 7, the hysteresis was taken into account by measuring the lift and pitching moment for flap travel in both directions, and then establishing the correct curve laterally halfway between the two curves thus determined. This procedure involves the assumption simply that the time lag is a constant. Near full flap travel the correct curve was determined only from the data for the flap approaching maximum deflection using the time lag determined from the data near zero flap deflection. As a result of the necessity for correcting for hysteresis it is possible that some error may be incurred where an abrupt change in slope of a curve occurs. As will be seen later, this possibility applied almost exclusively to the data for very large flap deflections. Because of the large number of test points and curves involved in determining the airfoil characteristics as a function of flap deflection, these curves are presented without showing the actual test points in the interests of clarity.

Figures 8 to 13, inclusive, present the measured lift, pitching-moment, and hinge-moment characteristics as a function of flap deflection for the various angles of attack tested. Figures 14, 15, and 16 show the lift, pitching-moment, and hinge-moment characteristics as a function of angle of attack for zero flap deflection. The data in figures 14 to 16 were cross-plotted from figures 8 to 13. Figure 17 is a summary plot of the lift effectiveness of both the airfoil and the flap as well as the relative effectiveness of the flap, all plotted against Mach number. Figure 18 is a summary plot showing the rate of change of measured pitching-moment coefficient with angle of attack and with flap deflection versus Mach number. Also included in figure 18 is the location of the center of pressure due to flap deflection and the location of the aerodynamic center relative to the mean aerodynamic chord. Figure 19 shows the variation with Mach number of the rate of change of hinge-moment coefficient with flap deflection. All the slopes shown in figures 16 to 19 were taken for either zero flap deflection or/and zero angle of attack; however, an inspection of the original data of figures 8 to 13 indicates that these slopes usually apply to rather large ranges of flap angle or angle of attack.

DISCUSSION OF RESULTS

An inspection of figures 8 and 9 reveals that, in general, the variation of lift with flap deflection is almost rectilinear over nearly the entire range of flap deflection tested ($\pm 20^\circ$) for angles of attack up to 5° , regardless of Mach number. Also, the slopes of the curves through zero flap deflection for a given Mach number are nearly the same for angles of attack up to 5° . At higher angles of attack a definite change in slope of the lift versus flap-deflection curve occurs for conditions where the flap is blanketed by the forward portion of the airfoil. This change in slope is most pronounced at a Mach number of 0.95. It may be noted that no data were obtained for an angle of attack of 15° in the level-flight runs above a Mach number of 0.75. These tests were purposely omitted in order to retain a reasonable strength margin against breaking the airfoil at the root. As it was, lift forces up to 62 pounds were obtained on the model in a high-dive run at a Mach number of 1.10. This fact indicates it is possible to obtain lift forces up to 700 pounds per square foot of area at 20,000 feet altitude on an airfoil of the type tested at a Mach number of 1.10.

The pitching-moment curves, given in figures 10 and 11, show much the same trends as the lift curves because of the far forward position of the reference axis (16 percent M.A.C. ahead of leading edge of M.A.C.). As in the case of the lift curves, the general shapes of the pitching-moment curves are largely unaffected by Mach number for low angles of attack, and for high angles of attack the most pronounced nonrectilinearity occurs near a Mach number of 0.95. The pitching moment falls off a greater amount than the lift at large flap deflections; also, the nonlinearity in the pitching-moment curves for moderate flap deflections when the flap is blanketed by the airfoil (large angles of attack) is more pronounced. These characteristics indicate the center of pressure due to flap deflection moves forward at large flap deflections.

The variations of hinge-moment coefficient with flap deflection, shown in figures 12 and 13, are also seen to be nearly rectilinear particularly for angles of attack close to zero. As the angles of attack increase the hinge-moment curves for Mach numbers between 0.95 and 1.10 become steeper for a few degrees of flap deflection near zero flap angle. Aside from this, it may be noted the hinge-moment curves undergo a gradual increase in over-all steepness as the Mach number is increased.

The variation of lift with ~~angle of attack~~ flap at zero flap deflection (fig. 14) was practically rectilinear for the first 10° . From figure 14(a) it can be seen that the changes in lift-curve slope in

the rectilinear range were very small over the entire range of Mach number tested. Although no attempt was made to establish accurately the maximum lift coefficient, figure 14(a) indicates clearly that the maximum lift coefficient increases sharply from a value of approximately 0.66 at $M = 0.90$ to value of about 0.91 at $M = 1.05$. Along with this large increase in maximum lift coefficient there was a corresponding large increase in the stalling angle of attack.

The pitching moment increased almost rectilinearly with angle of attack up to an angle of attack of about 10° for all test Mach numbers (fig. 15). Such a trend is to be expected because the pitching moment is largely a reflection of the lift when the moment axis is far forward of the aerodynamic center as was the case in these tests. However the slight nonrectilinearity in the moment curves for the angle-of-attack range from 0° to 10° in combination with the straight C_L versus α curves indicates a small rearward shift in the aerodynamic center with increasing angle of attack. At very large angles of attack the pitching-moment curves again show changes reflecting those found for the lift variation with angle of attack; rectilinearity of the curves extends over a progressively larger angle-of-attack range from a Mach number of 0.95 to a Mach number of 1.10. A close inspection of figure 15(a) shows that the over-all steepness of the pitching-moment curves increases with Mach number particularly at Mach numbers above 0.90. This, of course, corresponds to a rearward shift of the aerodynamic center for zero angle of attack with increasing Mach number.

In figure 16 it is seen that, in general, the change in hinge-moment coefficient with change in angle of attack is practically zero for the first 5° of angle of attack. At high angles of attack the hinge-moment coefficient becomes strongly negative indicating a strong tendency of the flap to float with the relative wind. This negative floating tendency is magnified by increasing Mach number and extends down to lower angles of attack with increasing Mach number.

The summary curves of lift effectiveness for the high dive runs (fig. 17) show that the lift curve slope $dC_L/d\alpha$ is essentially invariant with Mach number up to a Mach number of at least 1.05. The data from the level-flight runs indicate some rise in lift curve slope as the Mach number increased to 0.80 but very little further rise in lift curve slope above $M = 0.80$. In general, the values for lift curve slope shown by figure 17 agree well with values found for similar wing plan forms tested at low Mach numbers in various wind tunnels. The foregoing results indicate that any increase in lift curve slope due to Prandtl-Glauert effect is small in the present tests. The relative effectiveness of the flap $d\alpha/d\delta$ is seen to have a relatively low value (0.32) at the lowest Mach number tested and this low value is further reduced by nearly one-half when a Mach number of 1.06 is reached. Similarly, the flap

lift effectiveness $dC_L/d\delta$ is reduced by about 40 percent from an initial low value (0.0165) at $M = 0.55$. It is not yet known how sealing the flap gap will affect the flap lift characteristics. In connection with flap effectiveness it should be remembered that in the present tests the flap angles were measured in a plane perpendicular to the hinge line, whereas the angles of attack were measured in a plane parallel to the wind direction; this convention partly accounts for the low values of flap effectiveness measured for the sweptback model as compared with corresponding values for an unswept airfoil. The values of lift curve slope shown in figure 17 are uncorrected for the effects of model flexibility.

A ground calibration was made to determine the stiffness of the model and the location of its zero twist line. This calibration showed that the line along which lift loads caused no change in angle of attack due either to twist or to lateral deflection was located an appreciable distance ahead of the measured aerodynamic center so that lift forces caused the outboard portion of the airfoil model to twist in the direction that reduced the lift load thereon. This phenomenon resulted in a decrease of lift curve slope that depended on air density as well as Mach number. It is estimated that the value of lift curve slope presented for the high dive runs is reduced by 1.5 percent and that for the level-flight runs is reduced by 3.4 percent at a Mach number of 0.85 as a result of model flexibility.

Regarding the Reynolds number effects indicated by figure 17, it appears that the lift curve slope experiences a small decrease with increasing Reynolds number. For example, at a Mach number of 0.85, increasing the Reynolds number from 650,000 to 1,270,000 decreased the lift curve slope about 4 percent. As pointed out previously, however, model flexibility was responsible for about 2 percent of this total difference in lift curve slope at $M = 0.85$ so that only the remaining 2-percent change in lift curve slope is attributable to Reynolds number effects. It is noteworthy that within the accuracy of the measurements there was no effect of Reynolds number on the flap effectiveness $dC_L/d\delta$ over the Reynolds number range tested. In the case of relative effectiveness of the flap $da/d\delta$, it appears the effect of Reynolds number decreases with increasing Mach number.

The summary of pitching-moment characteristics (fig. 18) shows that beginning at a Mach number of 0.90, the rate of change of pitching-moment coefficient with angle of attack ($dC_M/d\alpha$) increases steadily to a Mach number of 1.05; the resulting aerodynamic center moves rearward steadily from 17 percent of the mean aerodynamic chord at a Mach number of 0.90 to 33 percent of the mean aerodynamic chord at a Mach number of 1.10. The small random variations of

aerodynamic center location shown at Mach numbers below 0.90 are believed to be due partly to experimental error. In connection with the seemingly far forward position of the aerodynamic center at the lower speeds as indicated by these tests, an attempt was made to determine analytically the effect on aerodynamic center location of the vertical velocity gradient above the wing door. It was found that the measured aerodynamic centers are probably on the order of 1 percent mean aerodynamic chord farther forward than they would be if the model were tested in a uniform flow field (disregarding secondary effects). Leakage of air through the relatively large flap gap may have contributed to the forward position of the aerodynamic center at low speeds. The center of pressure due to flap deflection, disregarding the apparent random scatter, moves rearward gradually from 65-percent mean aerodynamic chord at $M = 0.55$ to 85-percent mean aerodynamic chord at $M = 1.05$.

The summary of pitching-moment characteristics shown in figure 18 also indicates some definite effect of Reynolds number on the pitching moment due to angle of attack at low Mach numbers. The pitching moment due to flap deflection, on the other hand, is practically unaffected by the change in Reynolds number allowing for experimental error in the data for the lower speeds tested.

The rate of change of hinge-moment coefficient with flap deflection, shown in figure 19, increases negatively with increasing Mach number. It is seen that the control-centering tendency $dC_H/d\delta$ has a logical low-speed value of -0.0087 per degree at $M = 0.55$ that doubles in going to $M = 1.05$. Because of the excellent agreement between the data from the high-dive and level-flight runs, it is apparent that the large change in Reynolds number had no effect on the flap hinge-moment characteristics up to the highest Mach number for which comparable data were obtained ($M = 0.90$).

On the basis of the foregoing data, it is concluded that, for the Mach number range from 0.65 to 0.90, a change in Reynolds number from roughly 600,000 to 1,200,000 causes possibly a few percent change in the airfoil lift curve slope and aerodynamic-center location and no perceptible change in the flap-lift, pitching-moment, or hinge-moment characteristics for the model tested. These results are of great interest in view of the results obtained by Ackeret and by Liepmann as reported in references 2 and 3, respectively. Both Ackeret and Liepmann found that in a Reynolds number range similar to that covered by the wing-flow tests the manner of shock formation and attendant pressure distribution for two-dimensional transonic flow were highly dependent on the Reynolds number as it affected the condition of the boundary layer. From these facts it

might be supposed that the stability and control parameters of a finite-span airfoil (more especially the flap parameters) would also be affected considerably at the higher angles of attack by change in Reynolds number within the Reynolds number and Mach number ranges covered by the present tests. Such a supposition was not borne out by the present tests, however.

APPLICATION OF RESULTS TO ASSUMED TRANSONIC AIRPLANE

In order to gain an idea of the stability and control characteristics of a full-scale transonic flying-wing airplane, the model data were applied to an assumed flying-wing airplane geometrically similar to the model and possessing the characteristics listed below. Model data from the level-flight runs were used up to a Mach number of 0.90 and model data from the high-dive runs were used from $M = 0.95$ to $M = 1.10$, inclusive.

Wing area, square feet	200
Gross weight, pounds	15,000
Wing loading, pounds per foot ²	75
Span, feet	24.64
Mean aerodynamic chord, feet	8.24
Elevator span along hinge $\frac{g}{g}$, feet	29.62
Elevator root-mean-square chord perpendicular to hinge $\frac{g}{g}$, feet	1.673
Total stick travel, inches	18
Up-elevator travel, degrees	30
Down-elevator travel, degrees	10
Center-of-gravity position, percent M.A.C.	14

It was assumed that all the aerodynamic parameters were rectilinear and had the values indicated by the model data for $\alpha = 0$ and $\delta = 0$ over the angle-of-attack and flap-deflection ranges required to maintain level flight at all speeds up to a Mach number of 1.10. The effect of flap deflection on the total lift was taken into account. An altitude of 30,000 feet was assumed.

Results of the calculations for longitudinal characteristics in steady level flight are shown in figure 20. The top curve presents the airplane lift coefficient required to maintain level flight. The second plot gives the corresponding angles of attack and flap deflections required for trim. Neglecting the damping moment due to pitching velocity, which is small for an airplane of this type, these curves also give the elevator angle per g and the angle of attack per g in steady curvilinear flight so long as the airfoil and flap-lift and pitching-moment characteristics remain rectilinear. The third plot shows the stick force required to maintain level

flight. Unlike the elevator angle curve, the stick-force curve cannot be construed to give the stick-force per g in curvilinear flight because the model data indicate the nonrectilinear negative floating tendency begins to affect appreciably the stick-force characteristics at angles of attack above those required for level flight. In the calculations shown the parameter $dC_g/d\alpha$ was assumed to be zero.

On the basis of figure 20 it appears that such a transonic airplane will experience the familiar diving tendency at high Mach numbers that results from the large rearward shift in aerodynamic center (increase in static margin) due to compressibility phenomena. However, through the use of 35° of sweepback the tendency is delayed at least until a Mach number of 0.90 is reached. It is interesting to note the tremendous stick forces that would be required to fly such an airplane to a Mach number of 1.10. These stick forces might be reduced by many different methods. Some of these methods include the elimination of the less effective portions of the elevators, the use of a control booster, and the use of aerodynamic balance on the flap.

From the foregoing estimations it appears that, provided some method is used to cope with the tremendous stick forces that will be involved, there should be little difficulty from the standpoint of longitudinal trim and stability characteristics in flying a 35° sweptback flying-wing airplane to a Mach number of at least 1.10.

CONCLUSIONS

Wing-flow tests between Mach numbers of 0.55 and 1.10 of a 35° sweptback 65-009 airfoil model of aspect ratio 3.04 with a $\frac{1}{4}$ -chord full-span unsealed plain flap indicated the following conclusions:

1. The variations of lift and pitching moment with either angle of attack or flap deflection and the variation of hinge moment with flap deflection were approximately rectilinear at all Mach numbers tested for moderate angles of attack and flap deflections.
2. The lift curve slope increased slightly with increasing Mach number up to a Mach number of 0.80; above a Mach number of 0.80 there was no appreciable change in lift curve slope.
3. The maximum lift coefficient and the angle of attack for maximum lift coefficient increased markedly above a Mach number of 0.95.

4. The aerodynamic center was at approximately 17 percent of the mean aerodynamic chord below a Mach number of 0.90; increasing the Mach number to 1.10 caused a gradual rearward movement of the aerodynamic center to 33 percent of the mean aerodynamic chord.

5. Flap effectiveness $dC_L/d\delta$ was reduced 40 percent by increasing the Mach number from 0.55 to 1.00; between $M = 1.00$ and $M = 1.10$ the flap effectiveness remained constant.

6. Flap relative effectiveness $dx/d\delta$ decreased by about 50 percent between $M = 0.55$ and $M = 1.00$; further increase in speed to $M = 1.10$ caused a very slight recovery in relative effectiveness.

7. The center of pressure due to flap deflection moved rearward gradually from 65-percent mean aerodynamic chord at $M = 0.55$ to 85-percent mean aerodynamic chord at $M = 1.05$.

8. The flap-floating tendency $dC_H/d\alpha$ was zero for small angles of attack regardless of Mach number; at large angles of attack the flap had a large negative floating tendency that was magnified by increasing Mach number.

9. The flap-restoring tendency $dC_H/d\delta$ changed from -0.009 to -0.017 per degree when the Mach number increased from 0.55 to 1.05.

10. Increasing the Reynolds number from roughly 600,000 to 1,200,000 in the Mach number range from 0.65 to 0.90 caused possibly a few percent decrease in the lift curve slope, a slight forward shift in aerodynamic-center location, and no change in the flap-lift, pitching-moment, or hinge-moment characteristics.

Langley Memorial Aeronautical Laboratory
National Advisory Committee for Aeronautics
Langley Field, Va.

[REDACTED]
REFERENCES

1. Adams, Richard E., and Silsby, Norman S.: Tests of a Horizontal-Tail Model Through the Transonic Speed Range by the NACA Wing-Flow Method. NACA RM No. L7C25a, 1947.
2. Root, L. E., and Smith, A. M. O.: Swiss Aerodynamic Research on Compressible Flow Phenomena. Tech. Rep. No. 343-45, U.S. Naval Tech. Mission in Europe, Sept. 1945.
3. Liepmann, Hans Wolfgang: The Interaction between Boundary Layer and Shock Waves in Transonic Flow. Jour. Aero. Sci., vol. 13, no. 12, Dec. 1946, pp. 623-638.

NACA RM No. L7F13

Fig. 1



Figure 1.- View of 35° sweptback 65-009 airfoil with $\frac{1}{4}$ -chord plain flap mounted on right wing of P-51D airplane. Rectangular vane on right used for measuring angle of attack.

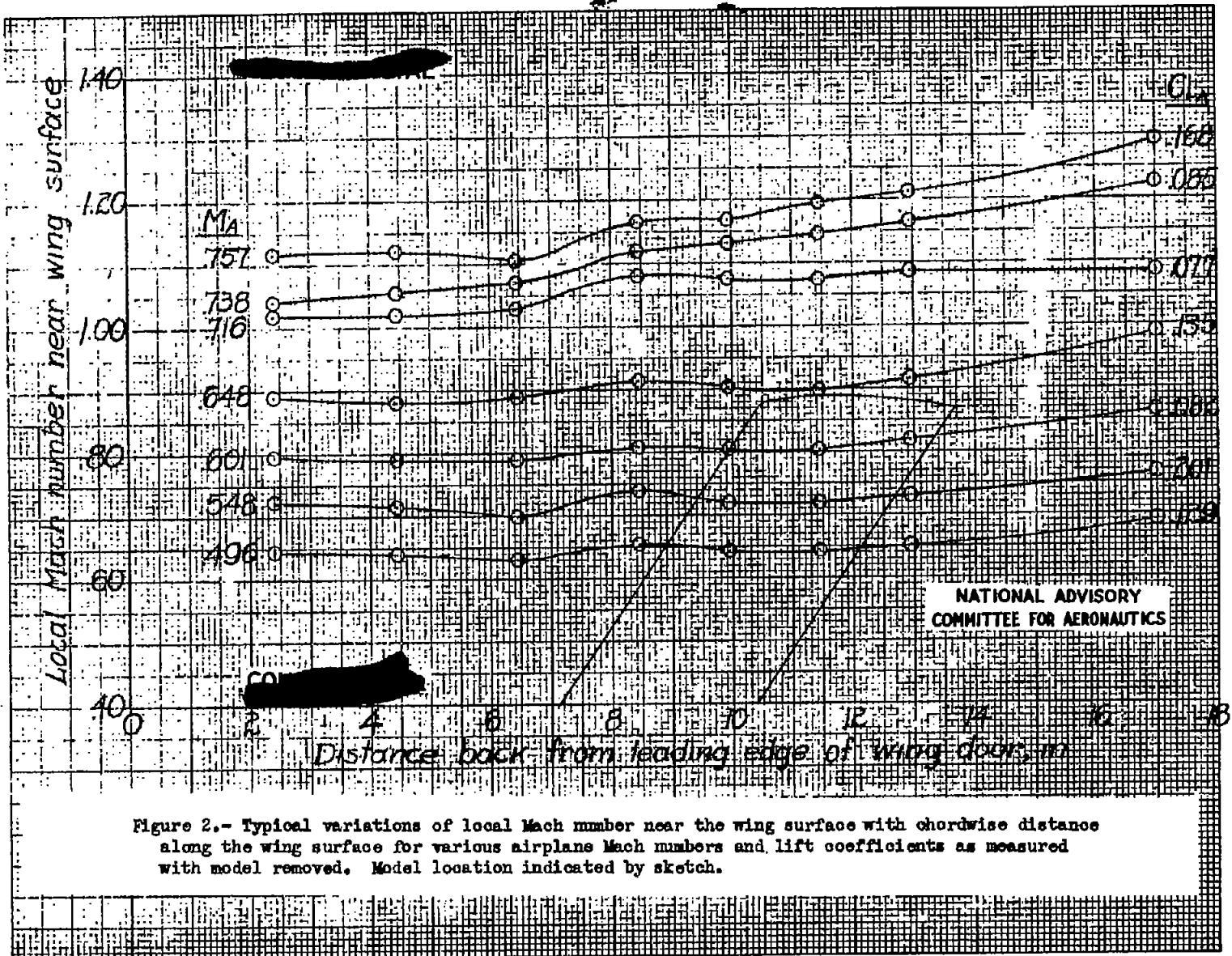


Figure 2.- Typical variations of local Mach number near the wing surface with chordwise distance along the wing surface for various airplanes Mach numbers and lift coefficients as measured with model removed. Model location indicated by sketch.

~~CONFIDENTIAL~~
NACA RM No. L7F13

Fig. 3

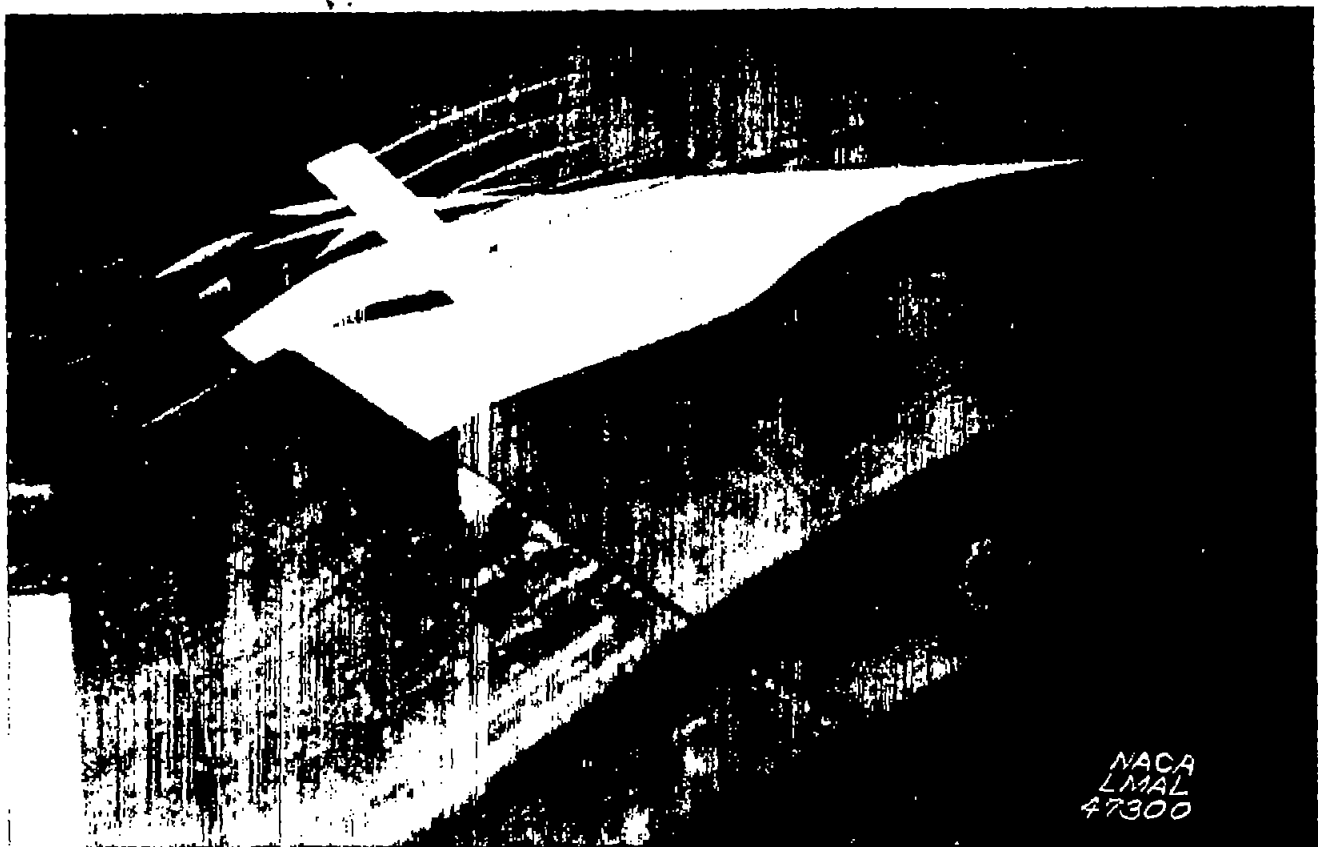
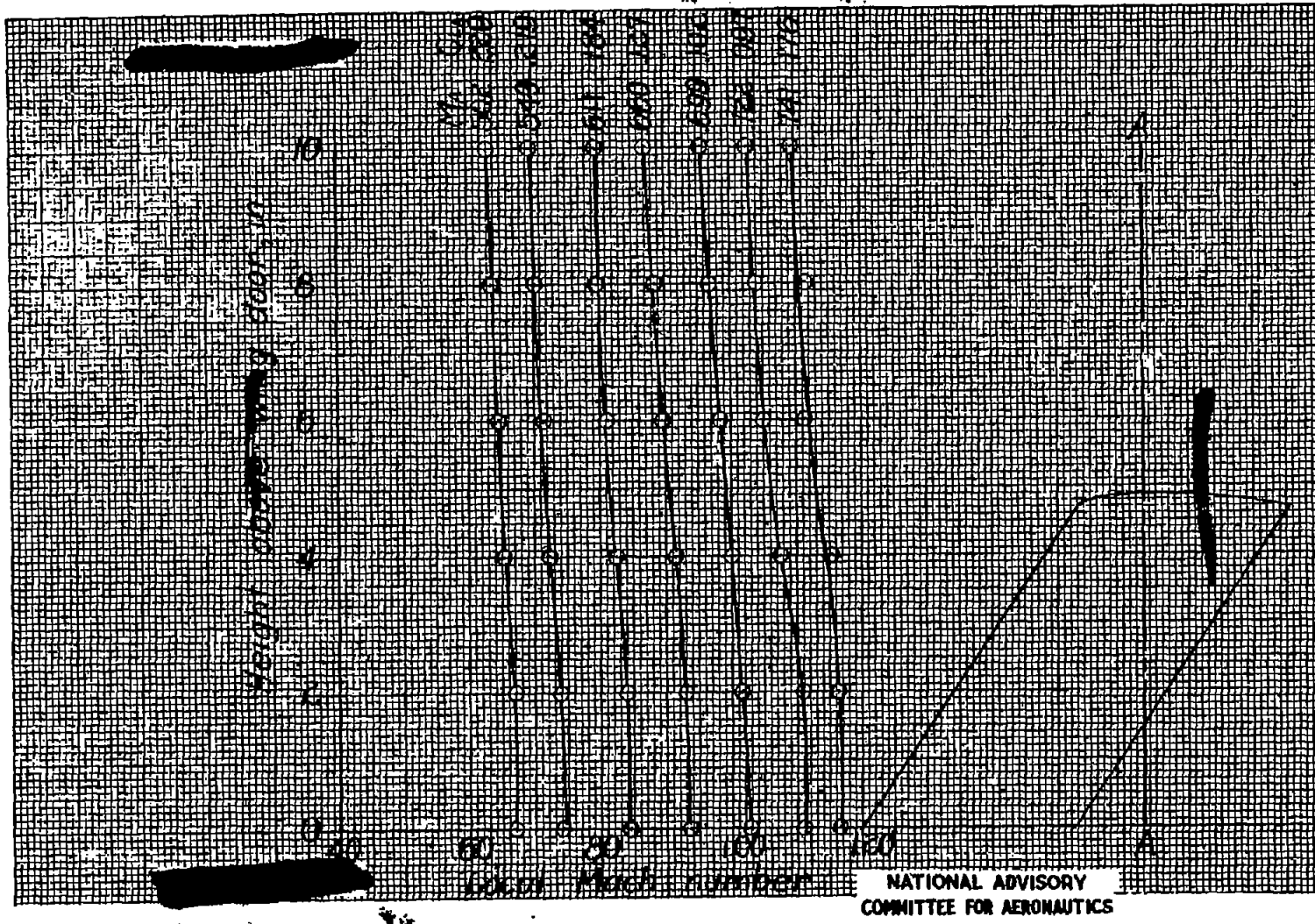


Figure 3.- View of rake used to measure velocity gradient above wing surface.

NACA RM No. L7F13

FIG. 4

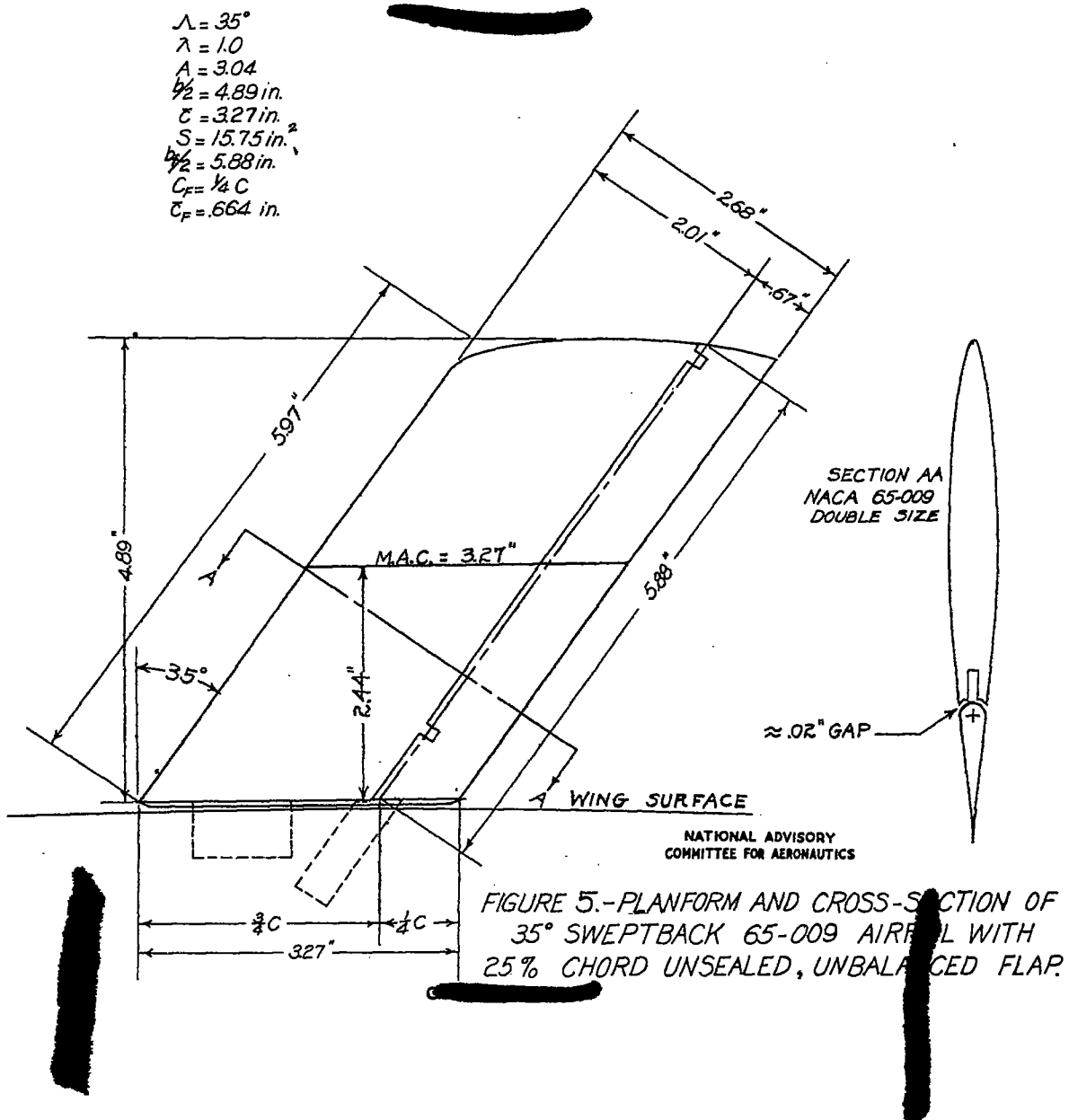


NATIONAL ADVISORY
COMMITTEE FOR AERONAUTICS

Figure 4.- Typical variations of local Mach number with vertical distance above wing surface as measured at chordwise station AA with model removed. These measurements made on left wing which had same contour as right wing.

Fig. 5

NACA RM No. L7F13



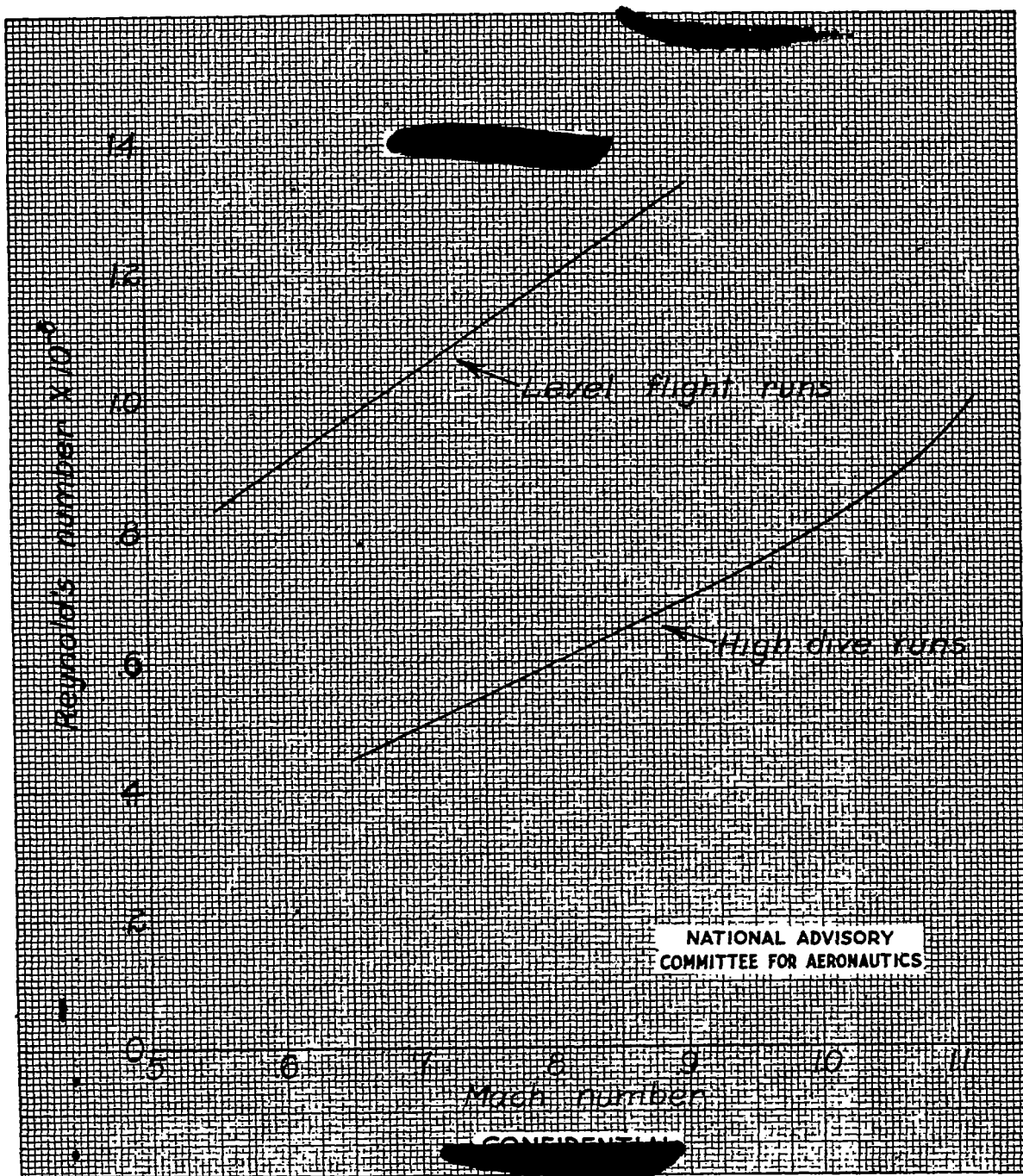


Figure 6.- Variation of Reynold's number with Mach number for tests of 35° Δ , 65-009 airfoil model with $\frac{1}{4}$ -chord plain flap by wing-flow method. Reynold's number based on airfoil chord parallel to direction of flow.

Fig. 7

NACA RM No. L7F13

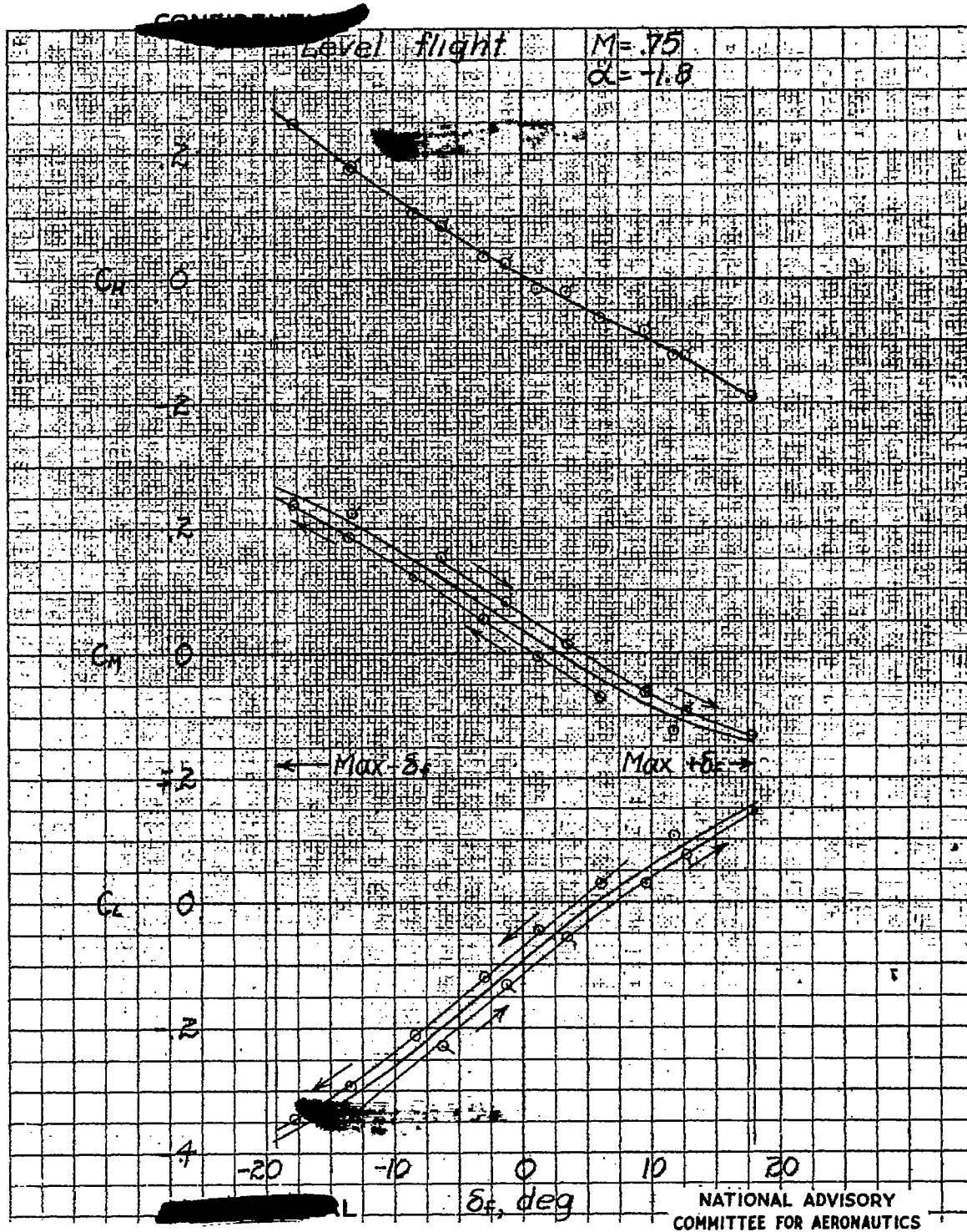


Figure 7.- Typical data obtained from the strain gage balance.

NACA RM No. L7F13

Fig. 8a

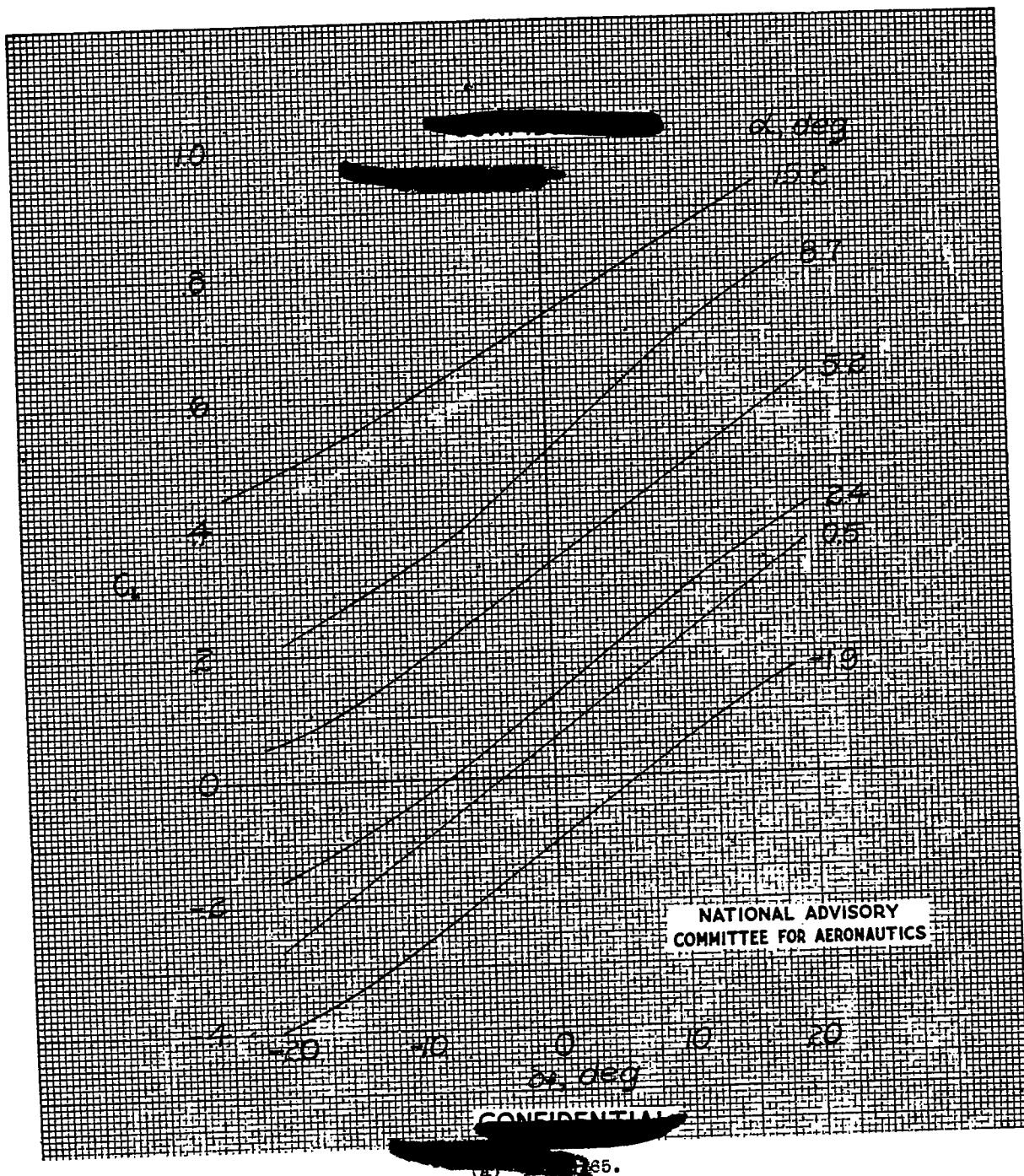
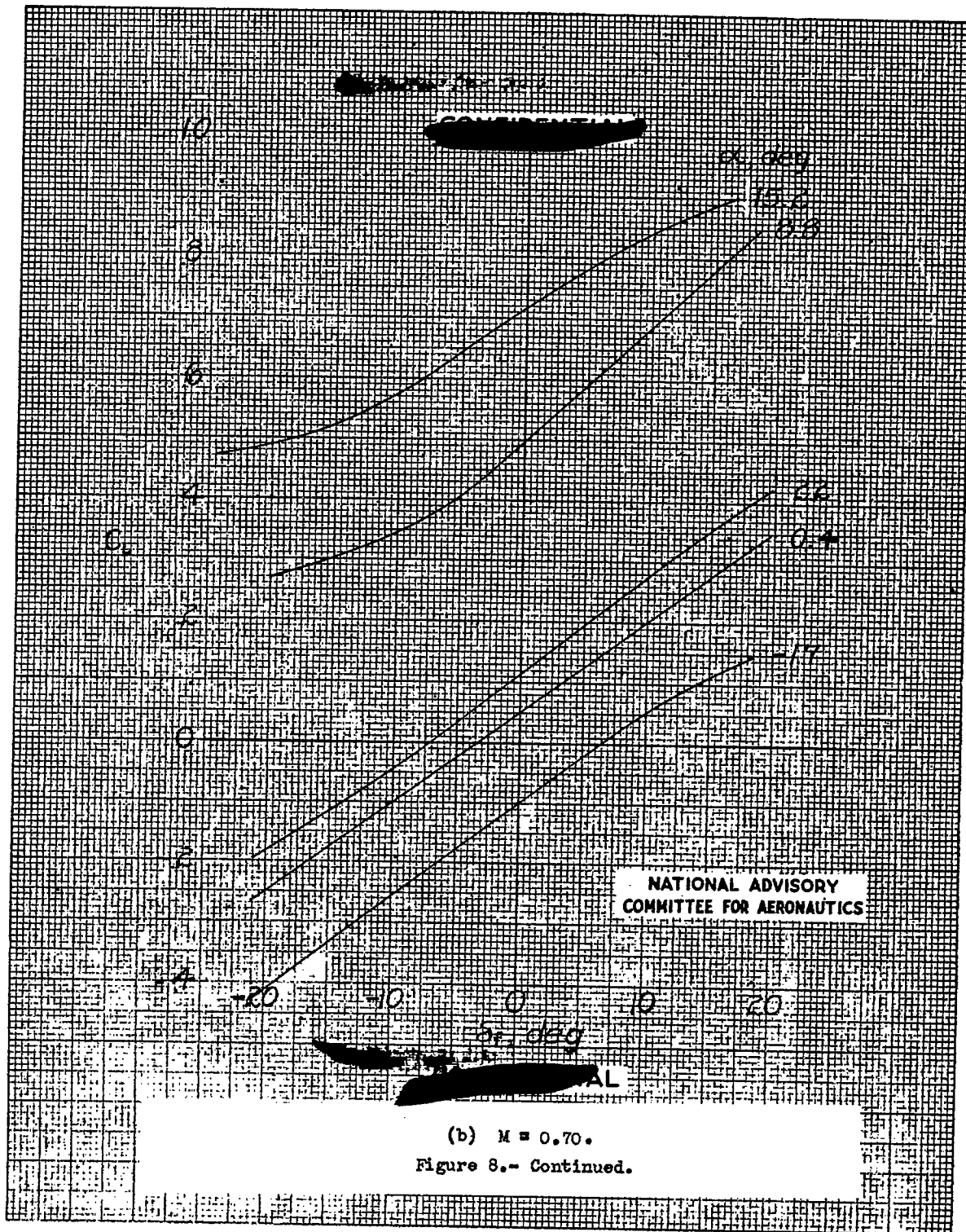


Figure 8.- Variation of lift coefficient with flap deflection from high dive runs.
NACA 65-009 airfoil, $A = 3.04$, $\Delta = 35^\circ$, $c_f/c = 0.25$, gap unsealed.

Fig. 8b

NACA RM No. L7F13



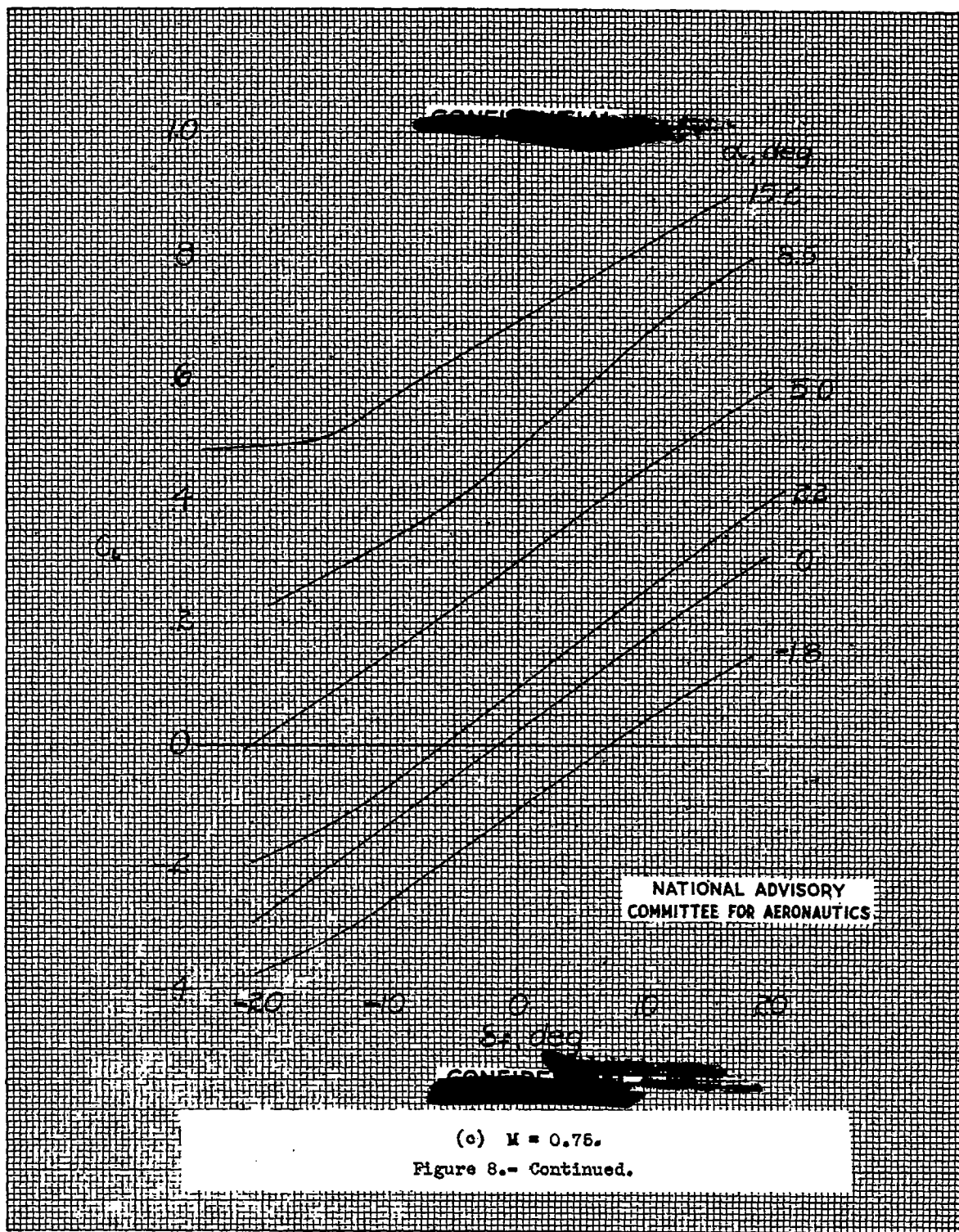
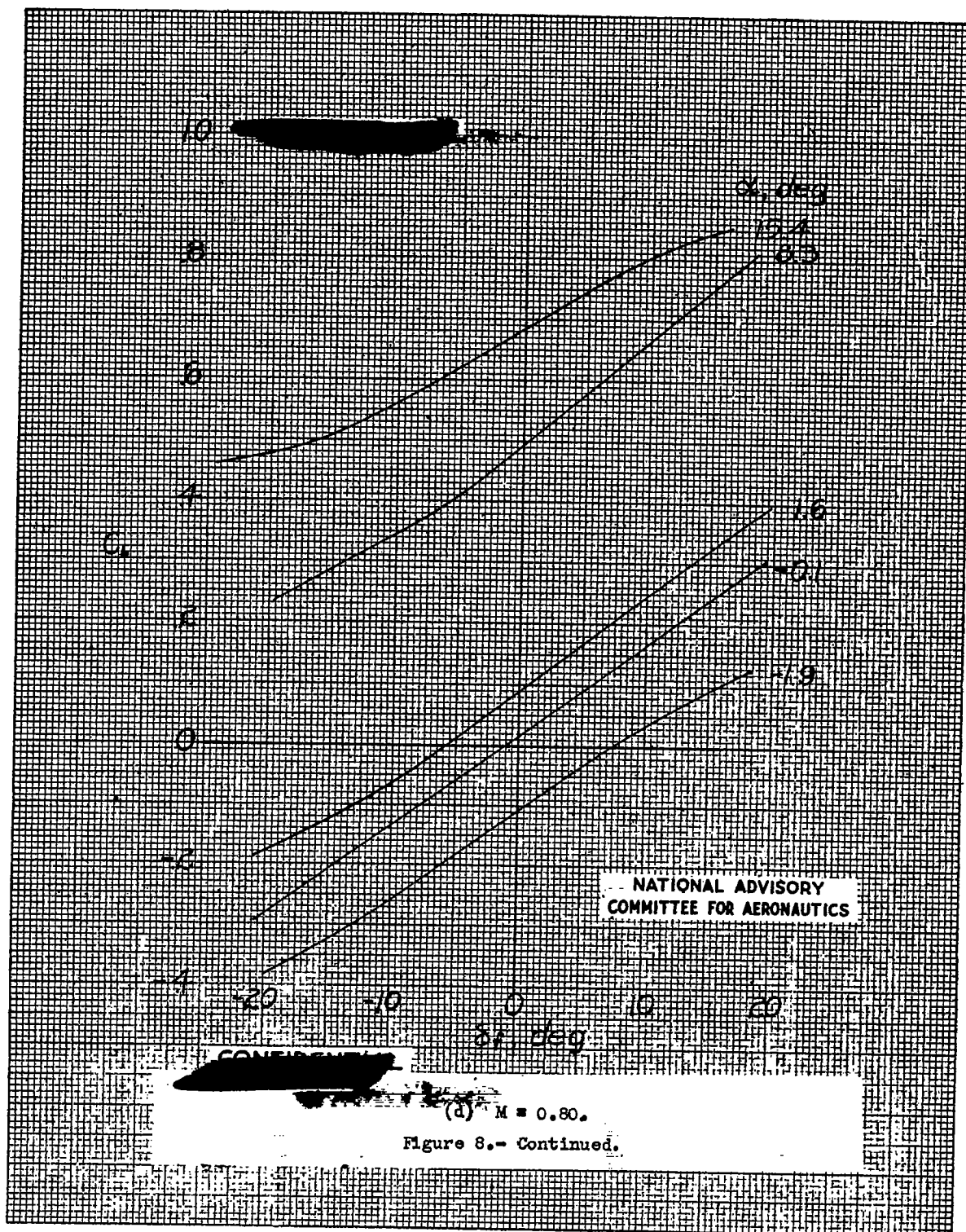


Fig. 8d

NACA RM No. L7F13



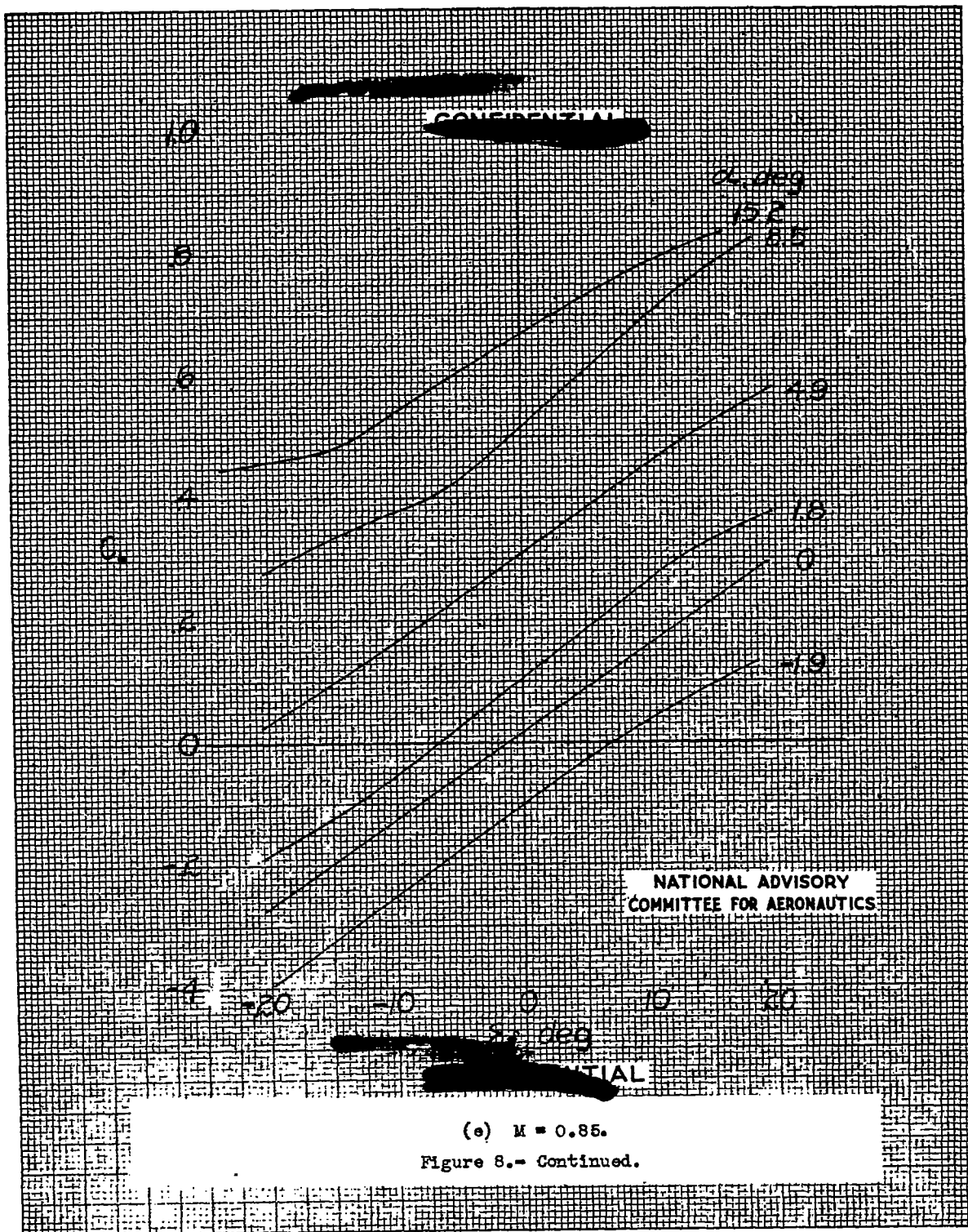
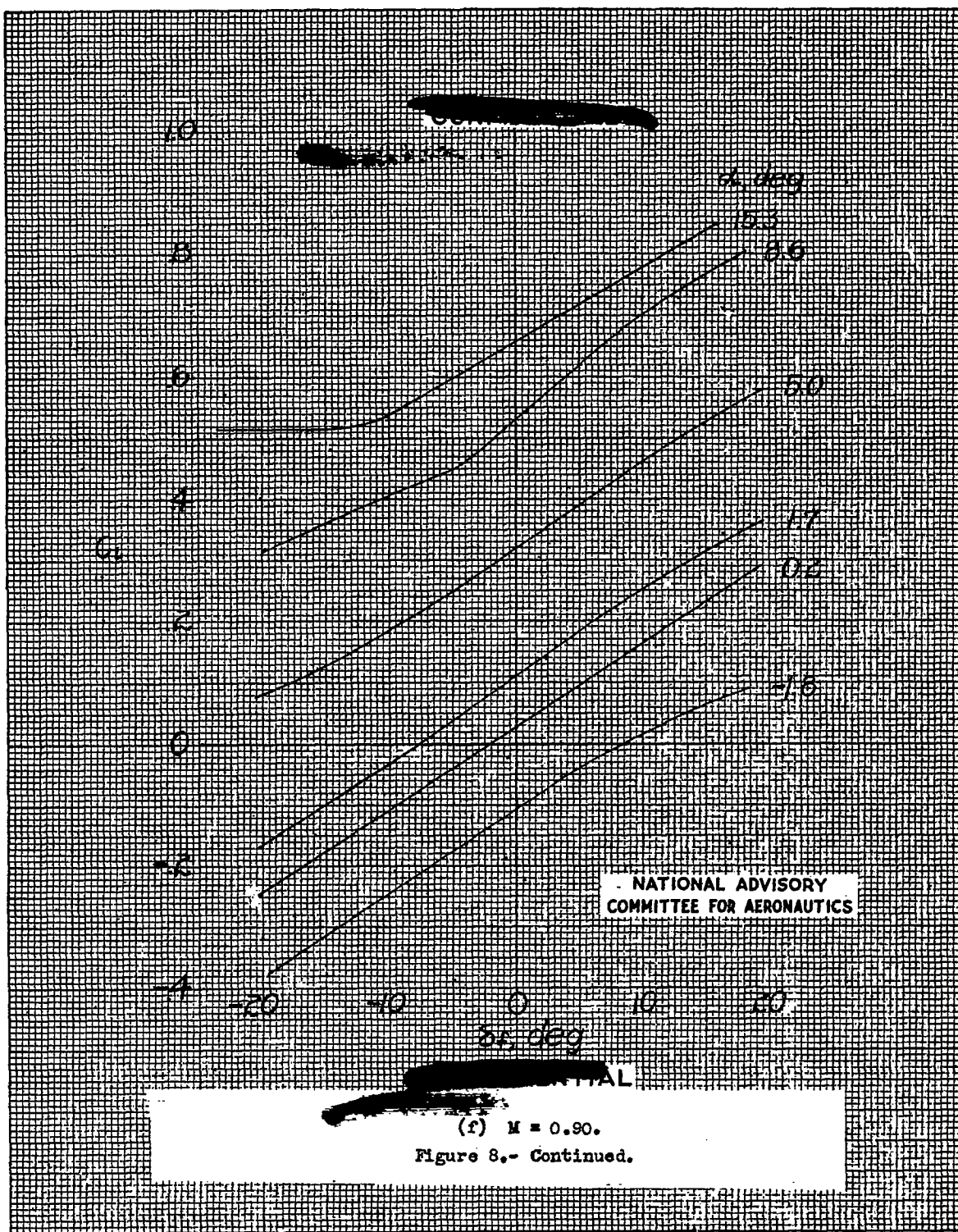


Fig. 8f

NACA RM No. L7F13



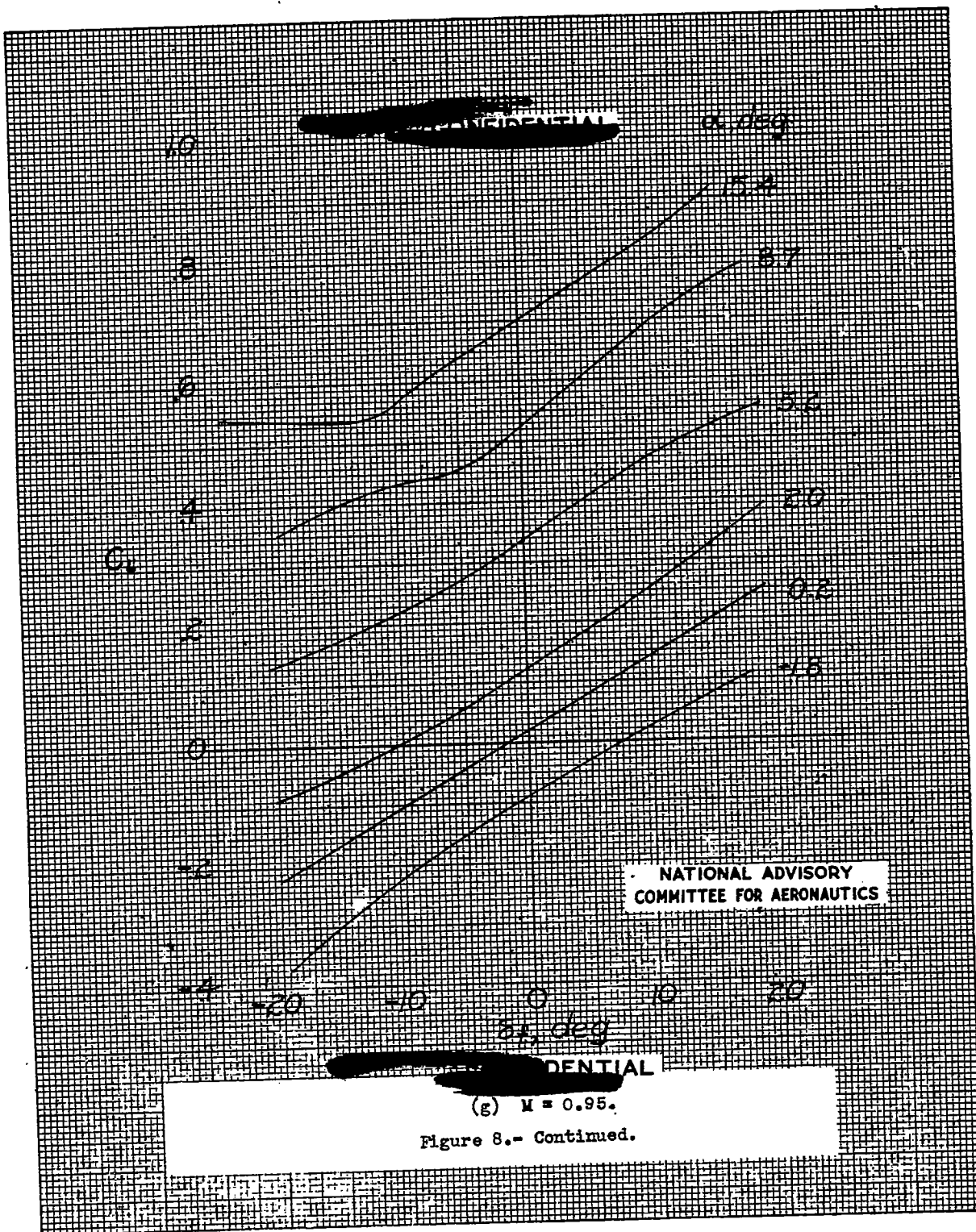
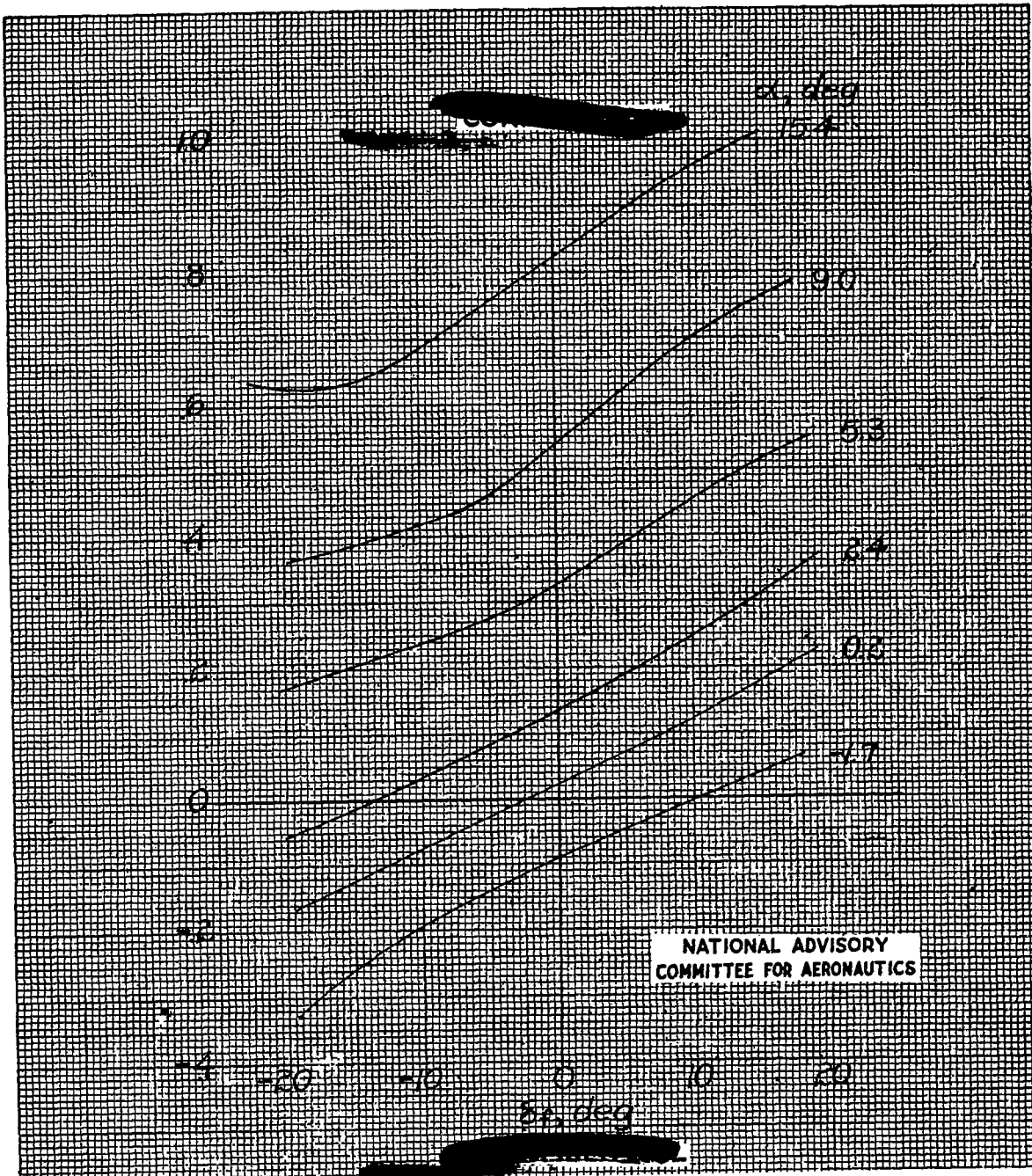


Fig. 8h

NACA RM No. L7F13



(h) $M = 1.00$.

Figure 8.- Continued.

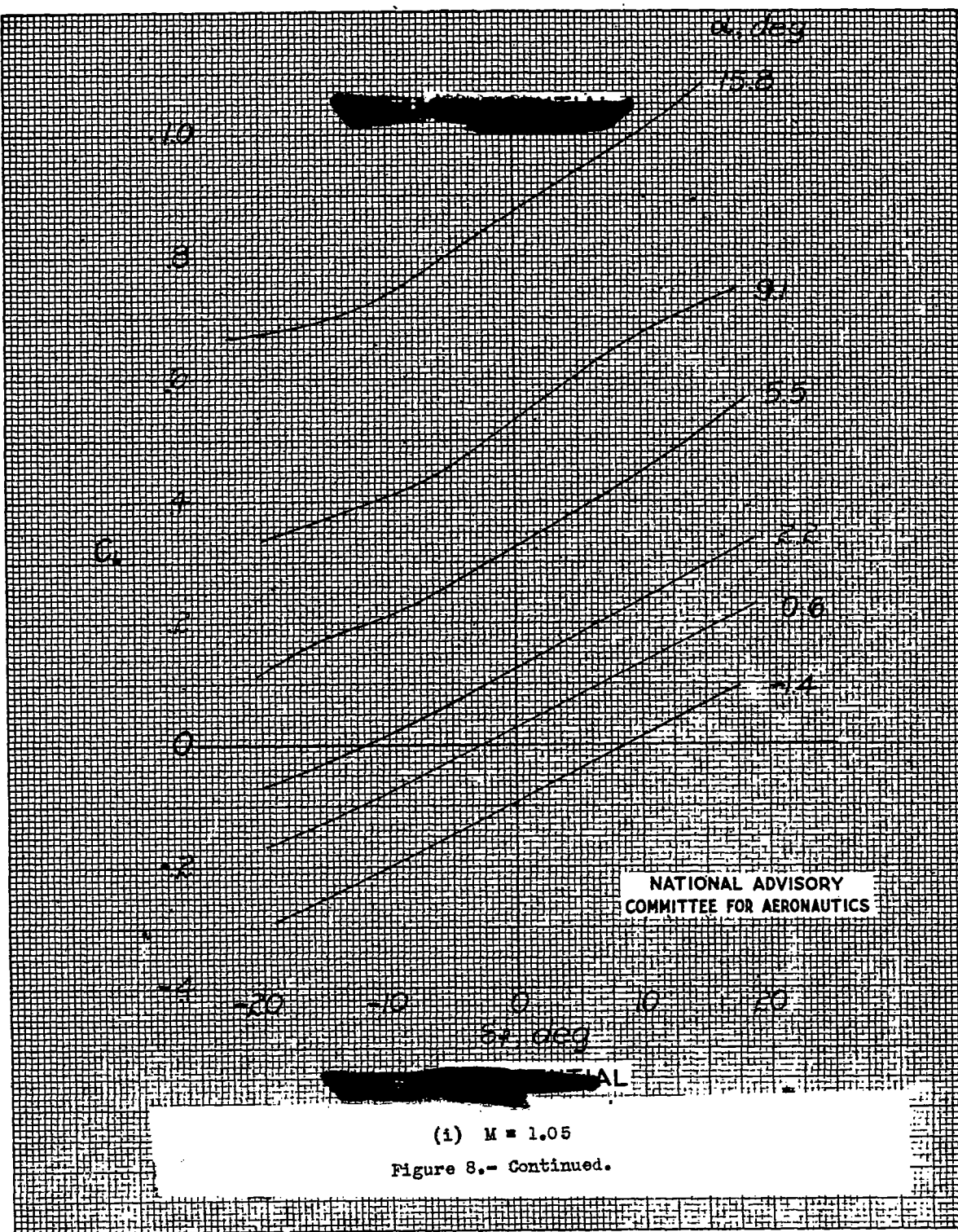
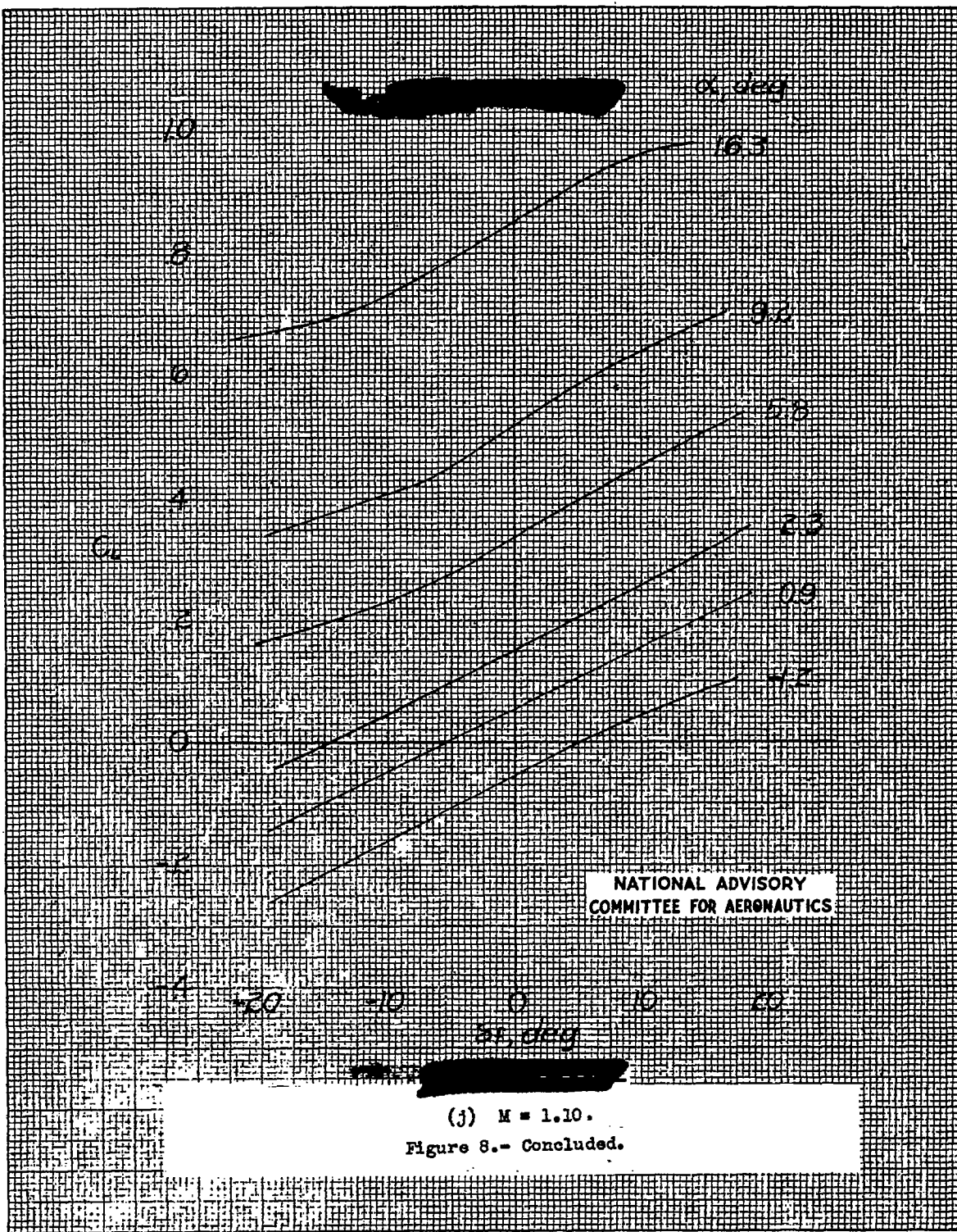


Fig. 8j

NACA RM No. L7F13



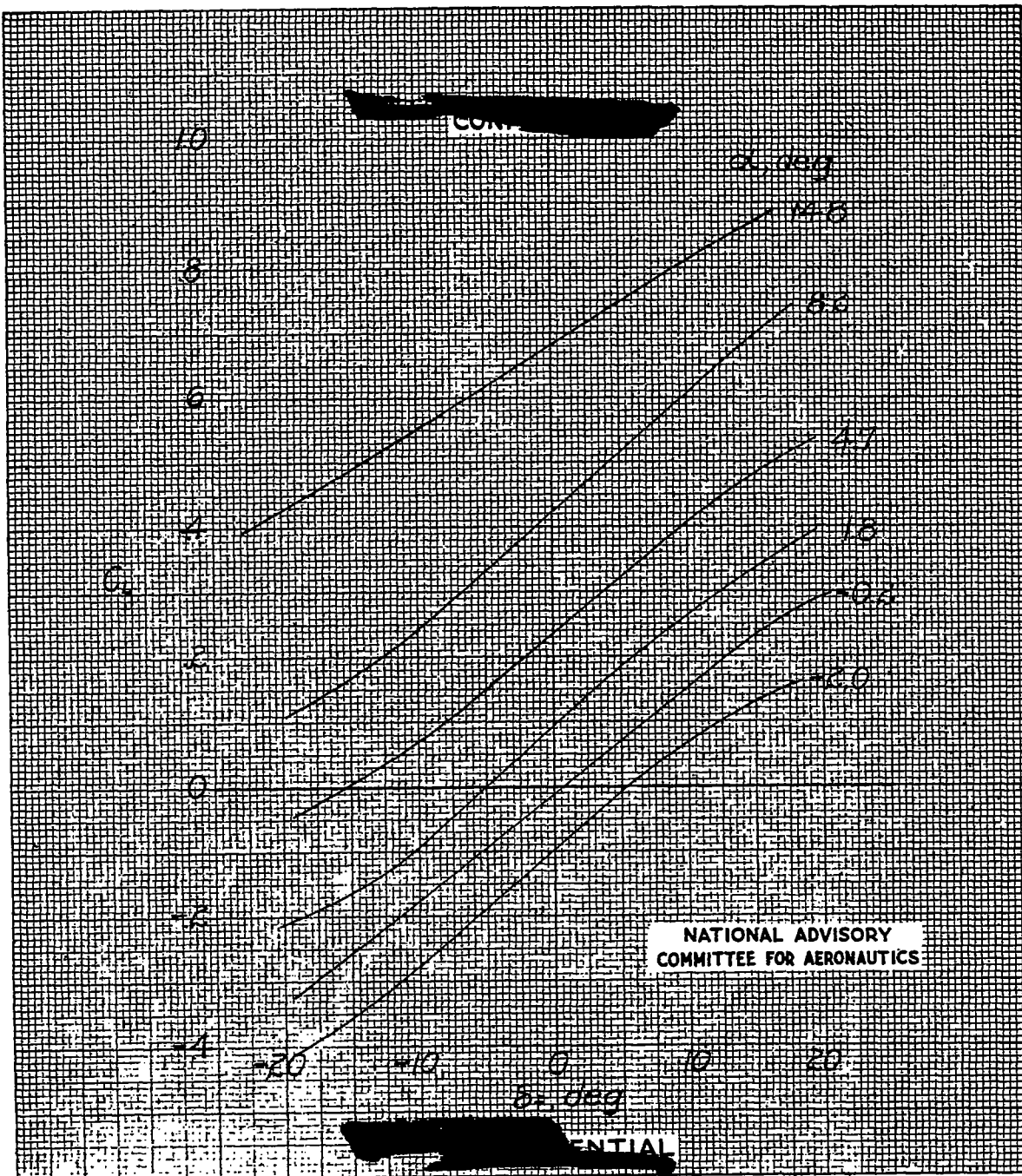
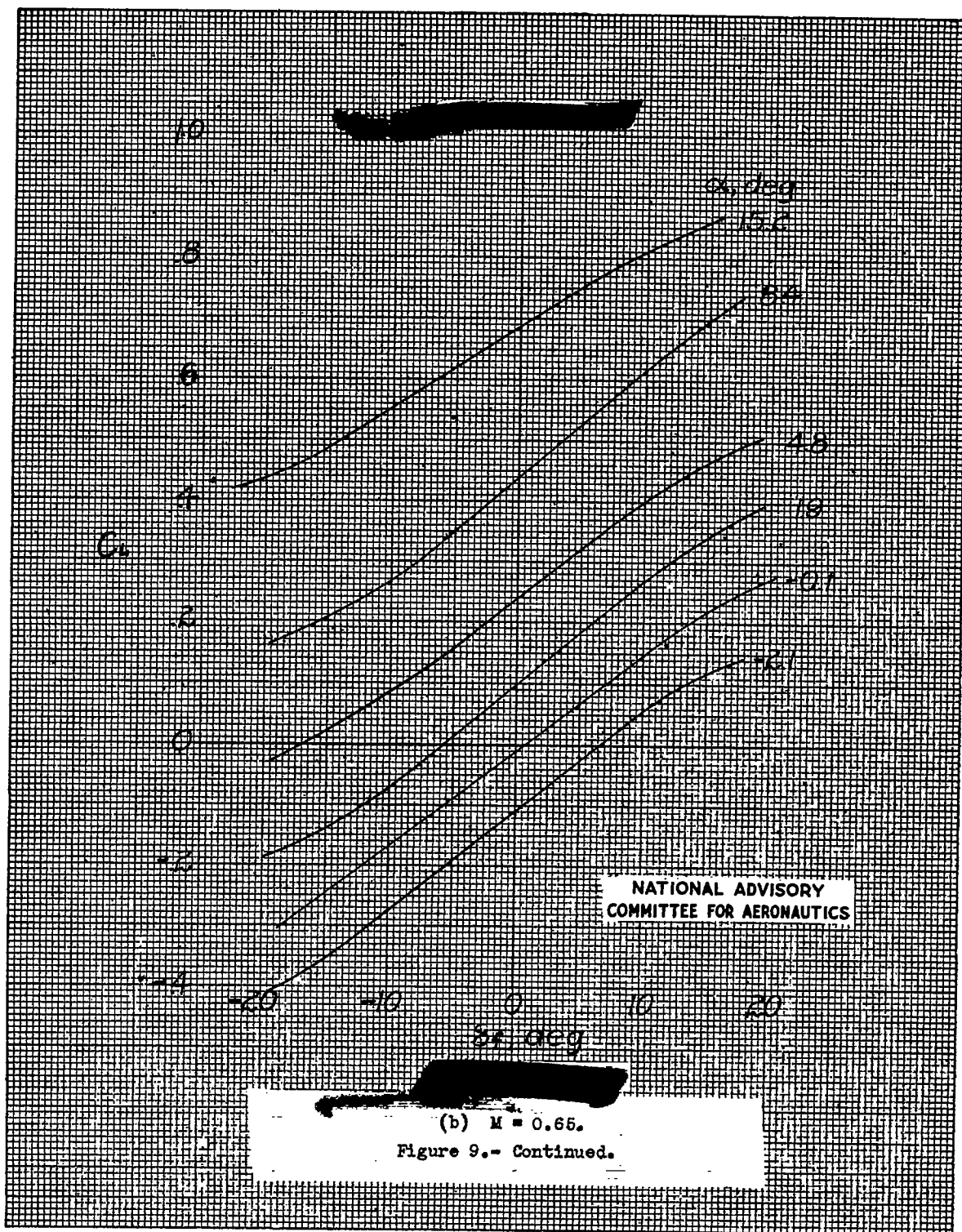
(a) $M = 0.55$.

Figure 9.- Variation of lift coefficient with flap deflection from level flight runs. NACA 65-009 airfoil, $A = 3.04$, $\Delta = 35^\circ$, $c_f/c = 0.25$, gap unsealed.

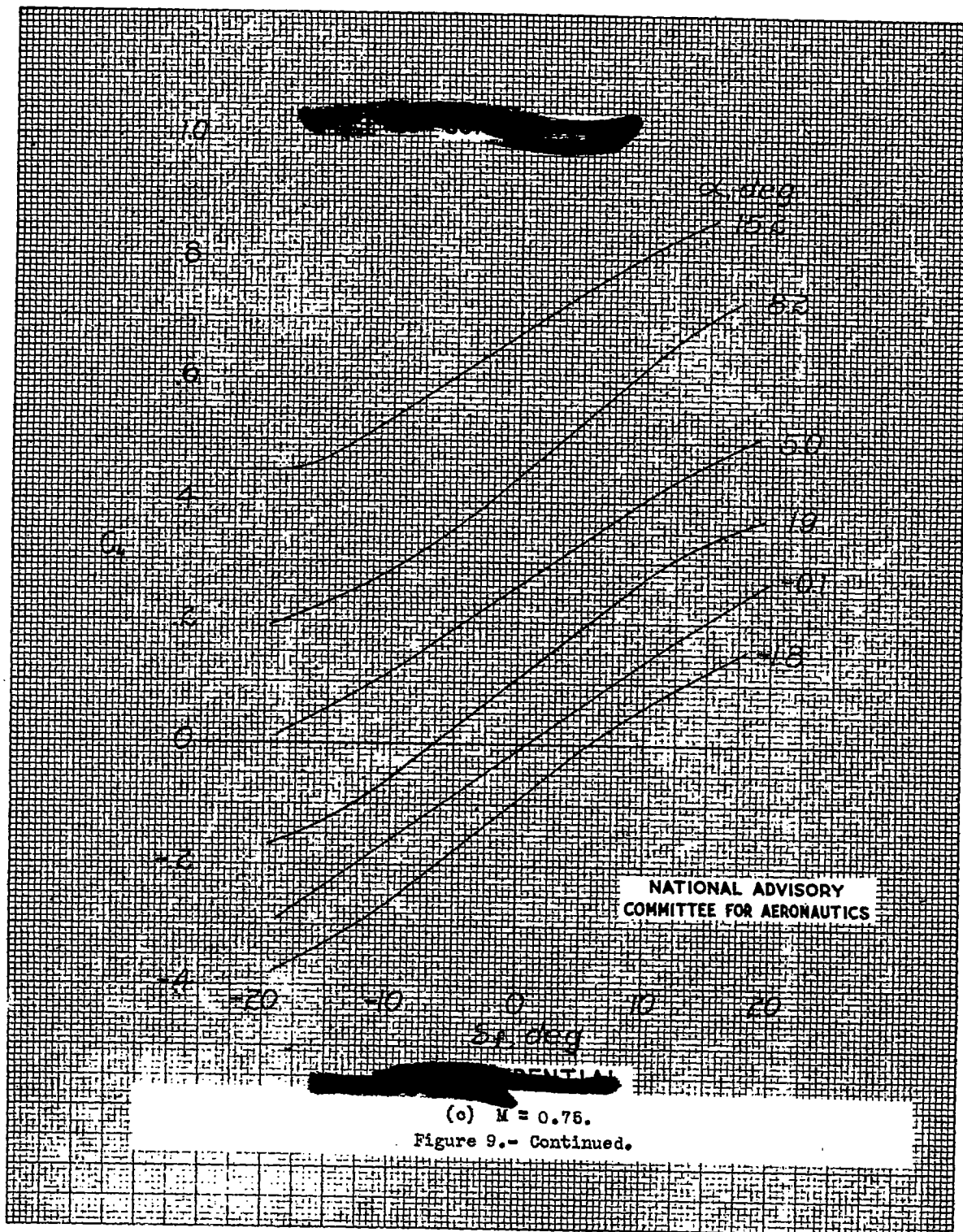
Fig. 9b

NACA RM No. L7F13



NACA RM No. L7F13

Fig. 9c



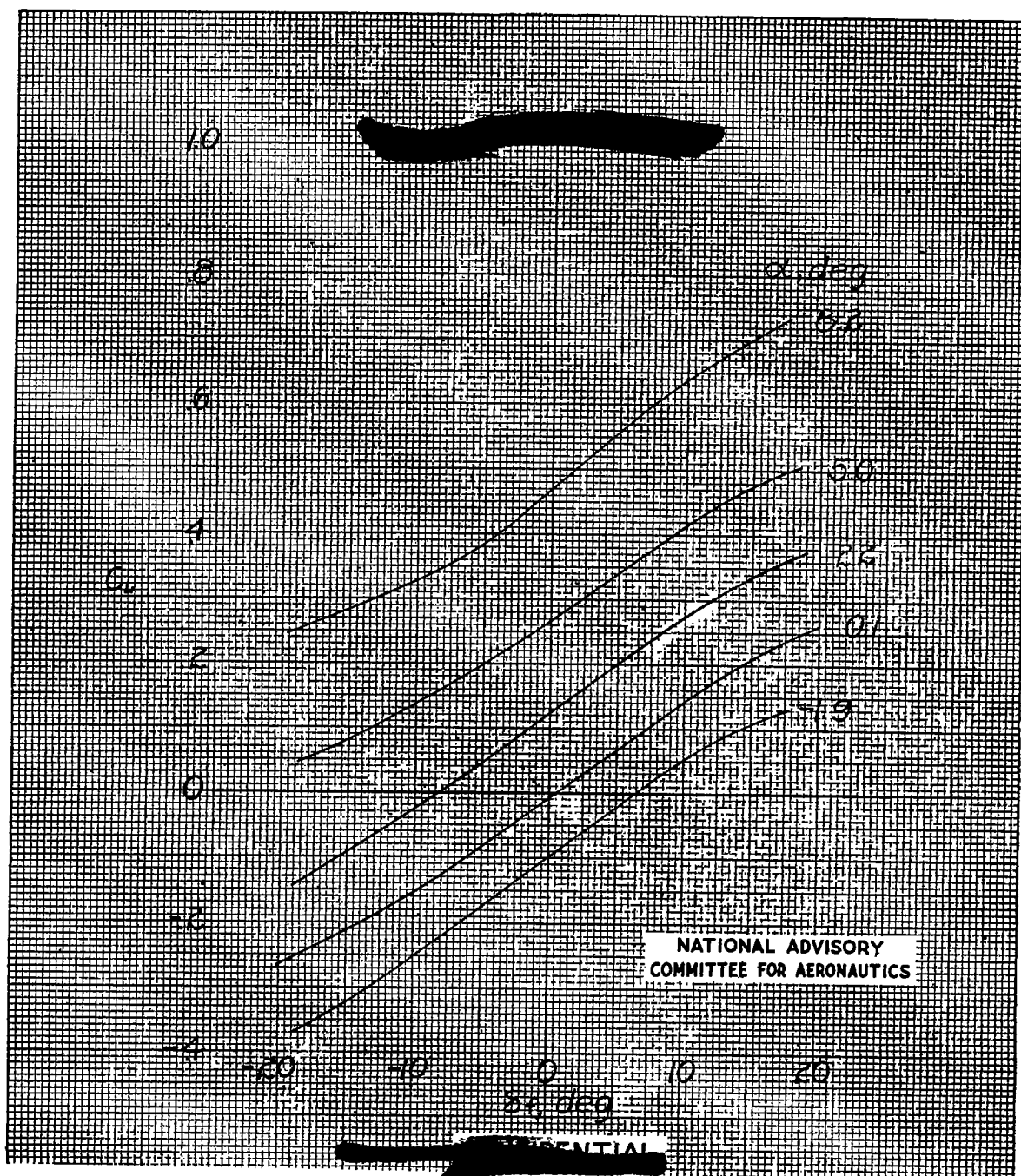
(d) $M = 0.80$.

Figure 9.- Continued.

NACA RM No. L7F13

Fig. 9e

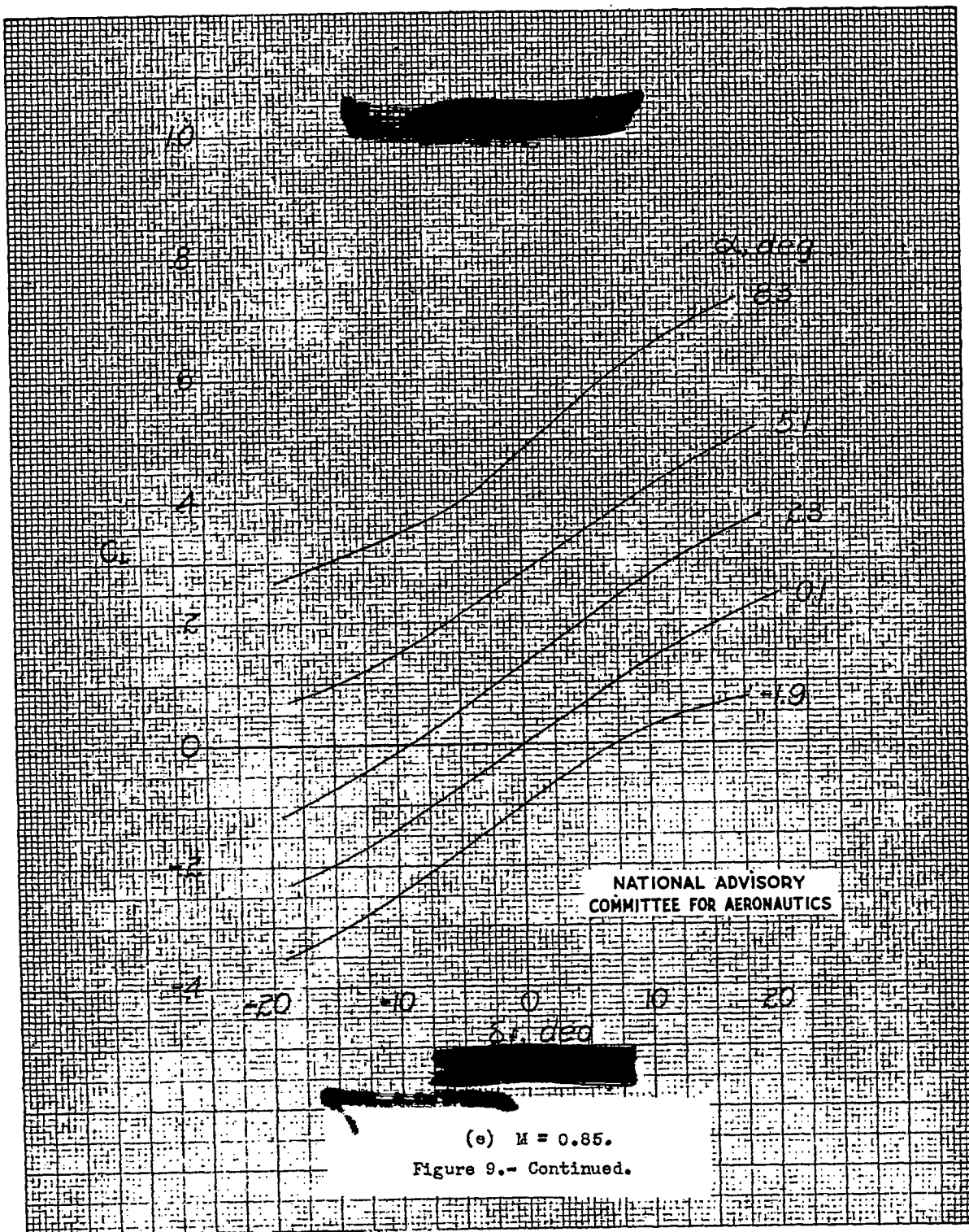
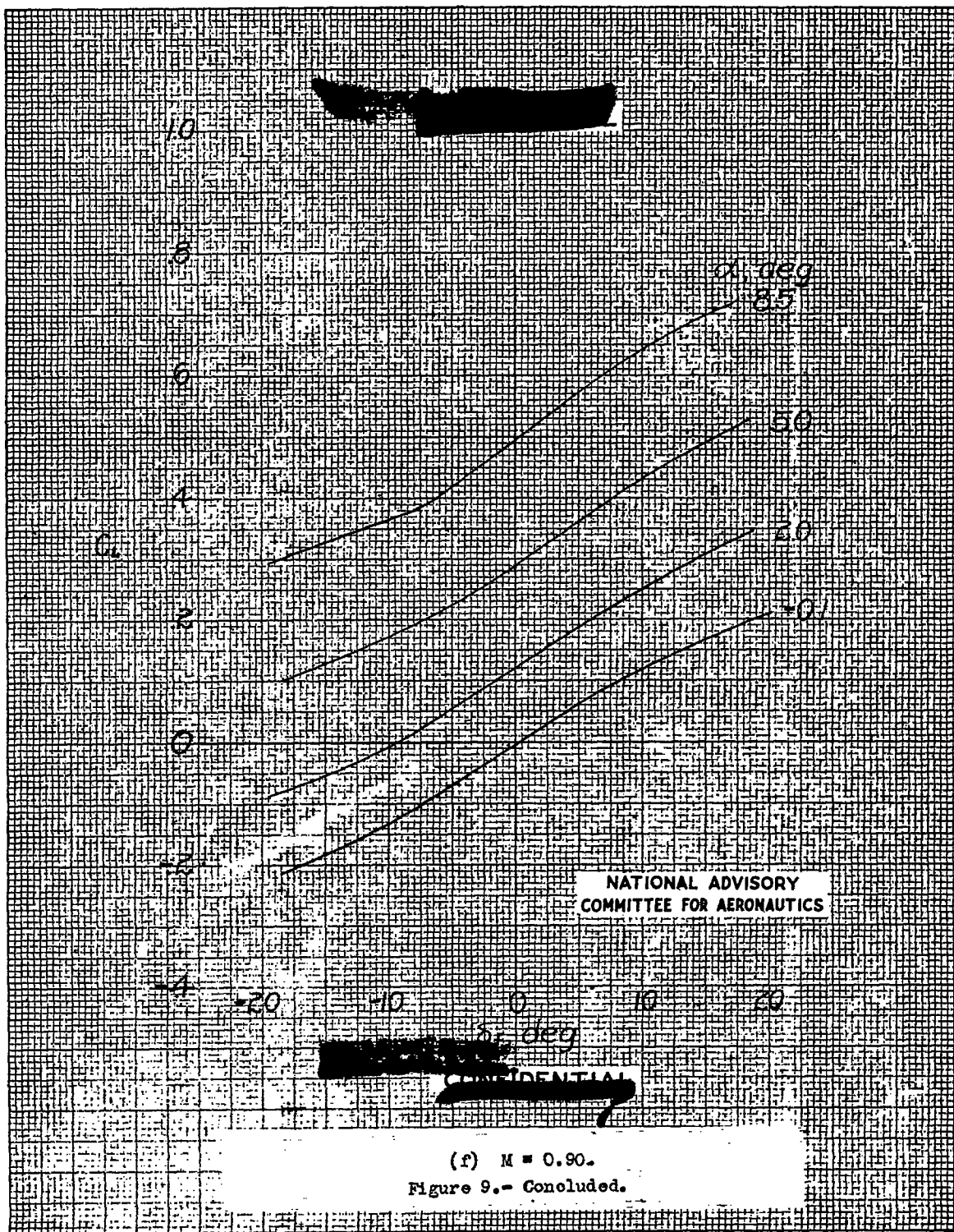


Fig. 9f

NACA RM No. L7F13



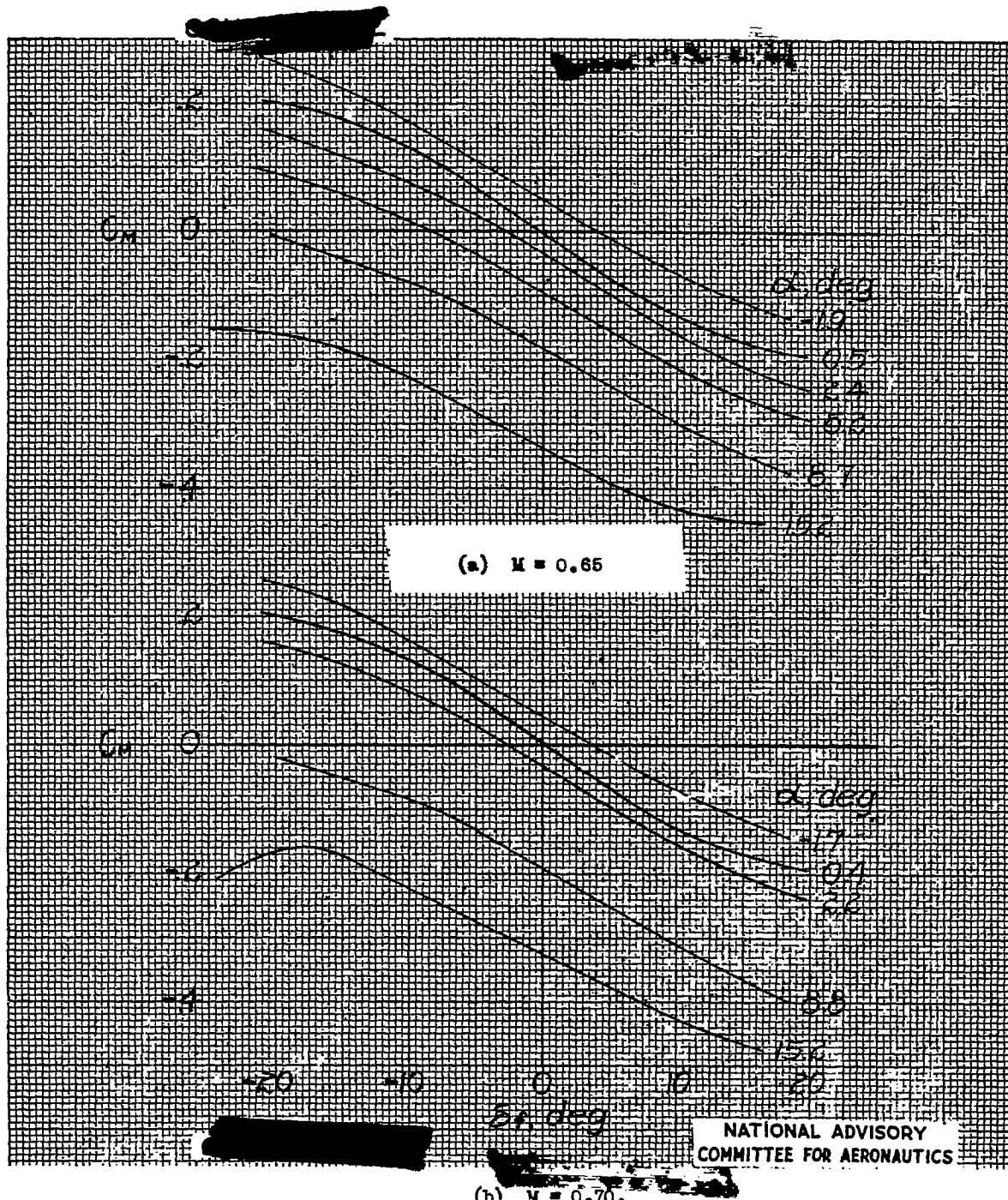
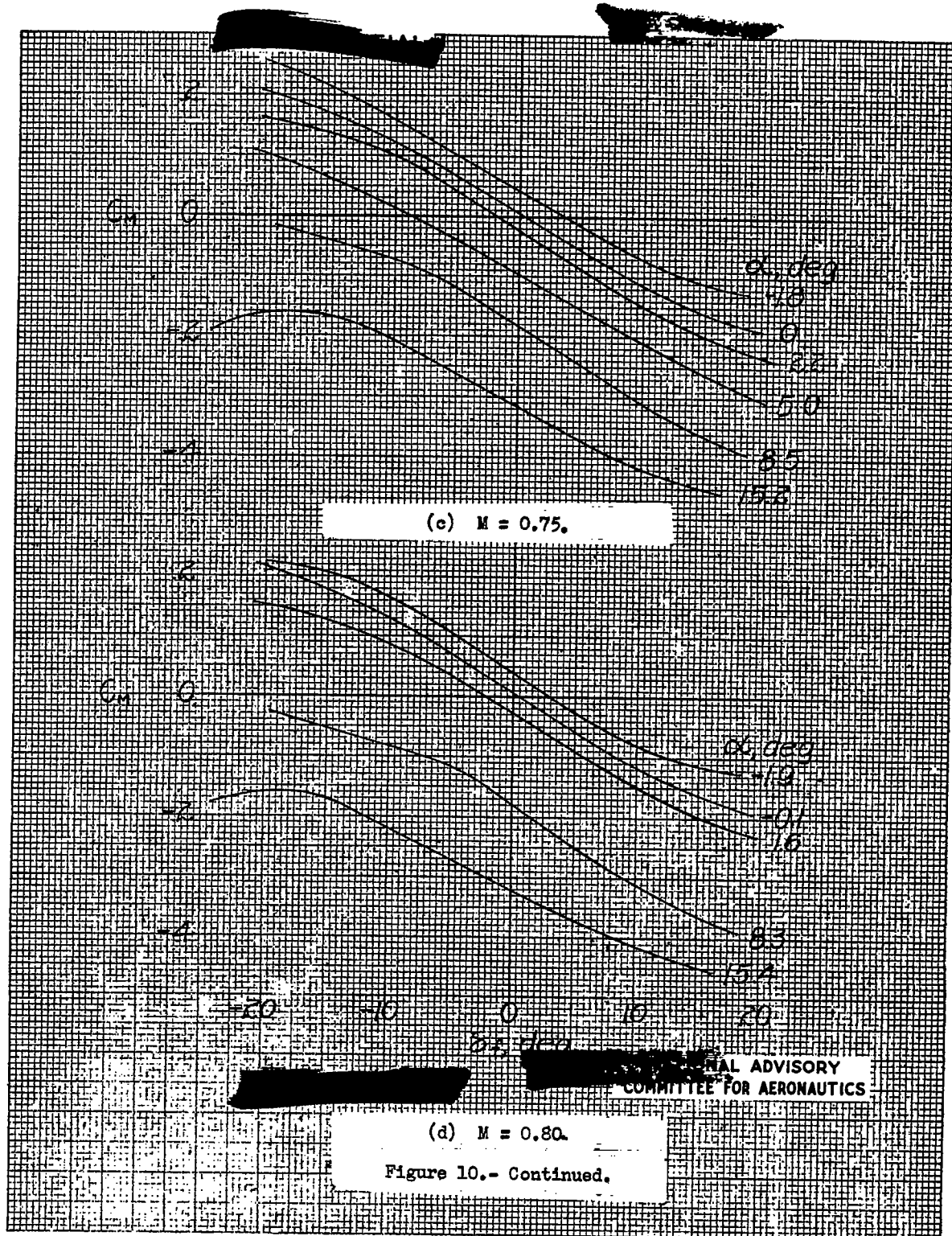


Figure 10.- Variation of pitching moment coefficient with flap deflection from high dive runs. NACA 65-009 airfoil, $A = 3.04$, $\Delta = 35^\circ$, $c_f/c = 0.25$, gap unsealed. Moment coefficient given about axis located 16 percent MAC ahead of leading edge of MAC.

Fig. 10c,d

NACA RM No. L7F13



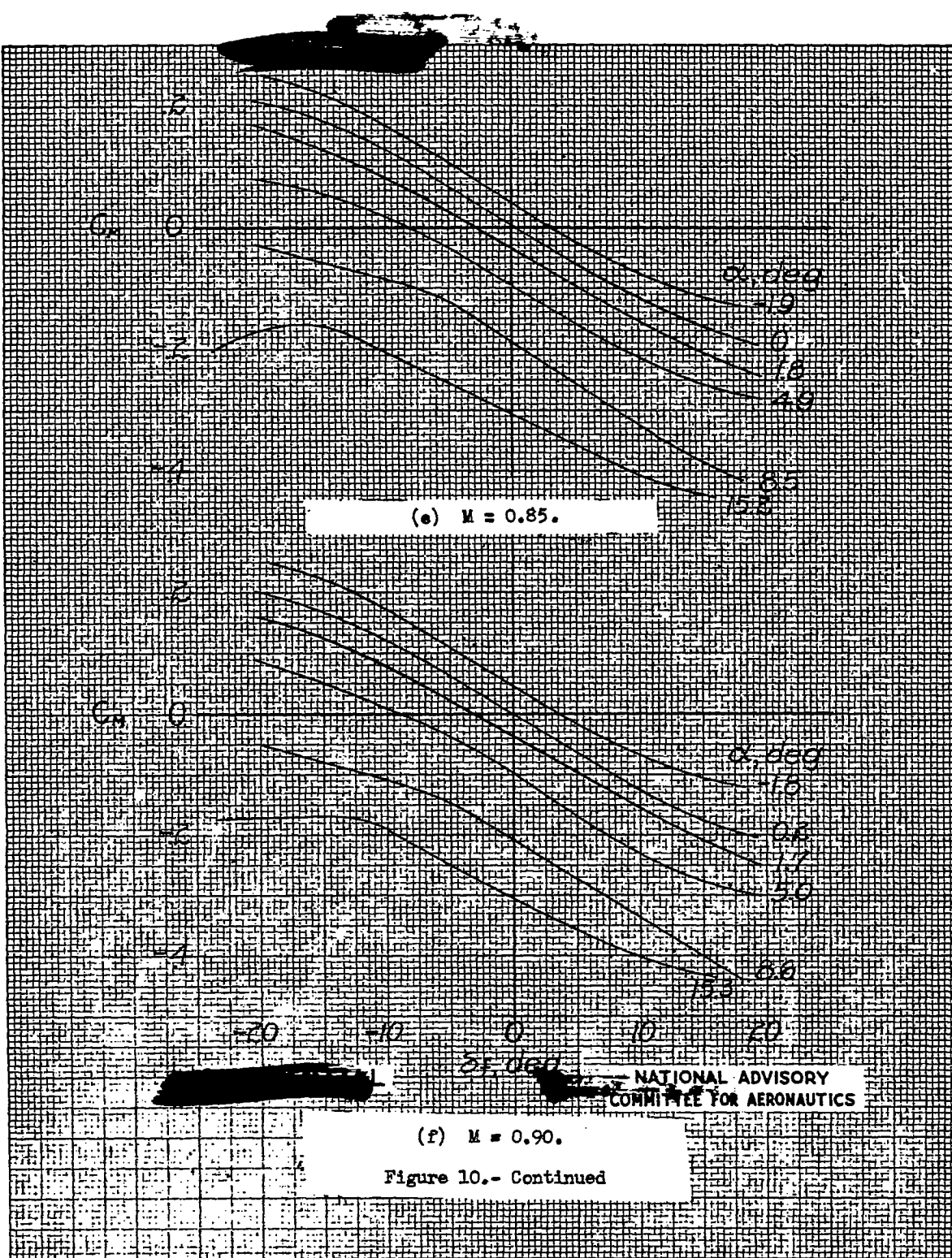
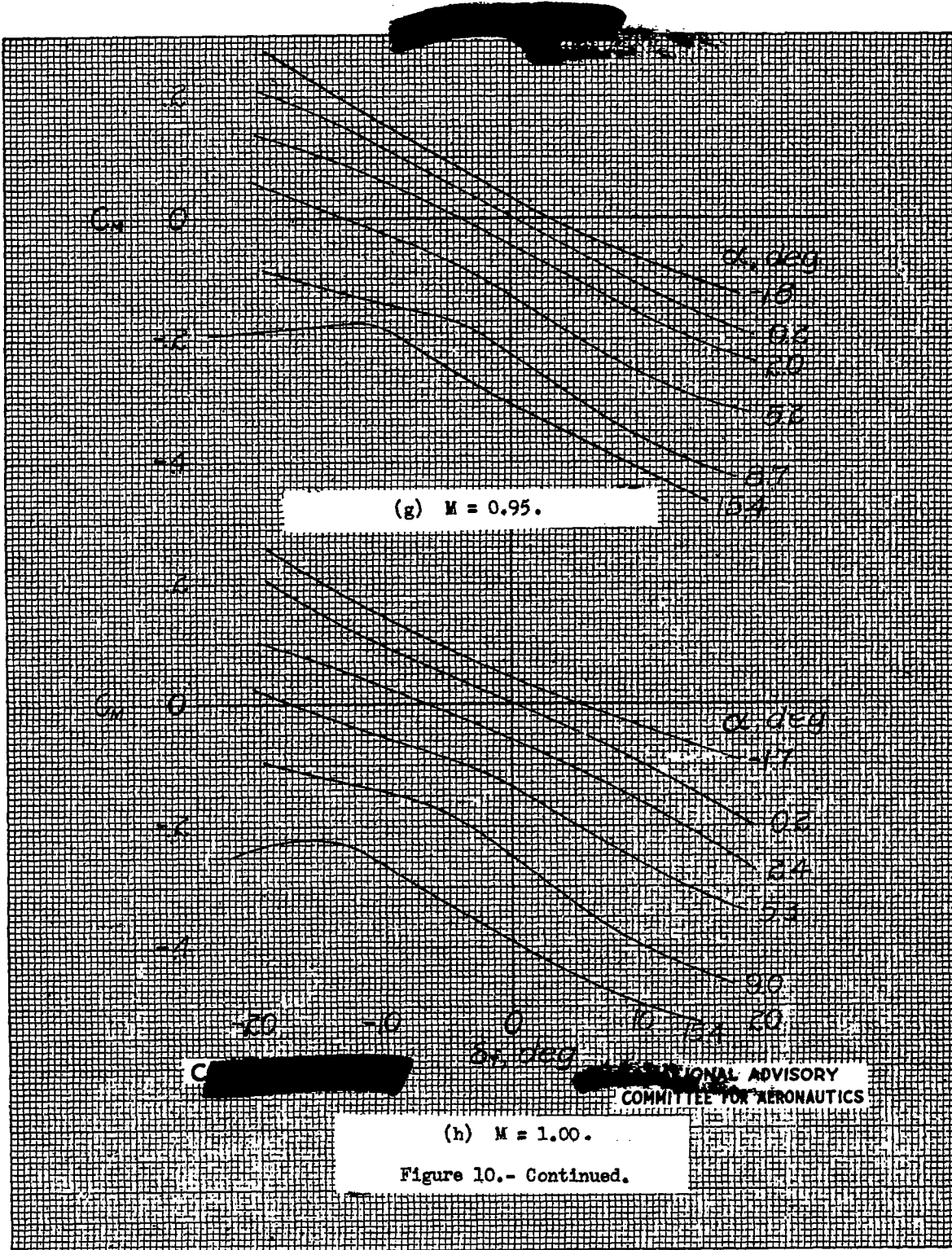


Figure 10.- Continued

Fig. 10g,h

NACA RM No. L7F13



NACA RM No. L7F13

Fig. 10i,j

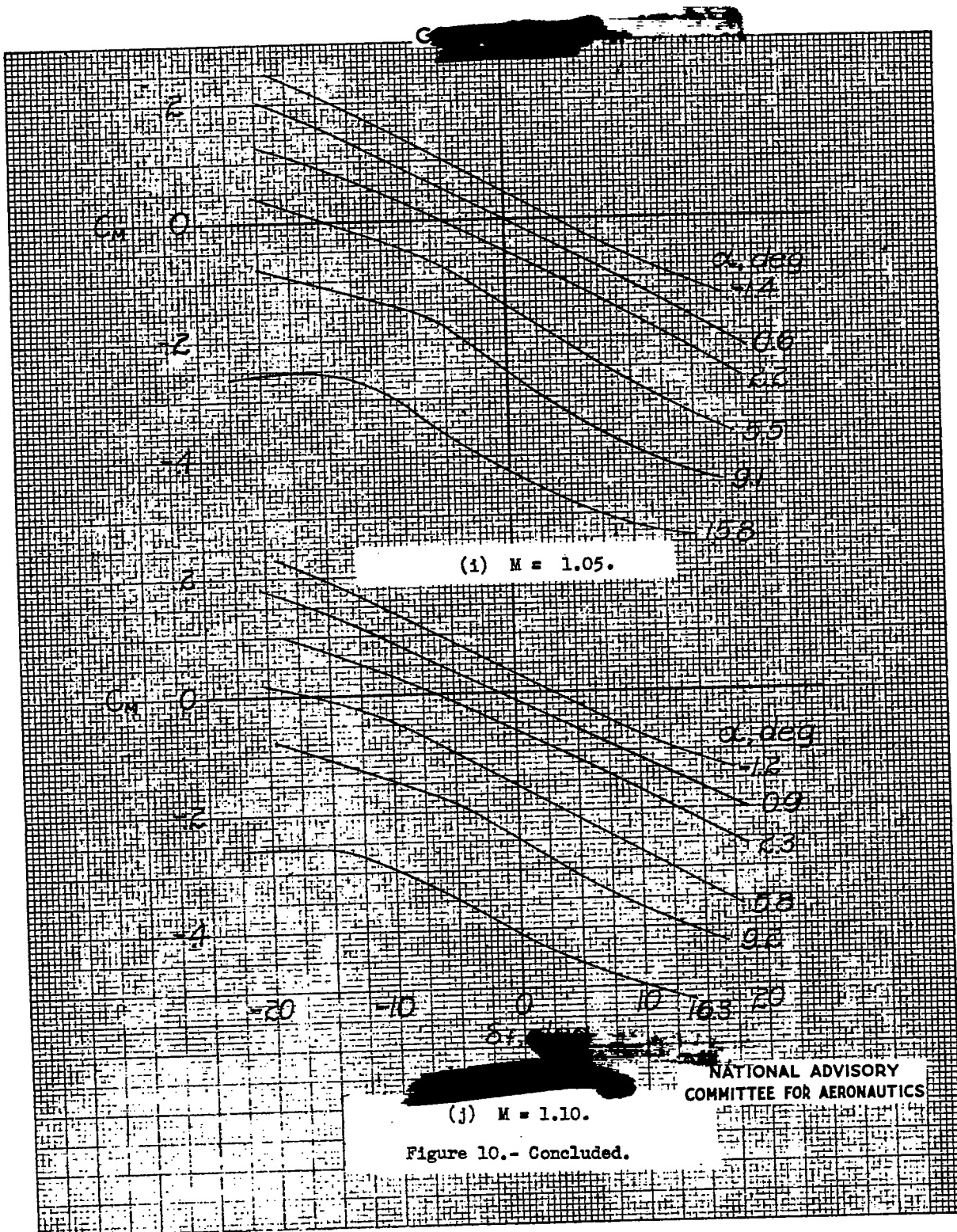


Fig. 11a,b

NACA RM No. L7F13

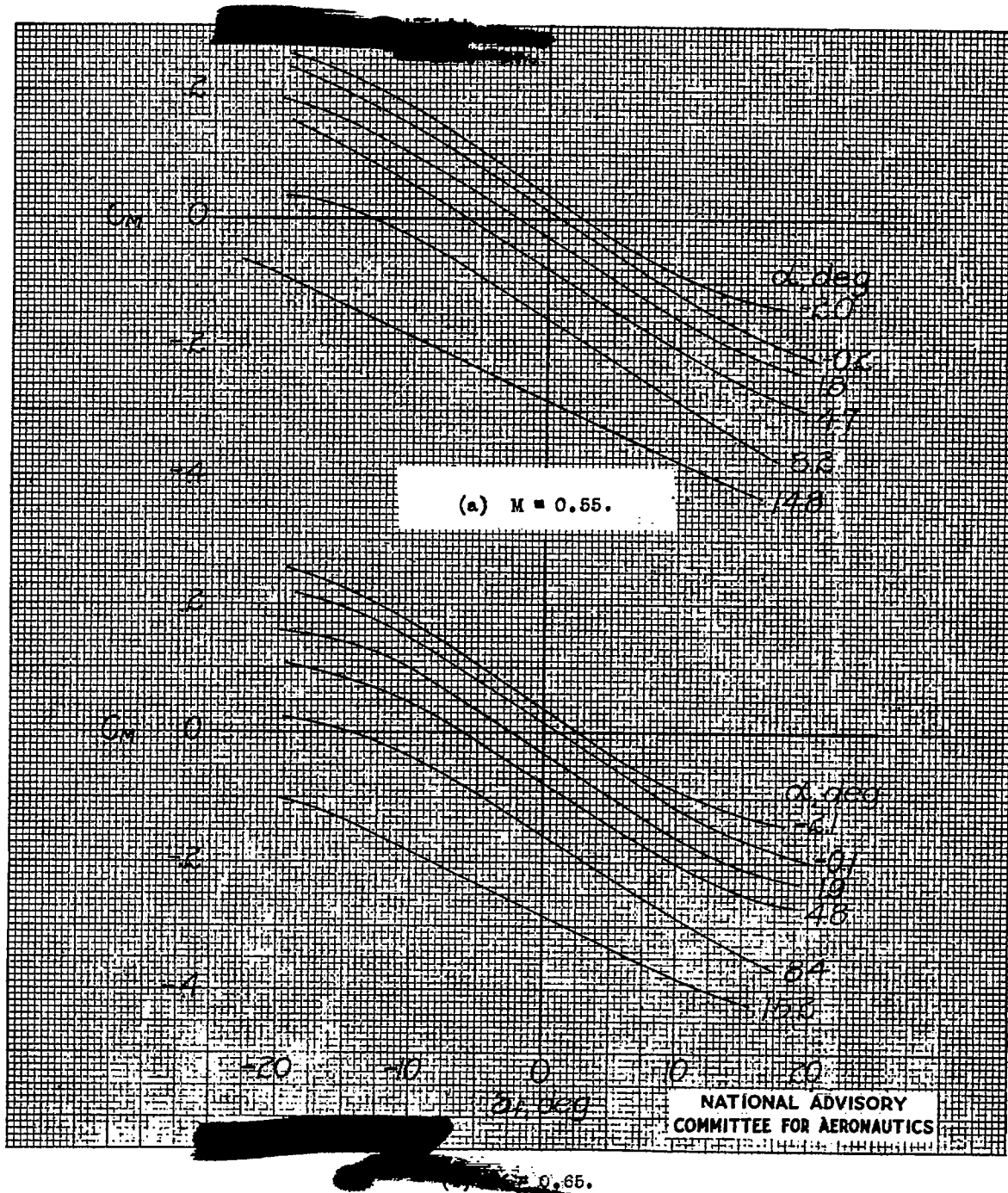


Figure 11.- Variation of pitching moment coefficient with flap deflection from level flight runs. NACA 65-009 airfoil, $A = 3.04$, $\Delta = 35^\circ$, $c_f/c = 0.25$, gap unsealed. Moment coefficient given about axis located 16 percent MAC ahead of leading edge of MAC.

NACA RM No. L7F13

Fig. 11c,d

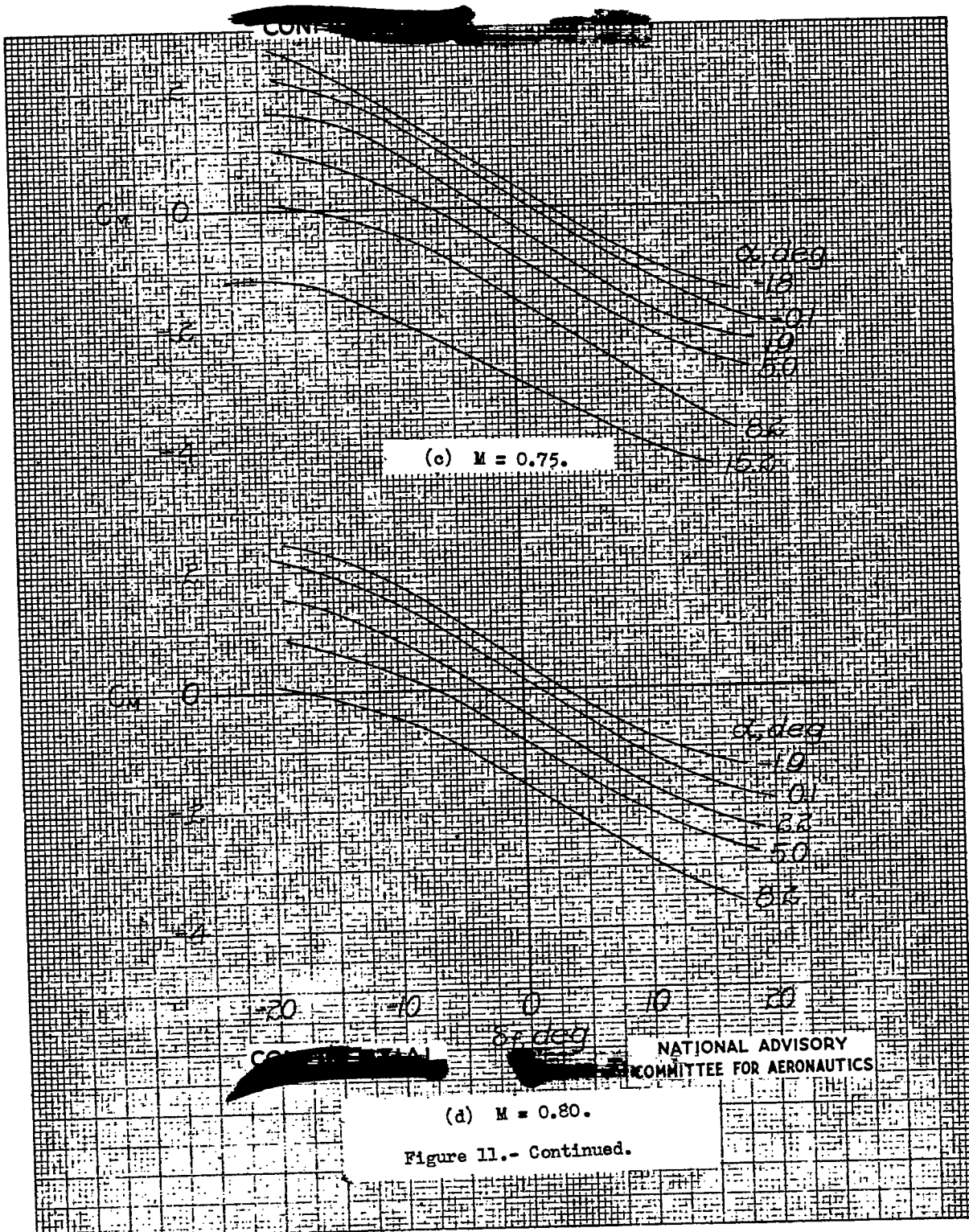
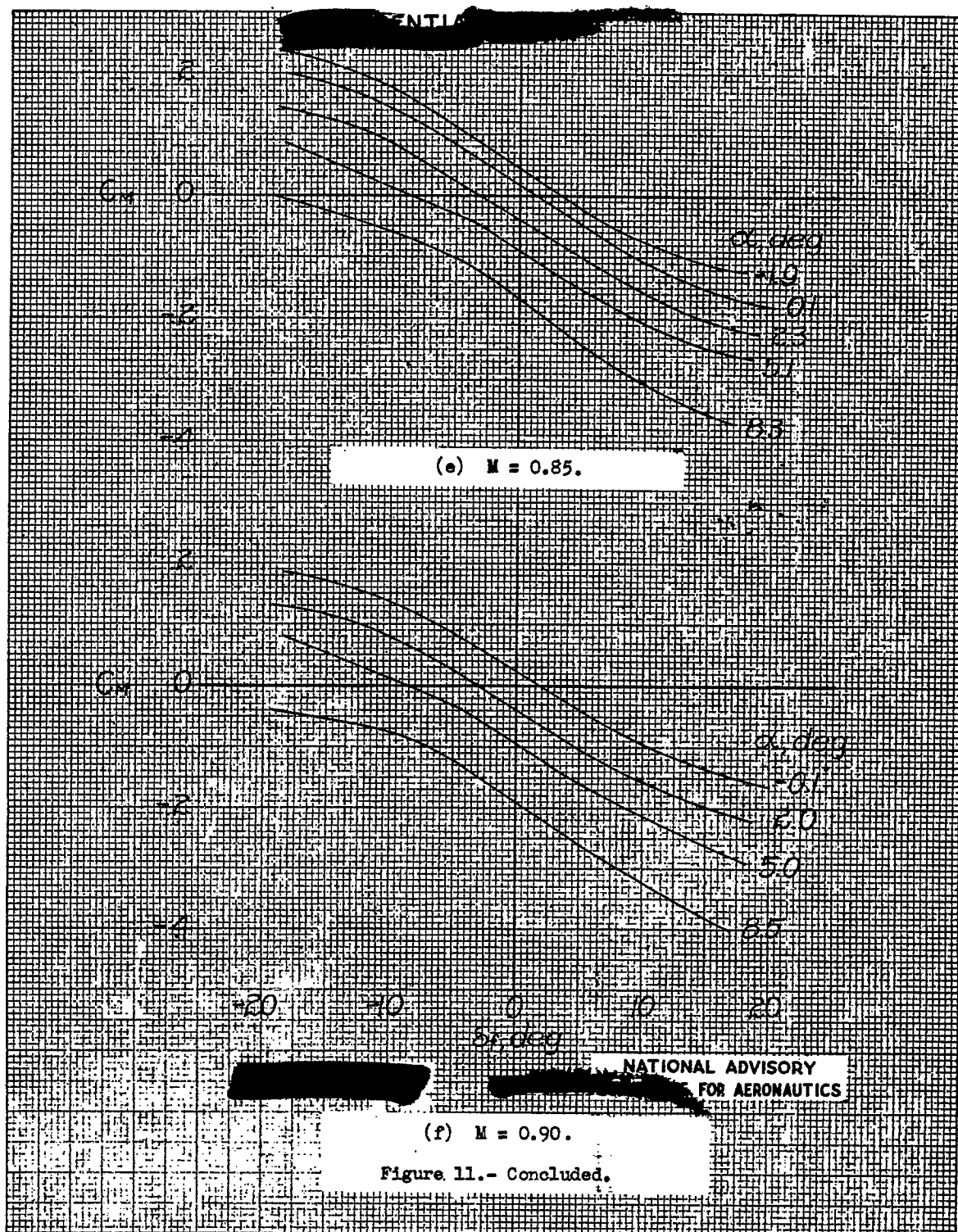


Figure 11.- Continued.



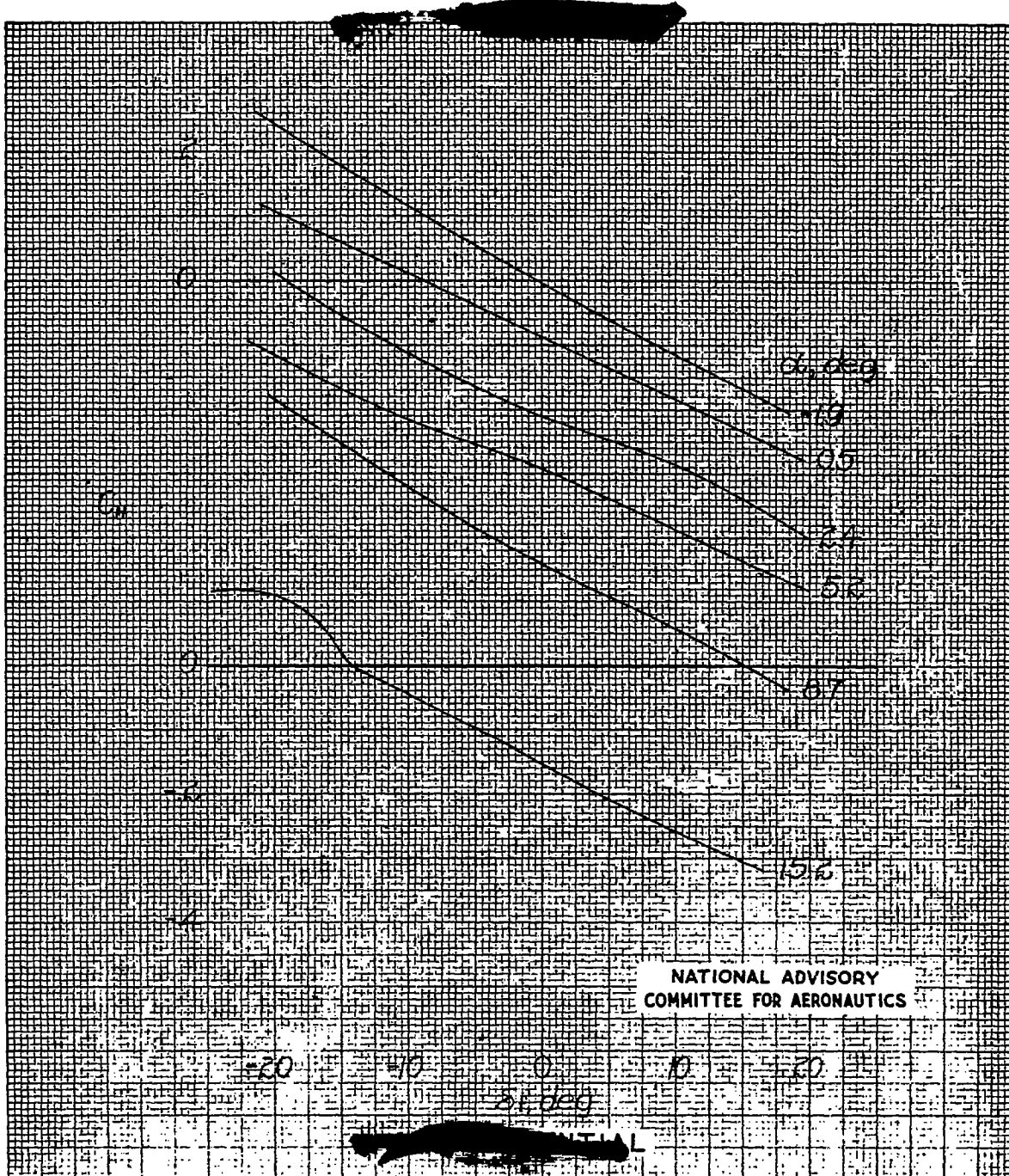
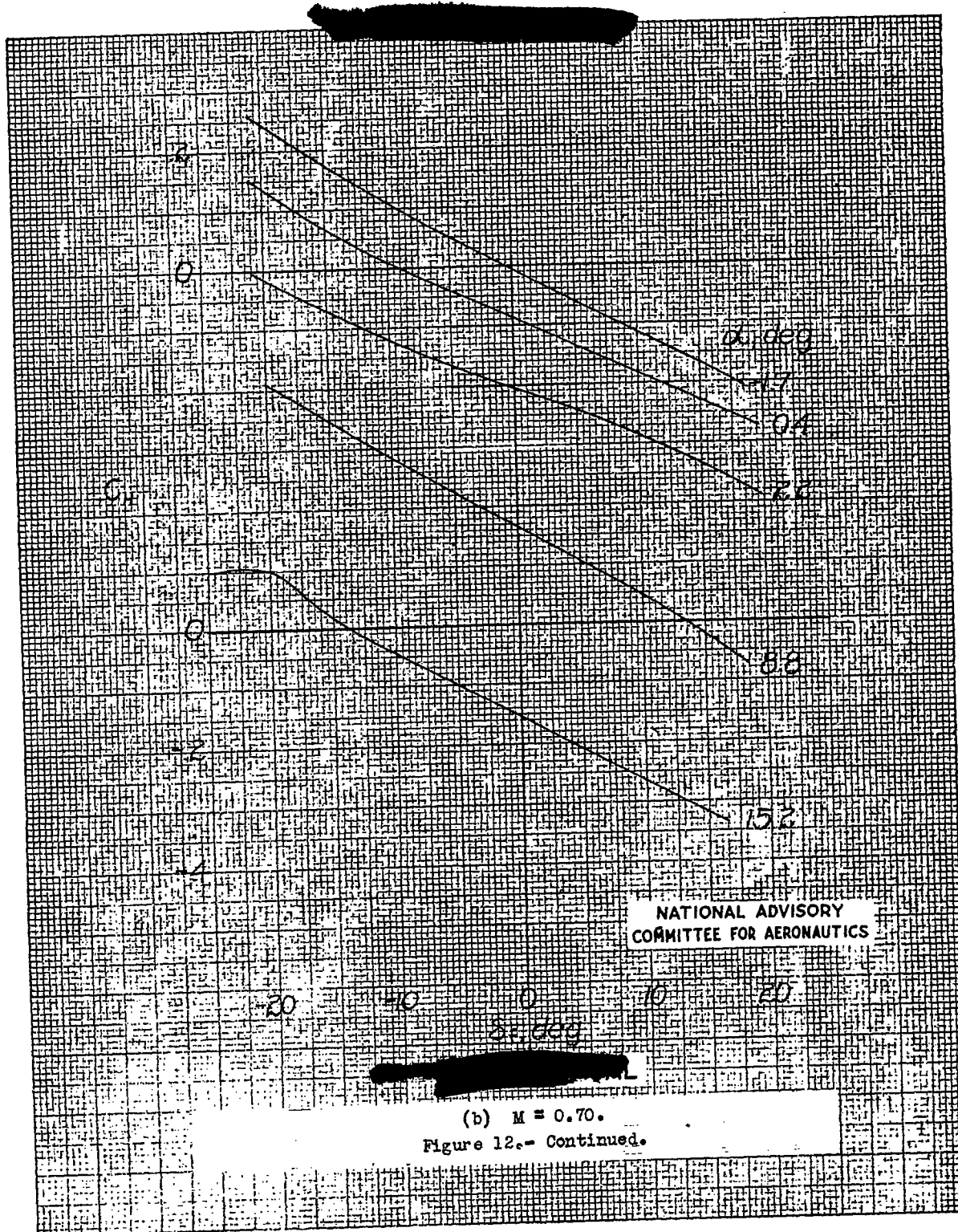
(a) $M = 0.65$

Figure 12.- Variation of hinge moment coefficient with flap deflection from high dive runs. NACA 65-009 airfoil, $A = 3.04$, $\Lambda = 35^\circ$, $c_f/c = 0.25$, gap unsealed. Note shift in zero ordinate for different angles of attack.

Fig. 12b

NACA RM No. L7F13



NACA RM No. L7F13

Fig. 12c

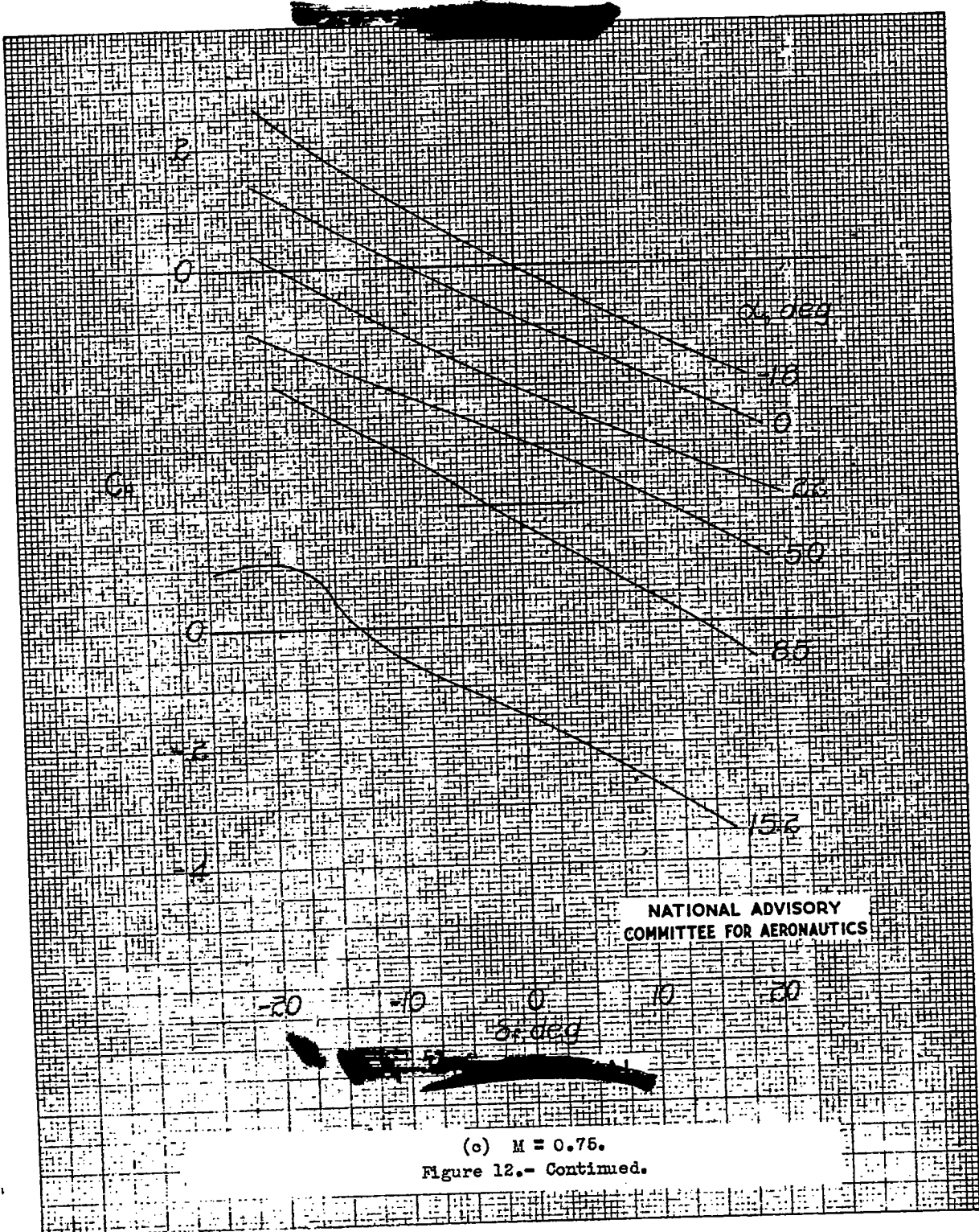
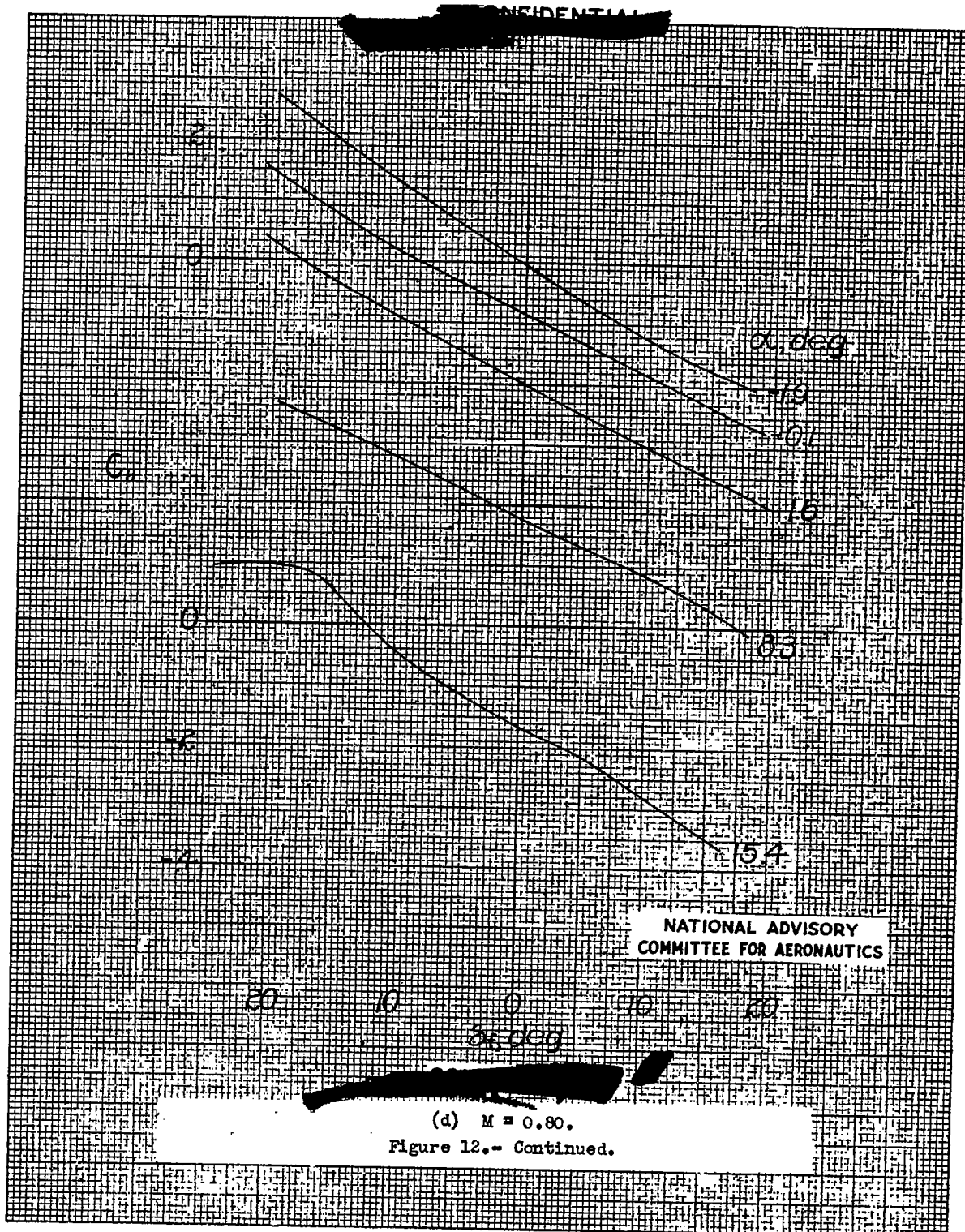


Fig. 12d

NACA RM No. L7F13



NACA RM No. L7F13

Fig. 12e

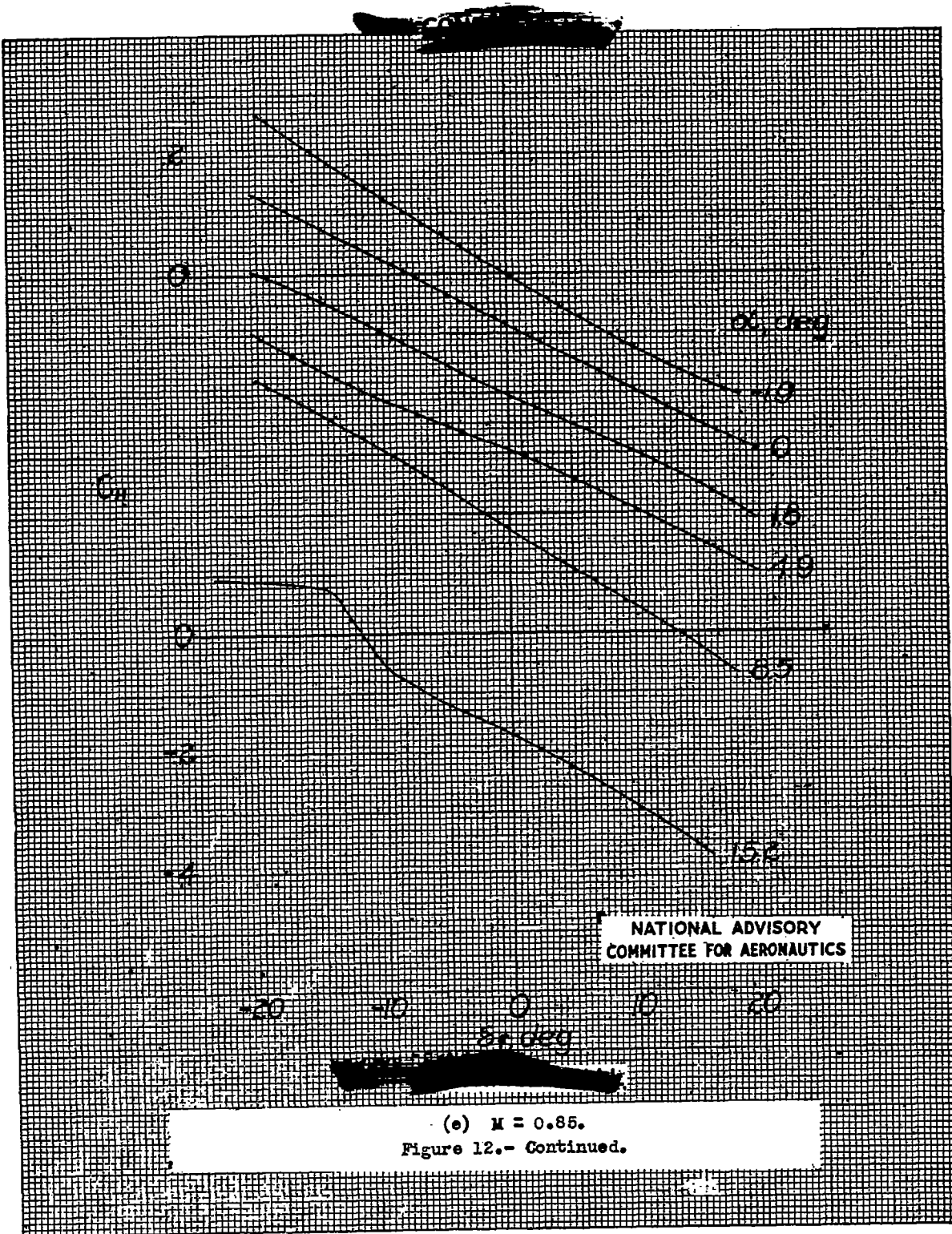
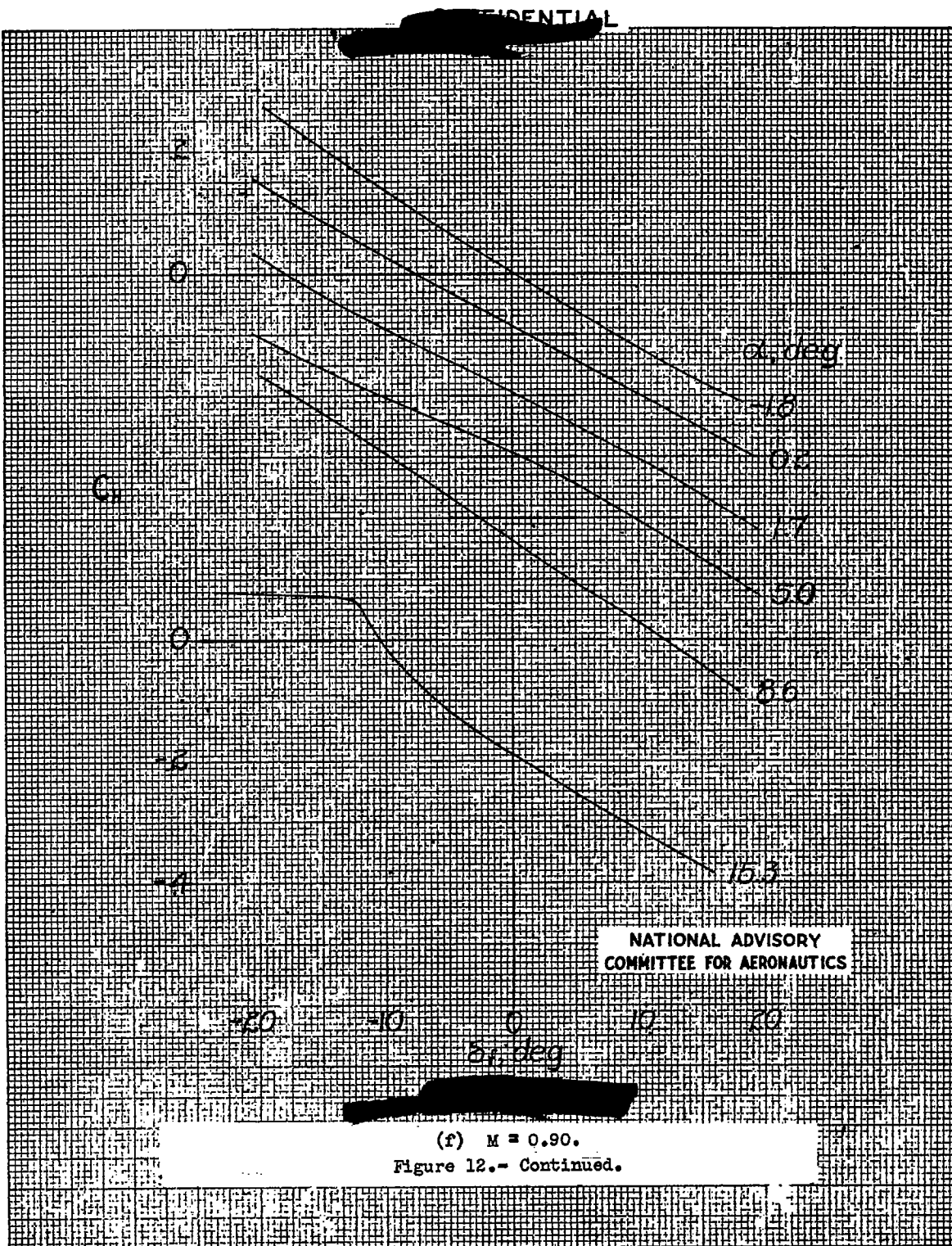


Fig. 12f

NACA RM No. L7F13



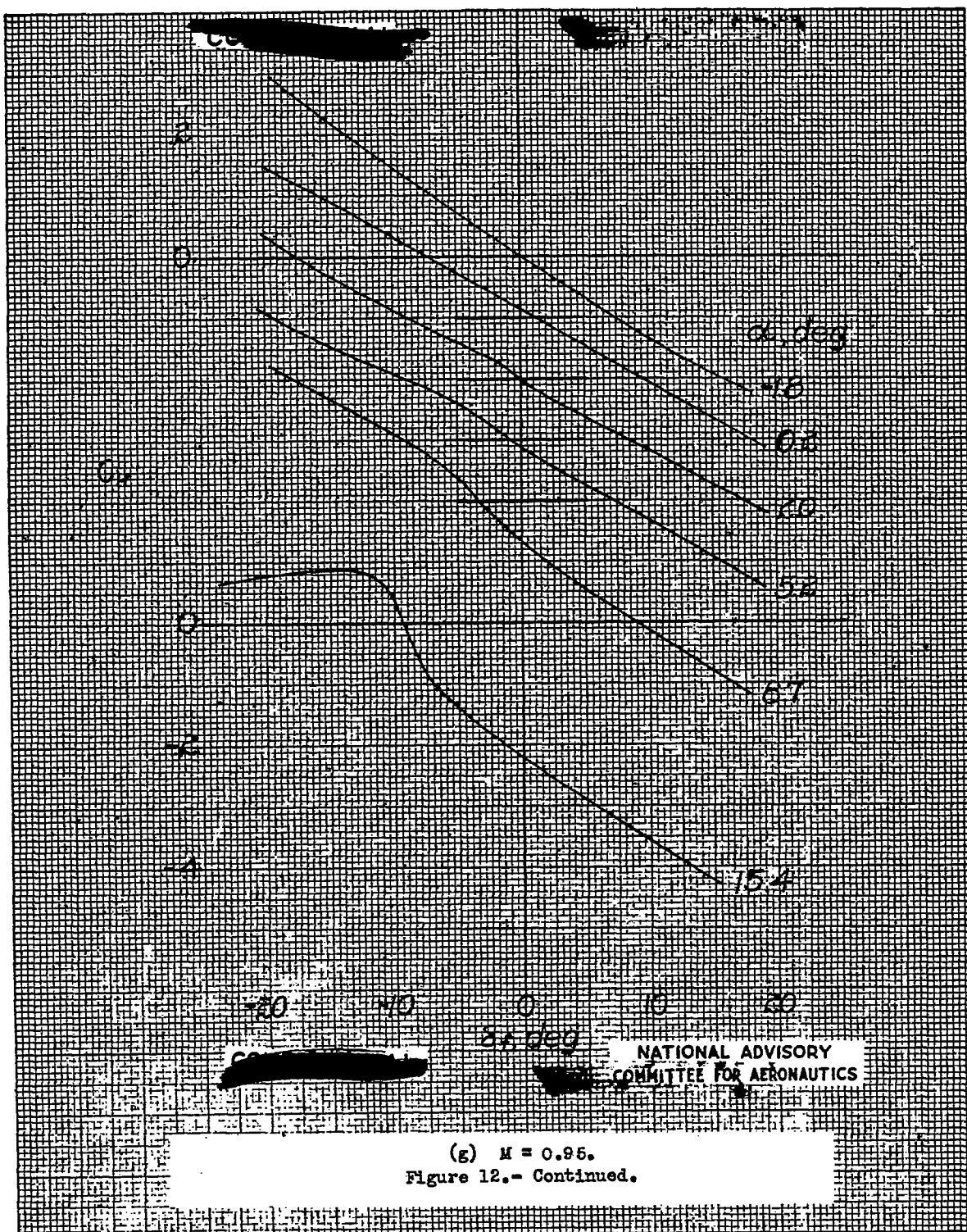
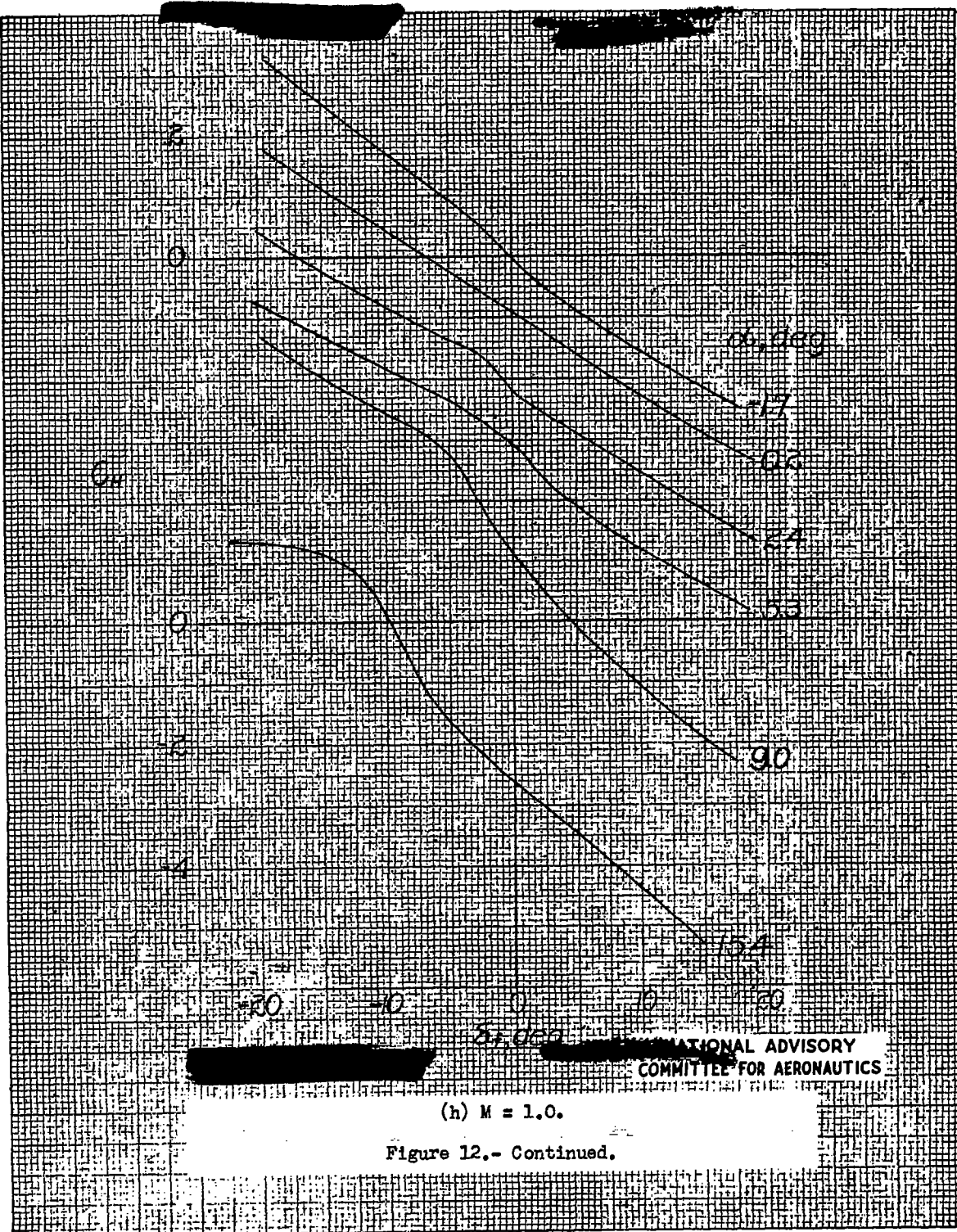


Fig. 12h

NACA RM No. L7F13



NACA RM No. L7F13

Fig. 12i

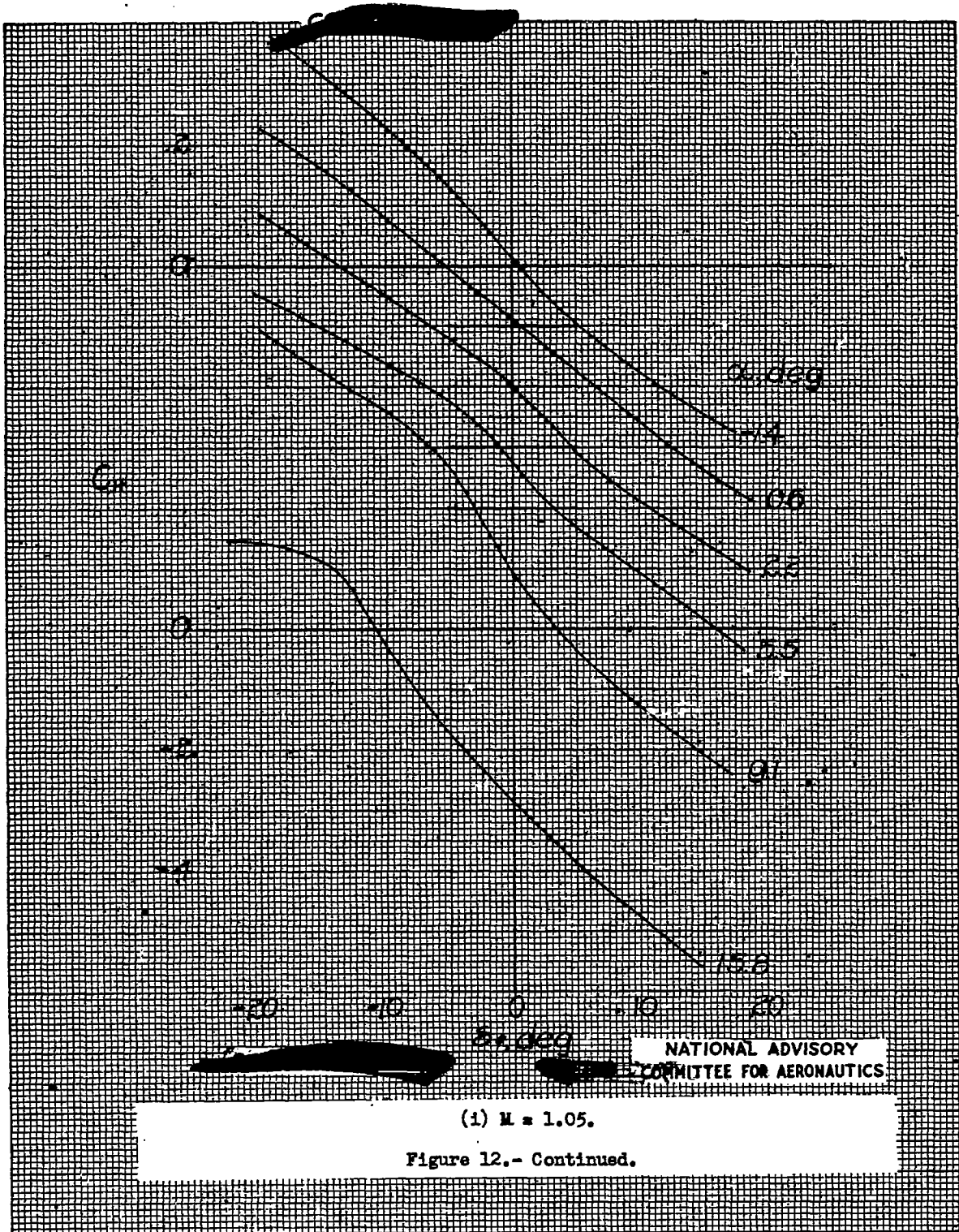
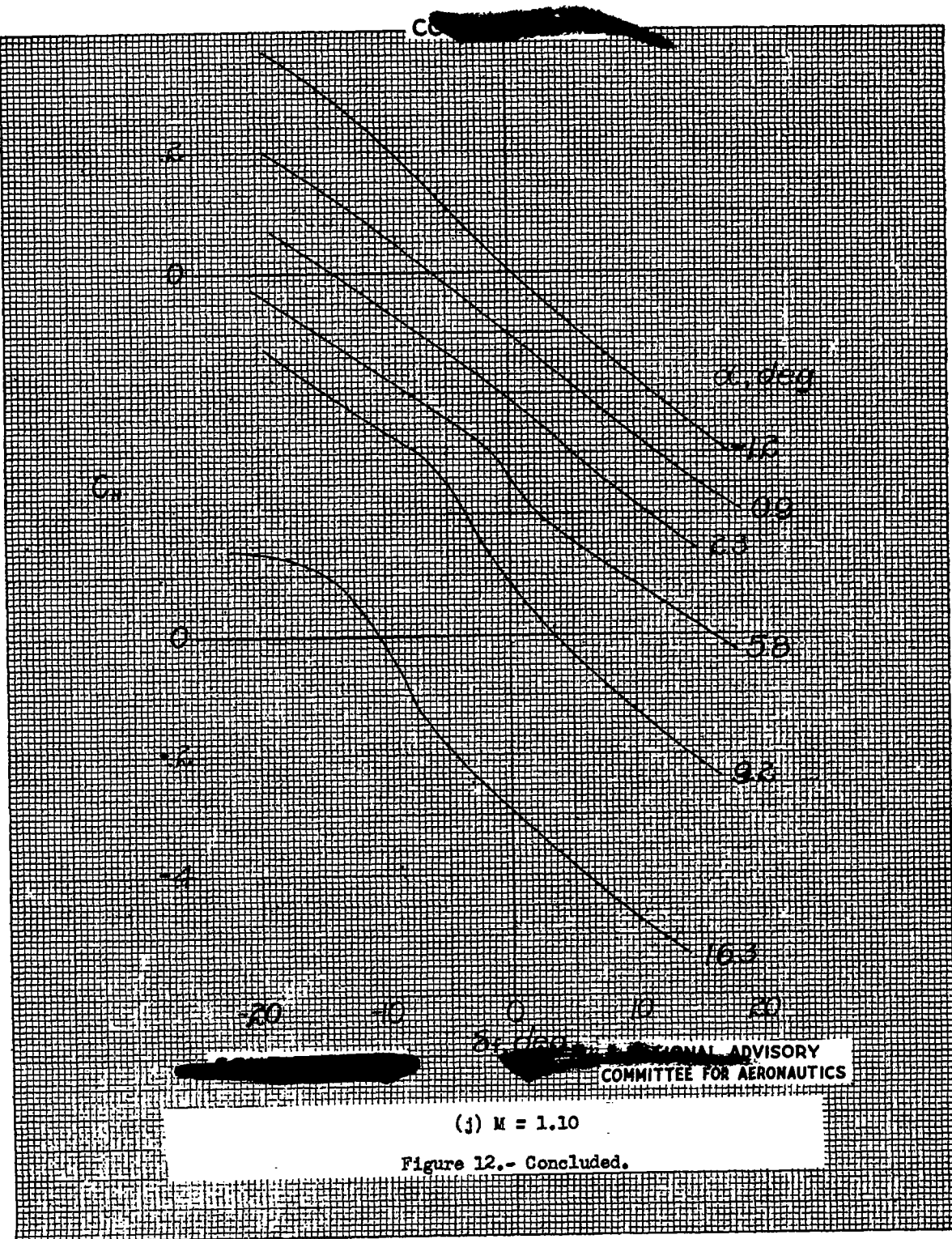


Fig. 12j

NACA RM No. L7F13



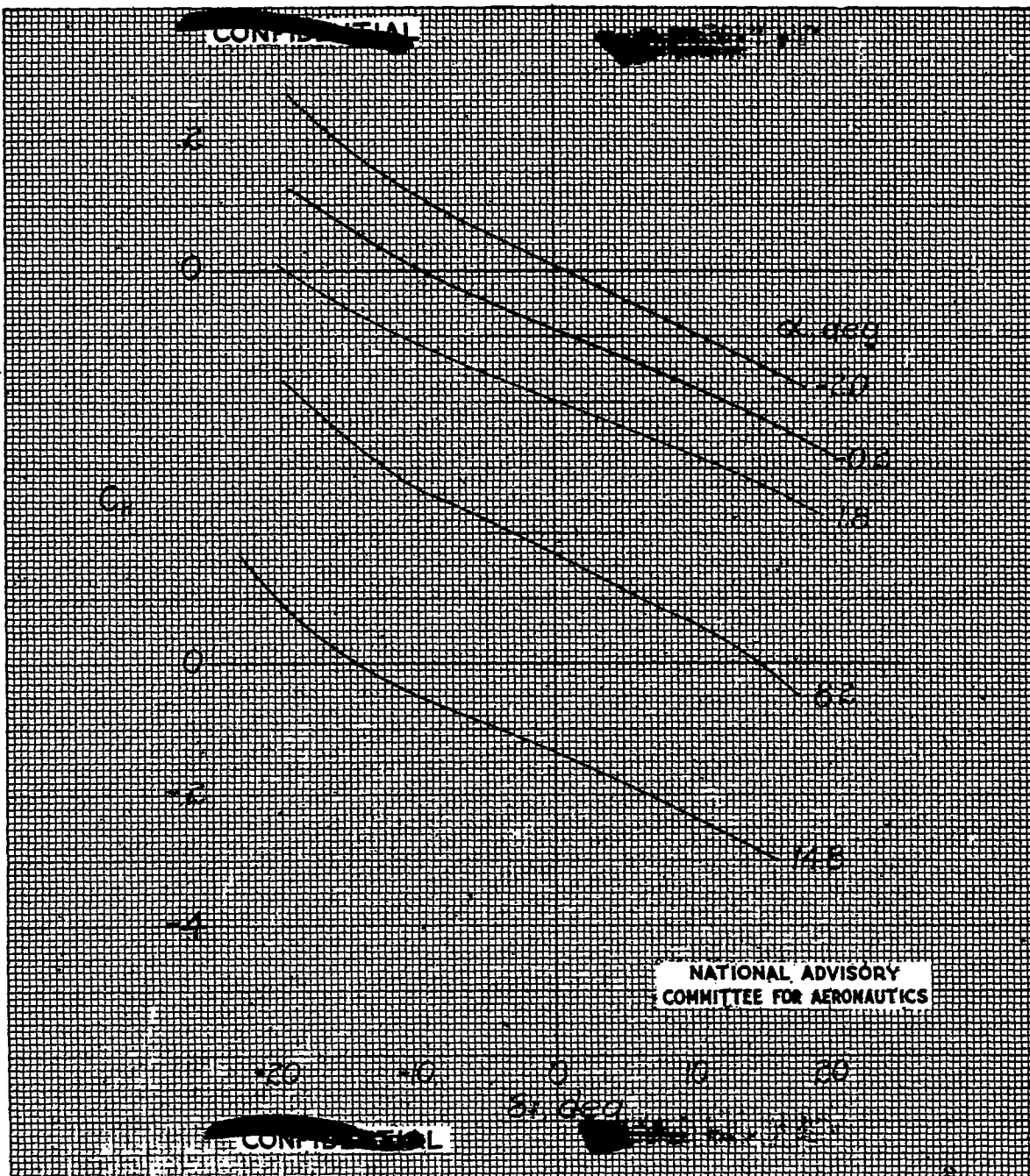
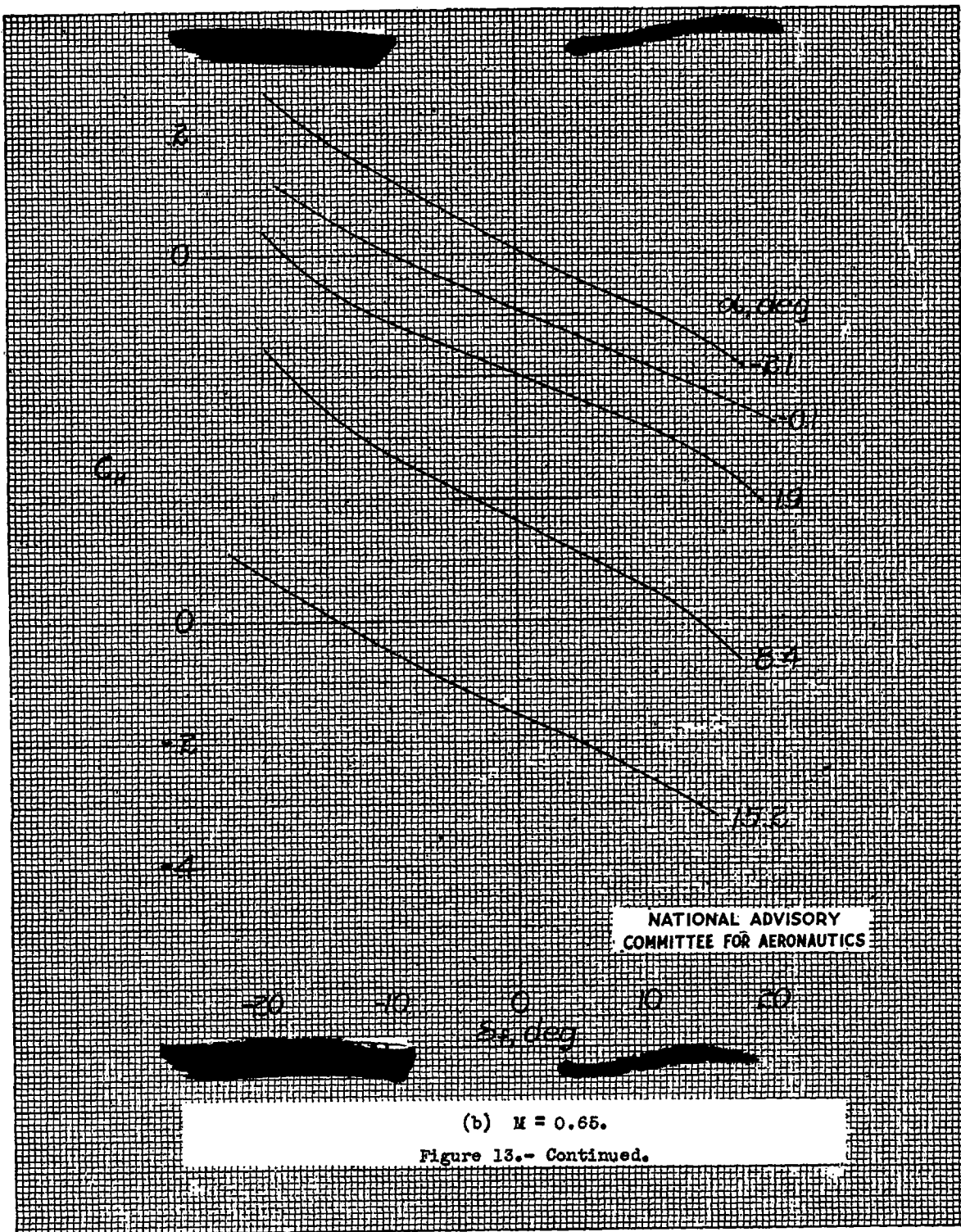
(a) $M = 0.55$.

Figure 13.- Variation of hinge moment coefficient with flap deflection from level flight runs. NACA 65-009 airfoil, $A = 3.04$, $\Delta = 35^\circ$, $c_f/c = 0.25$, gap unsealed. Note shift in zero ordinate for different angles of attack.

Fig. 13b

NACA RM No. L7F13



NACA RM No. L7F13

Fig. 18c

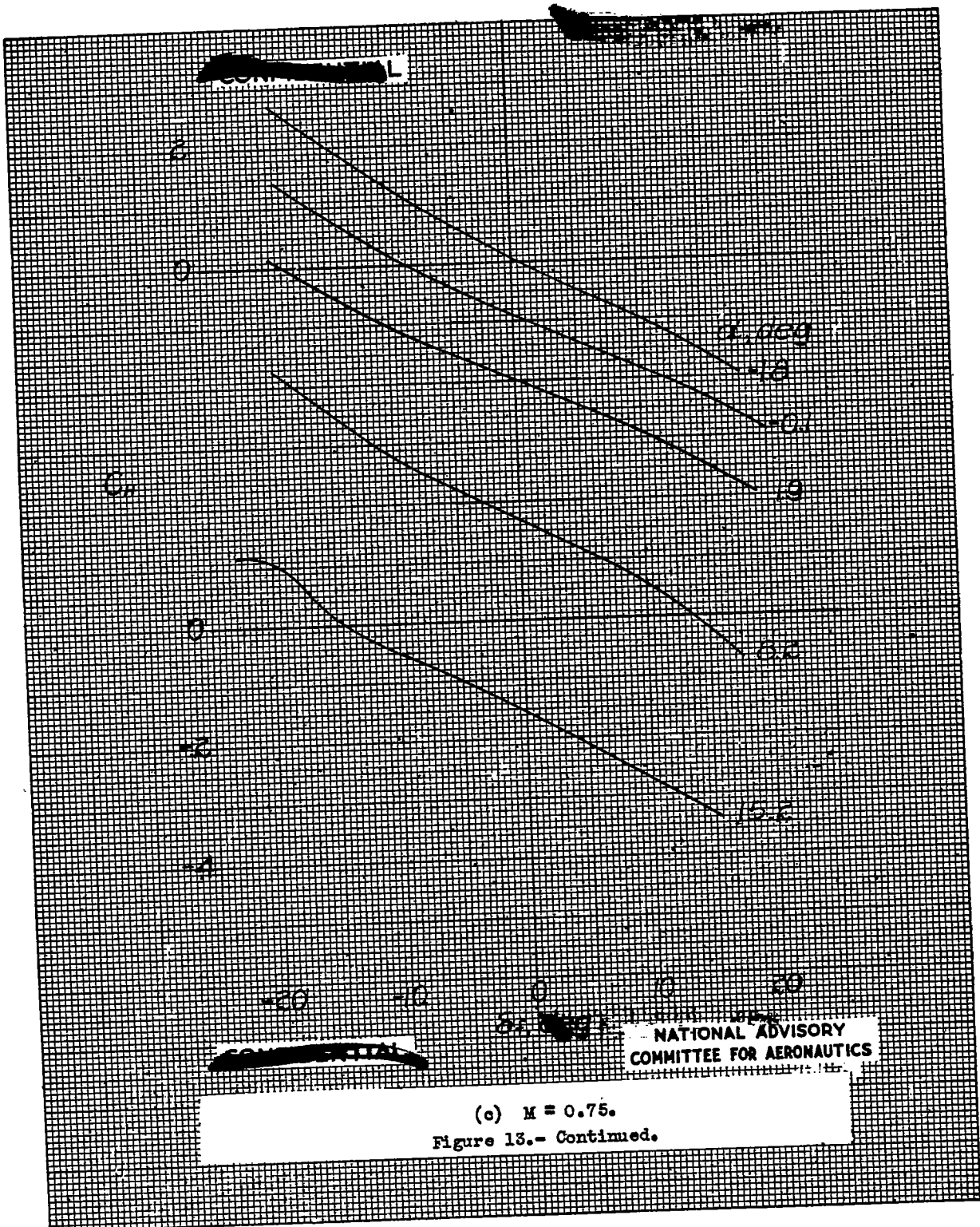
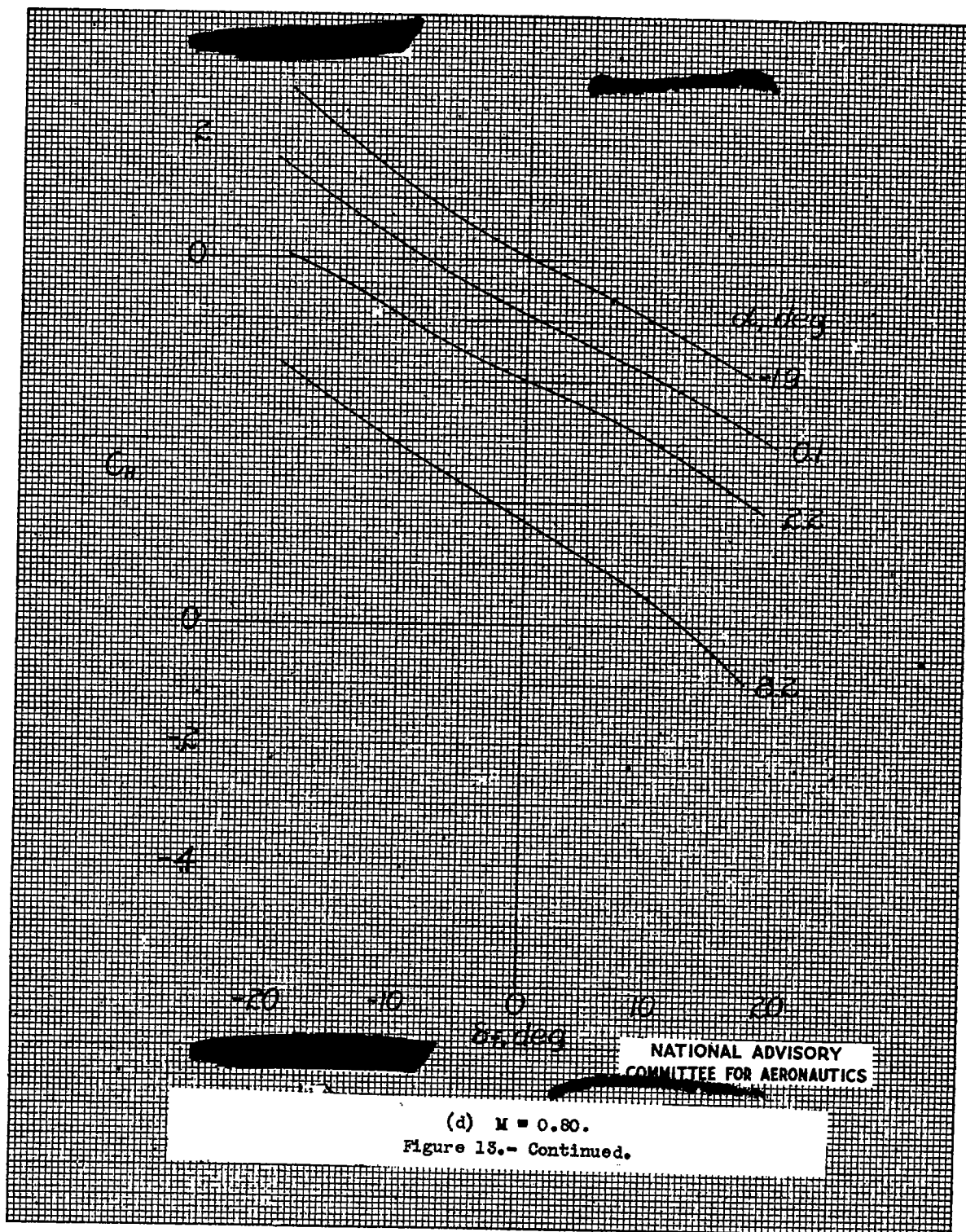


Fig. 13d

NACA RM No. L7F13



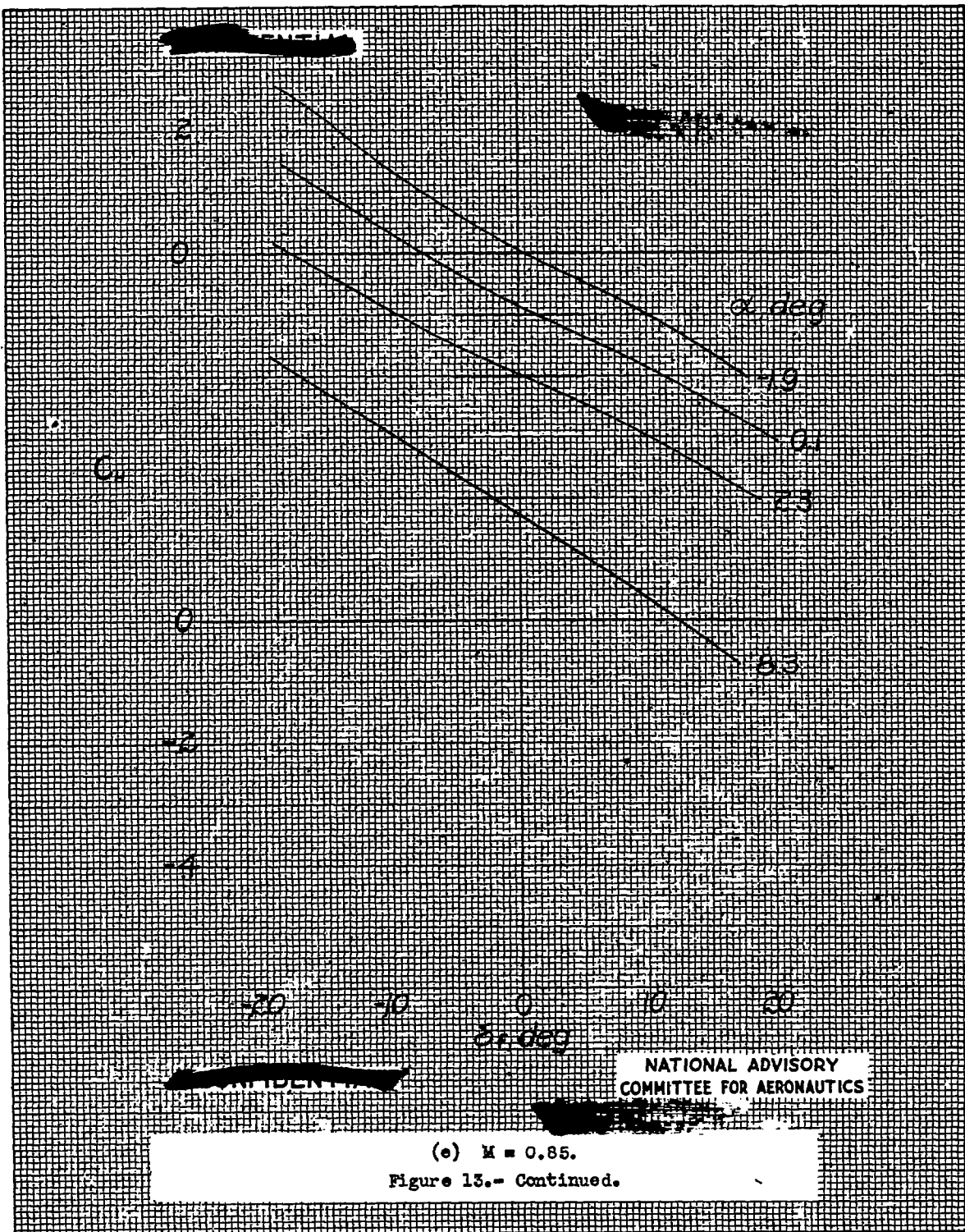
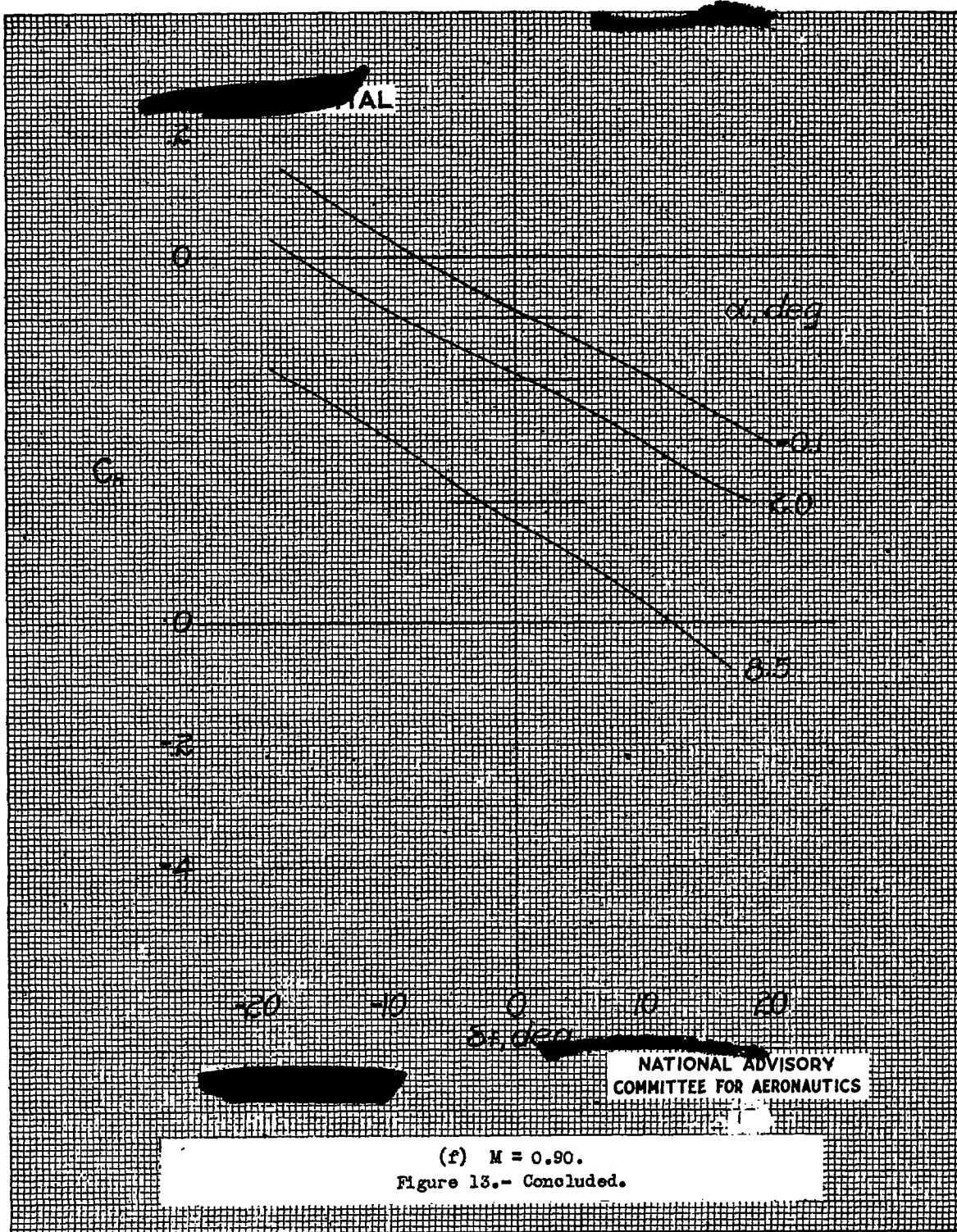


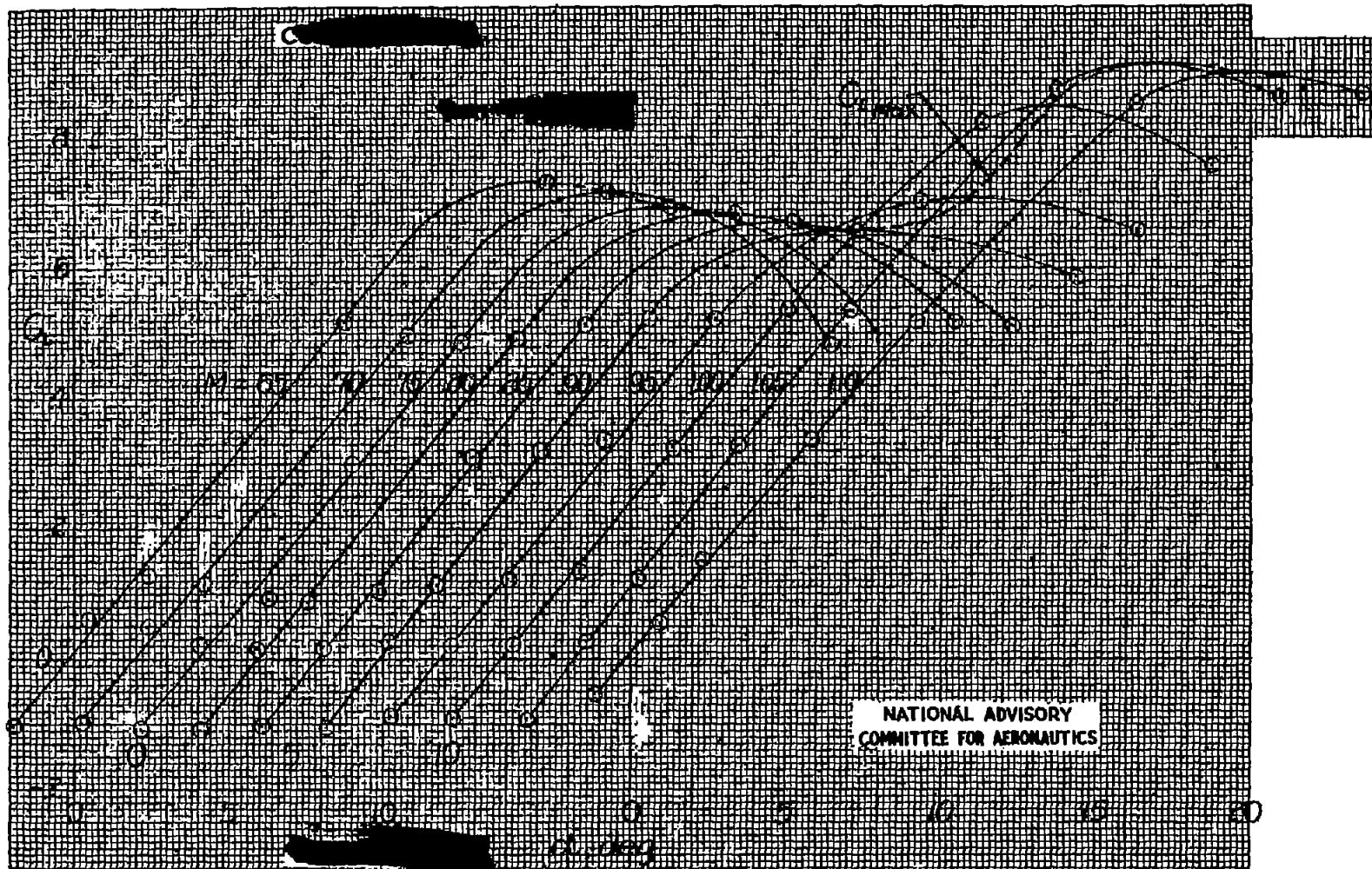
Fig. 13f

NACA RM No. L7F13



NACA RM No. 17F13

Fig. 14a

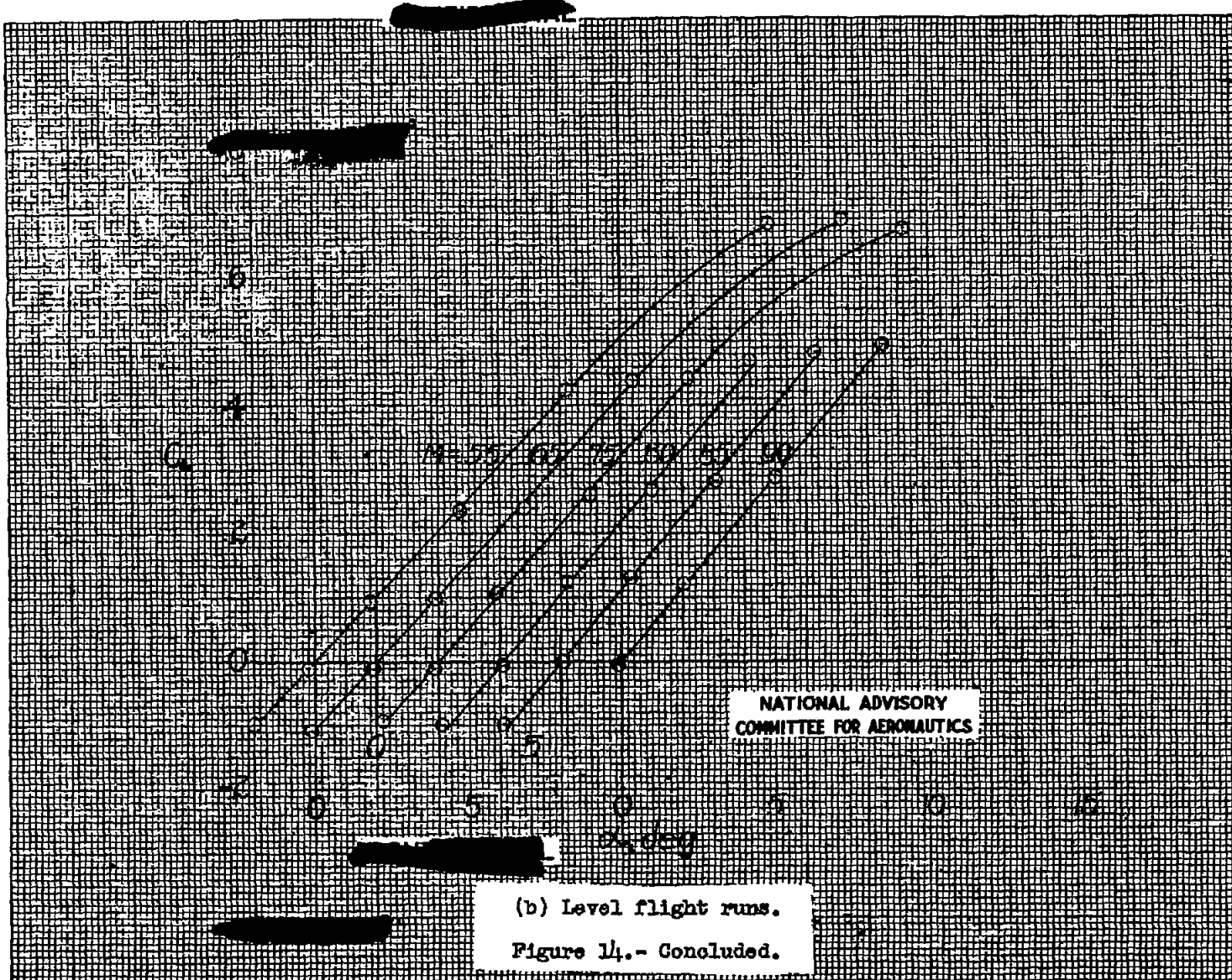


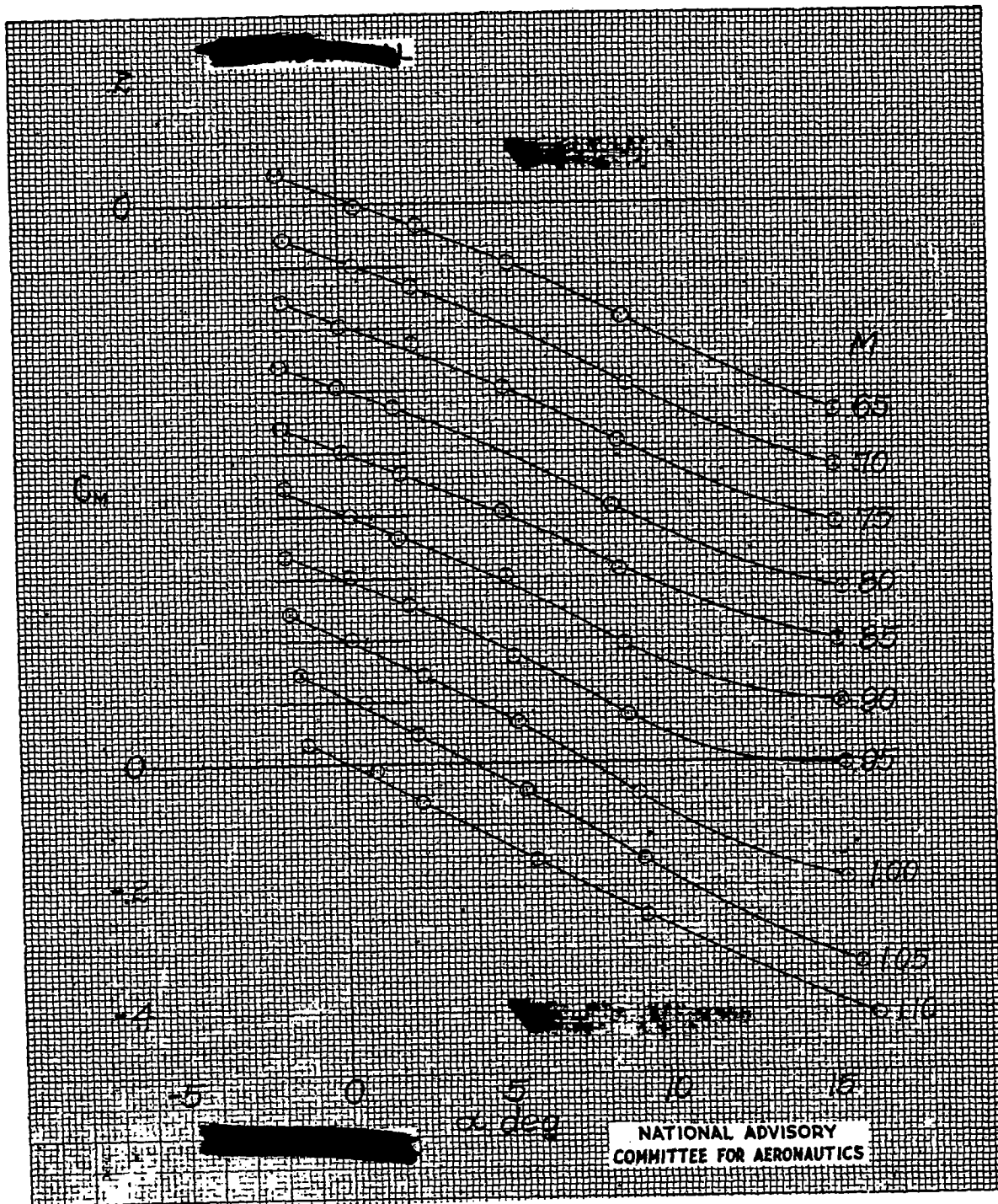
(a) High dive runs.

Figure 14a. Variation of lift coefficient with angle of attack. NACA 65-008 airfoil, $A = 3.04$, $\Delta = 35^\circ$, $c_p/c = 0.25$, gap unsealed, $\delta_e = 0^\circ$. Note shift in zero abscissa for different Mach numbers.

Fig. 14b

NACA RM No. L7F13



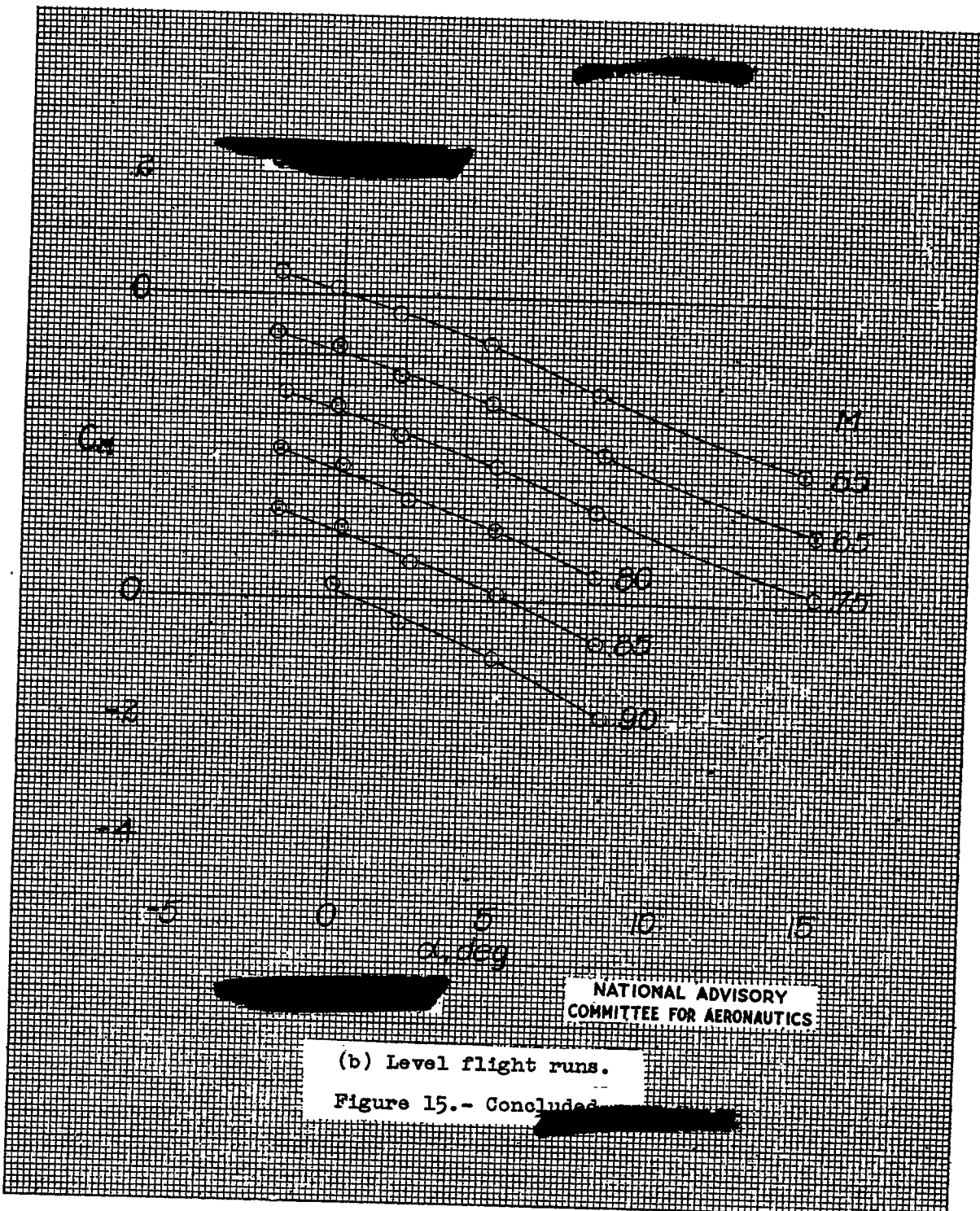


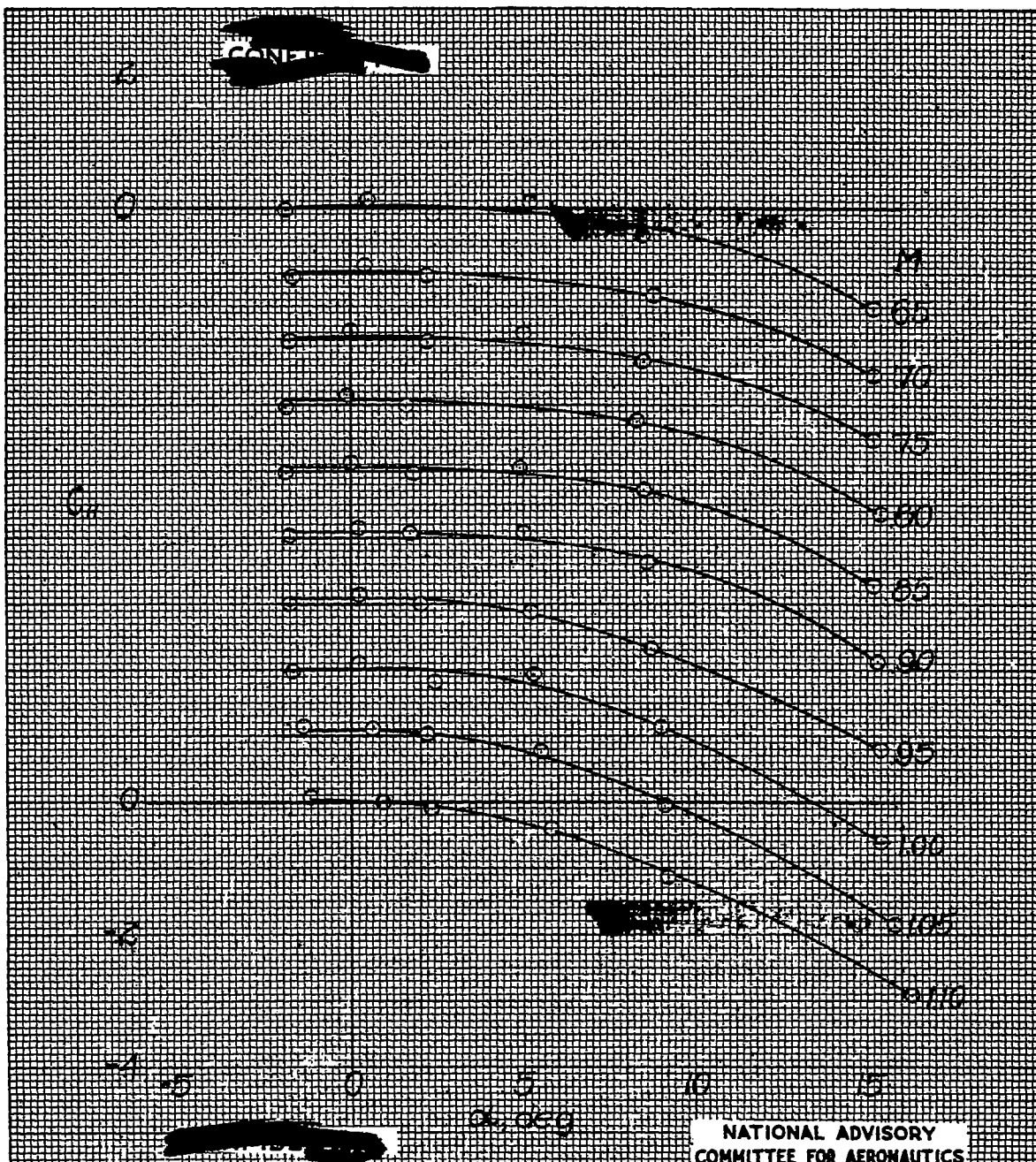
(a) High dive runs.

Figure 15.- Variation of pitching moment coefficient with angle of attack.
NACA 65-009 airfoil, $A = 5.04$, $\Delta = 35^\circ$, $c_f/c = 0.25$, gap unsealed,
 $\delta_e = 0^\circ$. Moment coefficient given about axis located 18 percent MAC
ahead of leading edge of MAC. Note shift in zero ordinate for different
Mach numbers.

Fig. 15b

NACA RM No. L7F13



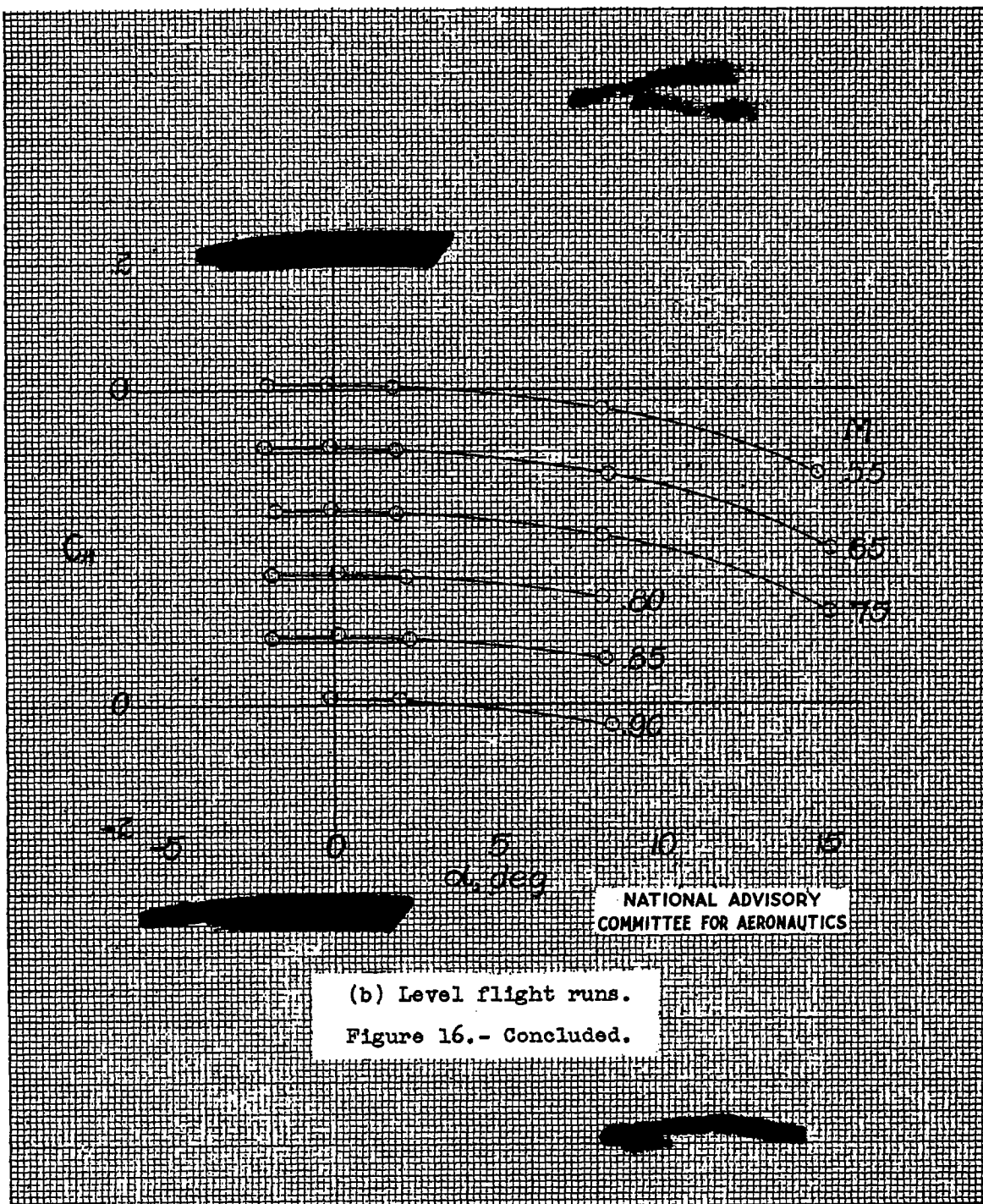


(a) High dive runs.

Figure 16.- Variation of hinge moment coefficient with angle of attack. NACA 65-009 airfoil, $A = 3.04$, $\Delta = 35^\circ$, $c_f/c = 0.25$, gap unsealed, $\delta_e = 0^\circ$. Note shift in zero ordinate for different Mach numbers.

Fig. 16b

NACA RM No. L7F13



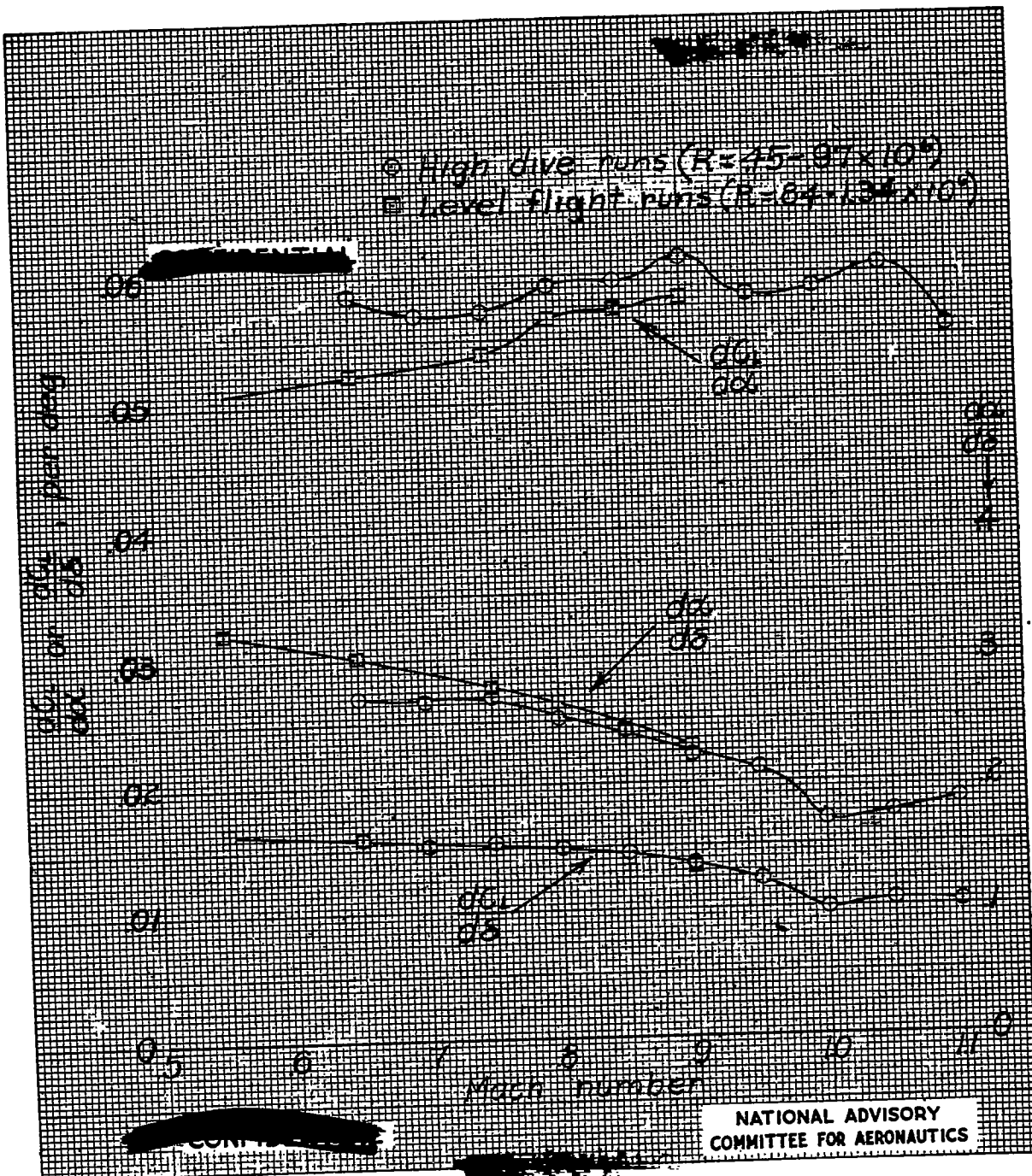


Figure 17.- Variation of airfoil and flap lift effectiveness with Mach number. NACA 65-009 airfoil, $A = 3.04$, $\Delta = 35^\circ$, $c_f/c = 0.25$, $\alpha \approx 0^\circ$, $\delta = 0^\circ$.

Fig. 18

NACA RM No. L7F13

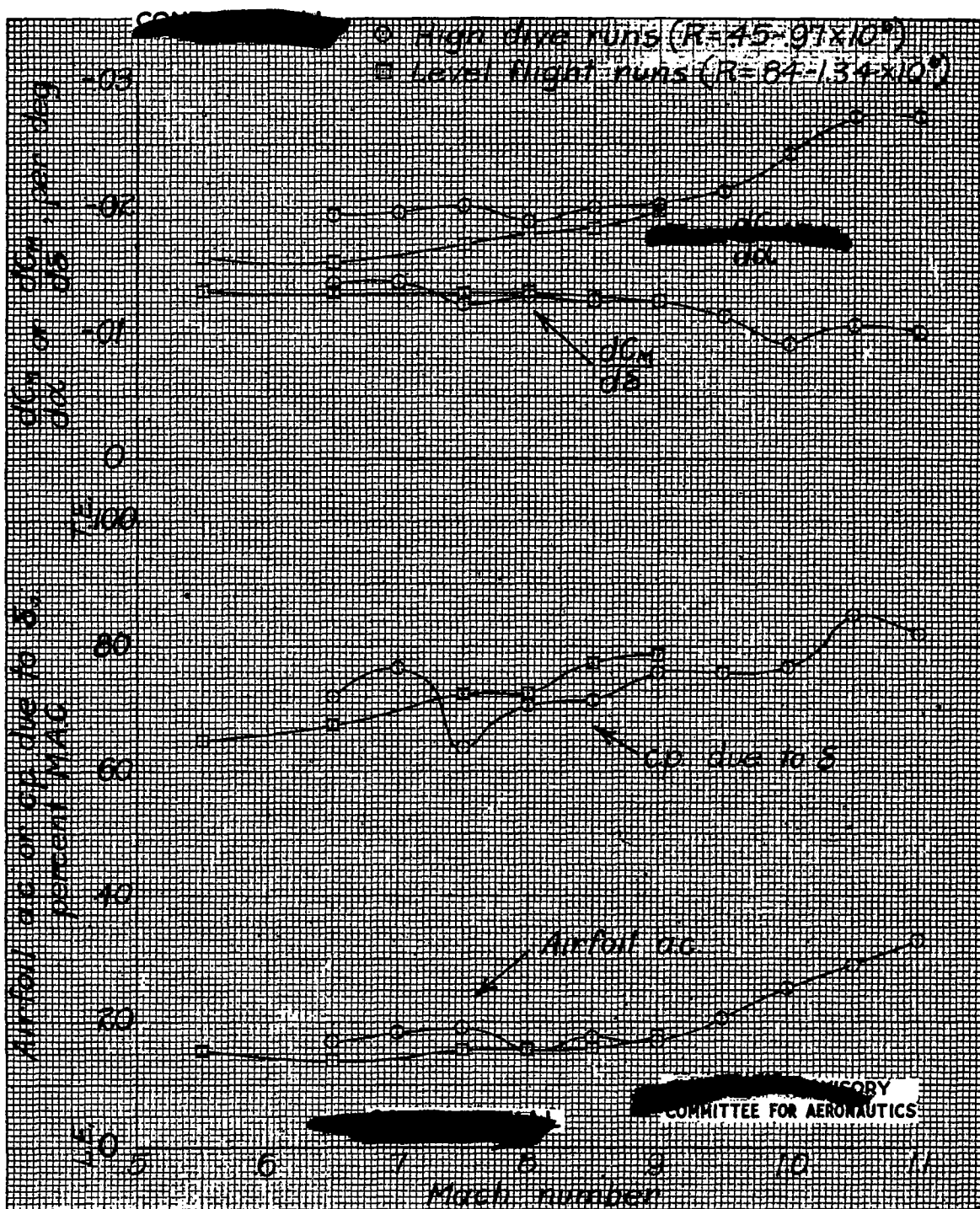


Figure 18.- Variation of airfoil and flap pitching moment characteristics with Mach number. NACA 65-009 airfoil, $A = 3.04$, $\Delta = 35^\circ$, $c_f/c = 0.25$, $\alpha \approx 0^\circ$, $\delta = 0^\circ$. Pitching moments measured about axis located 16 percent MAC forward of leading edge of MAC.

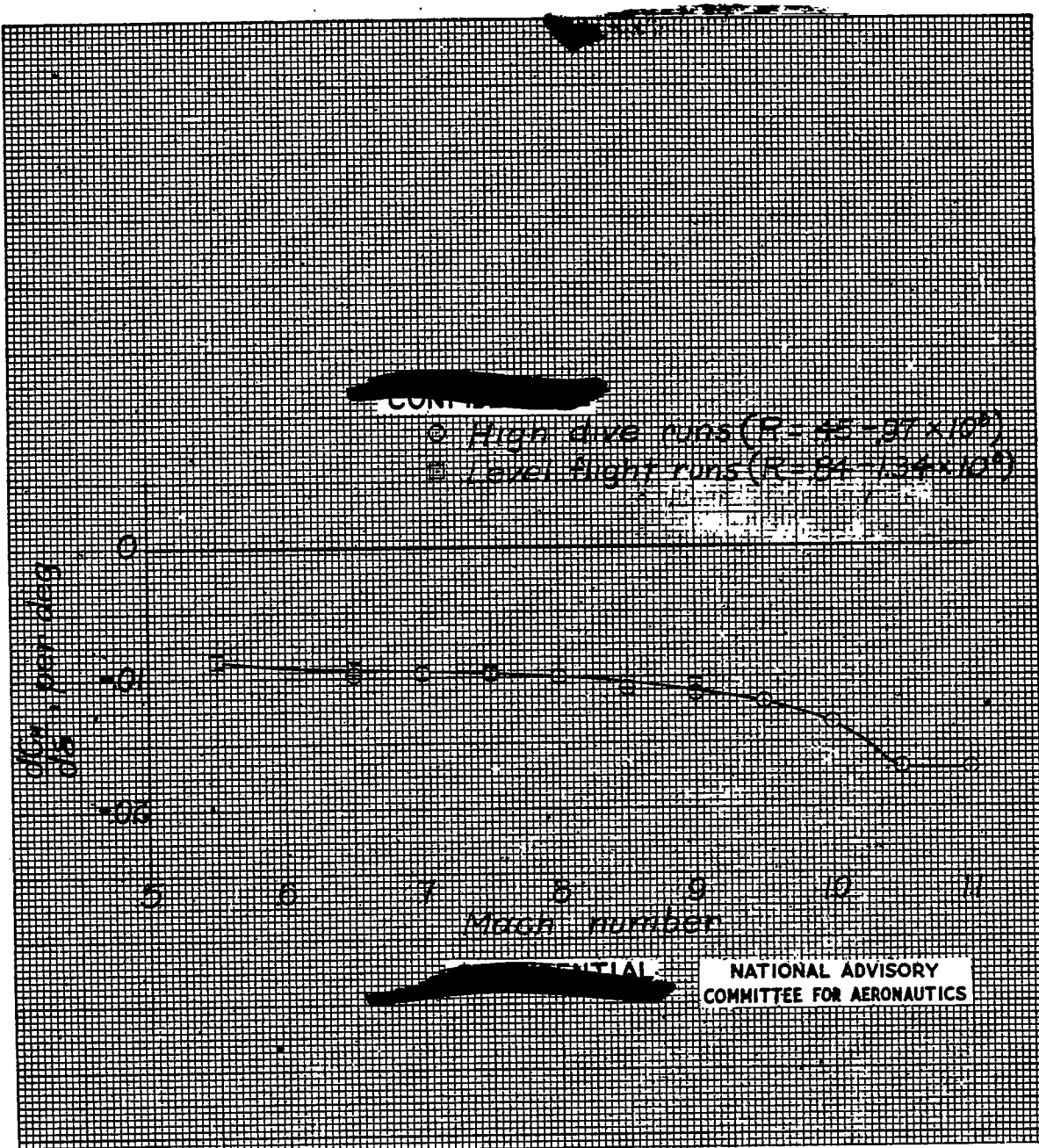


Figure 19.- Hinge moment coefficient versus Mach number. NACA 66-009, $A = 3.04$, $\alpha = 35^\circ$, $c_f/c = 0.25$, $\alpha \approx 0^\circ$.

Fig. 20

NACA RM No. L7F13

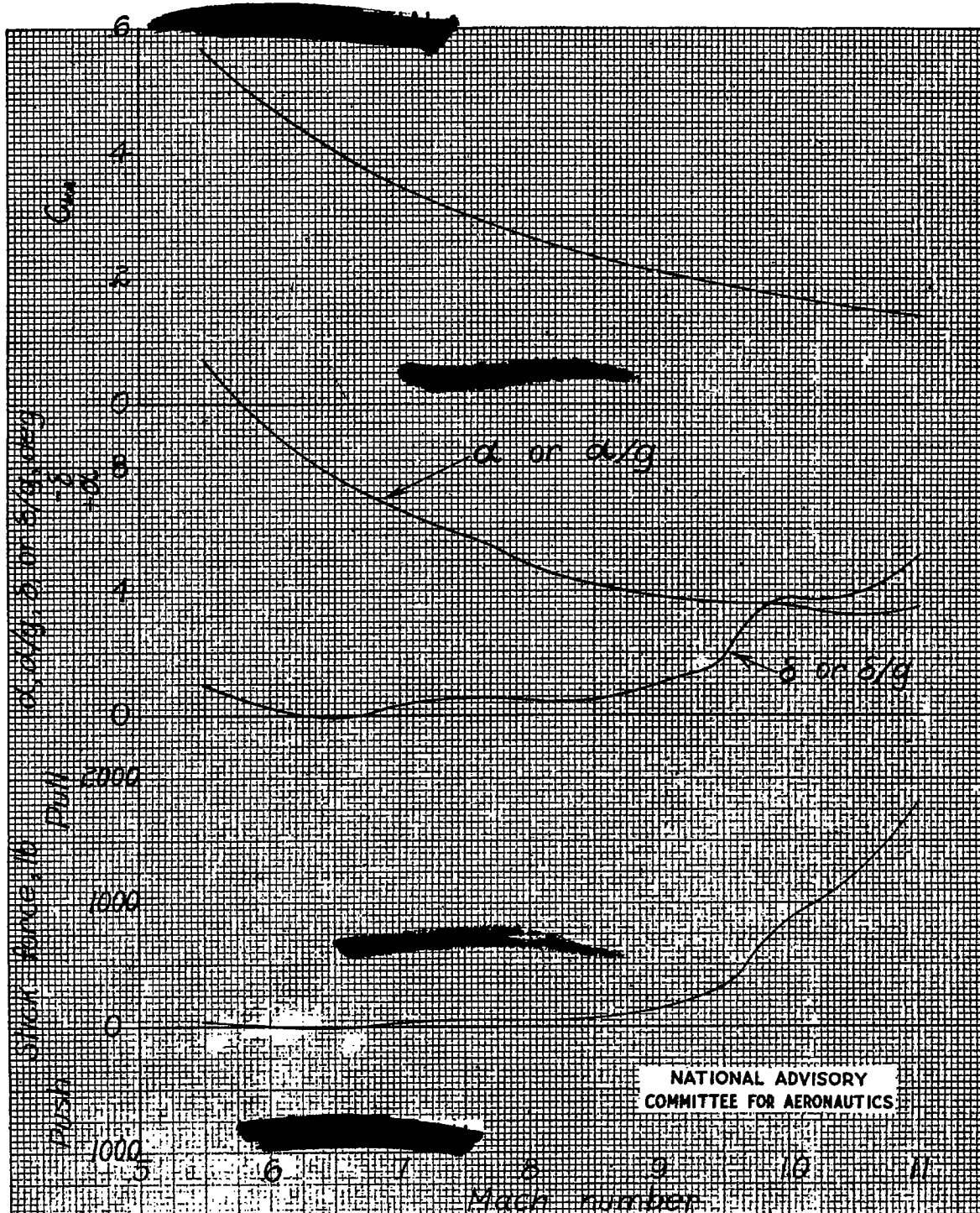


Figure 20.- Longitudinal trim characteristics of assumed 35° sweptback flying wing airplane in level flight at 30,000 feet altitude based on model data. $W = 15,000$ lbs, $S = 200$ sq. ft. Center of gravity at 14 percent mean aerodynamic chord.